Unveiling Cross-Kingdom Interactions in Natural *Arabidopsis thaliana* Leaf Microbial Communities

Dissertation

der Mathematisch-Naturwissenschaftlichen Fakultät

der Eberhard Karls Universität Tübingen

zur Erlangung des Grades eines

Doktors der Naturwissenschaften

(Dr. rer. nat.)

vorgelegt von

Samuel Quinzer

aus Heilbronn

Tübingen

2025

Gedruckt mit Genehmigung der Mathematisch-Naturwissenschaftlichen Fakultät der Eberhard Karls Universität Tübingen.

Tag der mündlichen Qualifikation:	23.10.2025
Dekan:	Prof. Dr. Thilo Stehle
1. Berichterstatter/-in:	Prof. Dr. Eric Kemen
2. Berichterstatter/-in:	Prof. Dr. Hannes Link

Contents

I Table of Figures

II Table of Tables

III List of Abbreviations and Acronyms

Abbreviation	Full Term
%	Percent
2FC	2-Foldchange
3-OC12-HSL	3-oxo-C12-homoserine lactone
ABC	ATP binding cassette
AHL	Acyl-homoserine lactone
AXP	AMPure XP beads
BSA	Bovine serum albumin
CAZyme	Carbohydrate active enzyme
cDNA	Complementary DNA
CV	Crystal violet
DCS	DNA control sample
DE	Differential expression
DNA	Deoxyribonucleic acid
EB	Elution buffer
EDTA	Ethylenediaminetetraacetic acid
EF1-α	Elongation factor 1 alpha
et al.	*et alii*, *et aliae*, *et alia*
FCT	Flow cell tether
FCF	Flow cell flush
g	Gram
Gb	Gigabases
GH	Glycoside hydrolase
GO	Gene ontology
IAA	Indole-3-acetic acid
ID	Identification
ITS	Internal transcribed spacer

Continued on next page

Abbreviation	Full Term
kbp	Kilobase pair
km^2	Square kilometres
LDB	Long fragment buffer
LIB	Library beads
log	Logarithmic
M	Molar
mL	Millilitre
min	Minute
mM	Millimolar
$MgCl_2$	Magnesium chloride
Mbp	Megabase pair
mRNA	Messenger RNA
NA	Native adapter
ng	Nanogram
NTP	Nucleoside triphosphate
OD	Optical density
OTU	Operational taxonomic unit
PDA	Potato dextrose agar
PDB	Potato dextrose broth
PCR	Polymerase chain reaction
padj	Adjusted *p*-value
pH	Negative decimal logarithm of H^+ concentration
PDR	Pleiotropic drug resistance
qPCR	Quantitative PCR
RCF	Relative centrifugal force
RNA	Ribonucleic acid
rpm	Rounds per minute
RT	Room temperature

Continued on next page

Abbreviation	Full Term
SB	Sequencing buffer
sec	Second
TE	Tris-EDTA
TMHMM	Transmembrane hidden Markov model
UV	Ultraviolet
VOC	Volatile organic compound
µ	Micro
µL	Microlitre
°C	Degree Celsius

IV Summary

Microbial colonizers of natural plant populations play a pivotal role in shaping microbial community composition, influencing host physiology, and either promoting or suppressing disease development. Investigating the microbiome of *Arabidopsis thaliana* populations in the Tübingen region provided valuable insights into community structure and its interaction with the obligate biotrophic pathogen *Albugo laibachii*. Identified as a hub species through correlation network analysis, *A. laibachii* emerged as a key player in the phyllosphere, actively shaping the surrounding microbial community. In the same study, basidiomycete yeasts were found to be more stable than bacteria and occurred both in the presence and absence of the oomycete pathogen. While many yeasts co-occur with *Albugo*, some — particularly *Moesziomyces bullatus* and *Cystofilobasidium* — were predominantly found in its absence. These yeasts were shown to significantly reduce pathogen infection, with glycoside hydrolase 25 (GH25) identified as the key effector enzyme in the case of *M. bullatus*.

In the present study, we sought to elucidate the mechanism behind the inhibitory effect of *Cystofilobasidium* and uncovered an intriguing cross-kingdom synergy with a *Pseudomonas extremaustralis* strain frequently co-isolated with *Cystofilobasidium* from natural *A. thaliana* populations. Initial analyses confirmed that neither GH25 nor its orthologs are present in the *Cystofilobasidium* genome, suggesting a previously uncharacterized mechanism. Confrontation assays showed that the antimicrobial activity of our *P. extremaustralis* isolate is enhanced in the presence of *Cystofilobasidium* yeasts against various *A. thaliana*-associated bacteria. Notably, co-cultures of *Cystofilobasidium* and *Pseudomonas* exhibited increased biofilm formation in the presence of these previously inhibited bacterial strains. Transcriptomic analysis of the yeast revealed a distinct response to *P. extremaustralis*, and subsequent qPCR validation identified two candidate genes: the ABC transporter g5886 and the glycoside hydrolase g4647.

Together, these findings support a model in which the inhibition of *A. laibachii* observed in initial infection assays results from a natural synergistic interaction between *Cystofilobasidium* and *P. extremaustralis*. This interaction likely enhances biofilm formation, thereby reducing pathogen adhesion, and promotes selective microbial inhibition that indirectly limits pathogen colonization.

V Zusammenfassung

Mikrobielle Besiedler natürlicher Pflanzenpopulationen spielen eine zentrale Rolle bei der Zusammensetzung mikrobieller Gemeinschaften, beeinflussen die Wirtspflanze und können Krankheitsverläufe fördern oder unterdrücken. Die Untersuchung des Mikrobioms von *Arabidopsis thaliana*-Populationen in der Region Tübingen lieferte wertvolle Einblicke in die Struktur der Gemeinschaft und ihre Wechselwirkung mit dem obligat biotrophen Pathogen *Albugo laibachii*. Als zentraler Hub in der Korrelationsnetzwerkanalyse identifiziert, erwies sich *A. laibachii* als Schlüsselfaktor in der Phyllosphäre, der die umgebende Mikrobiota aktiv mitgestaltet. In derselben Studie wurden die Basidiomyceten als robuster im Vergleich zu den Bakterien beschrieben und traten sowohl in Anwesenheit als auch in Abwesenheit des Oomyceten-Pathogens auf. Während viele Hefen mit *Albugo* koexistieren, wurden einige – insbesondere *Moesziomyces bullatus* und *Cystofilobasidium* – überwiegend in dessen Abwesenheit gefunden. Diese Hefen reduzierten die Pathogeninfektion signifikant, wobei im Fall von *M. bullatus* die Glycosid-Hydrolase 25 (GH25) als zentrales Enzym identifiziert wurde.

In dieser Studie untersuchten wir den Wirkmechanismus von *Cystofilobasidium* und entdeckten eine reichsübergreifende Synergie mit einem *Pseudomonas extremaustralis*-Stamm, der häufig gemeinsam mit *Cystofilobasidium* aus natürlichen *A. thaliana*-Populationen isoliert wurde. Erste Analysen zeigten, dass weder GH25 noch orthologe Sequenzen im Genom von *Cystofilobasidium* vorkommen, was auf einen unbekannten Mechanismus hindeutet. Konfrontationsassays ergaben, dass die antimikrobielle Aktivität des *P. extremaustralis*-Isolats in Anwesenheit von *Cystofilobasidium* gegenüber verschiedenen *A. thaliana*-assoziierten Bakterien verstärkt wird. Zudem wiesen Mischkulturen von *Cystofilobasidium* und *Pseudomonas* in Gegenwart dieser Bakterienstämme eine erhöhte Biofilmbildung auf. Die Transkriptomanalyse der Hefe zeigte eine deutliche Reaktion auf *P. extremaustralis*, und qPCR-Validierung identifizierte zwei Kandidatengene: den ABC-Transporter g5886 und die Glycosid-Hydrolase g4647.

Diese Ergebnisse stützen ein Modell, bei dem die beobachtete Hemmung von *A. laibachii* auf einer natürlichen Synergie zwischen *Cystofilobasidium* und *P. extremaustralis* beruht, die über verstärkte Biofilmbildung die Pathogenadhäsion reduziert und durch selektive Mikrobenhemmung die Besiedlung durch Pathogene indirekt einschränkt.

6 Introduction

Microbial communities play a major role in natural, as well as man-made environments and inhabit all known ecological niches, from extremophiles on the ocean floor (Bienhold et al., 2016) to biofilms forming on space flight equipment (Marra et al., 2023). Diverse habitats come with different challenges. Variable pH, temperature, salinity along with overall nutrient limitation or heavy metals and many more all need to be dealt with. Over time, many different methods of adaptation to the multitude of environmental conditions were developed. Slow-growing microbes take a more methodical approach, while fast-growers try to outpace the competition for nutrients and space. Other approaches include the formation of biofilms to produce a physical barrier or the construction of microbial communities. Complex microbial communities have the advantage that not all microbes have to adapt to all environmental challenges but can share the responsibilities.

6.1 The Plant Holobiont

One such example of a microbial community is the plant microbiome. Here, a multitude of interactions between the plant host, its associated microbes and among the microbes themselves take place. Many of these interaction are symbiotic by providing stability for the community and contributing to plant health (Newton et al., 2010). Combinations of host-microbe, microbe-microbe and host-microbe-microbe interactions are responsible for the establishment of the microbiome as we know it (Hunter et al., 2010, Bakker et al., 2014).

6.1.1 Plant-Microbe Interactions in the Rhizosphere

Microbial communities in the rhizosphere are distinct from those in bulk soil and often play a beneficial role for the plant. To attract specific microbes to the root zone, plants release various organic compounds, including sugars, amino acids, and phenolics, which promote microbial enrichment in the rhizosphere (Hu et al., 2018, Y. Liu et al., 2024). This recruitment process can be energy-intensive, with plants allocating up to 40% of their photosynthetic output for this purpose (Zhalnina et al., 2018). Different plants have different rhizosphere effects. For example, maize and lotus have a rather strong effect (Peiffer et al., 2013, S. Zhu et al., 2016, Zgadzaj et al., 2016) compared to *A. thaliana* (Edwards et al., 2015, Schlaeppi et al.,

2014). The acquired microbes in turn have multiple advantages for the plant. They provide an increased capability to take up nutrients by making limiting compounds, like nitrogen or phosphorus, more available (Richardson and Simpson, 2011). Through the increased availability of food and certain microbes being able to produce phytohormones like indole-3-acetic acid (IAA), plant growth is promoted (Gouda et al., 2018, Backer et al., 2018, P.-F. Sun et al., 2014). Plant-derived carbon is exchanged not only for growth-promoting phytohormones or enhanced nutrient solubilization but also for protection against pathogens. For example, commensal *Pseudomonas* strains can suppress pathogenic *Pseudomonas* (Eitzen et al., 2021, Shalev et al., 2022). Beyond just protecting directly from pathogens, microbes can also prime the plants immune system through induced systemic resistance (Pieterse et al., 2014, Peng et al., 2023). Necessarily, when enhancing plant immunity, microbes need the ability to evade host defenses or suppress the immune response, which is especially important for endophytes coming in closer contact with the host immune system (Zamioudis and Pieterse, 2012, Y. Liu et al., 2017). Additionally, it was shown that under different abiotic stresses, the microbial community surrounding the plant shifts to accommodate the changing environment and help the plant handle stress such as drought better and faster (Lau and Lennon, 2012, Gehring et al., 2017). Furthermore, the adaptation of plant responses to dry soil was inferred not by changes in plant genetics but rather by the microbial community, again displaying the importance of the microbiome (Lau and Lennon, 2012).

6.1.2 Composition and Colonization of Phyllosphere Microbiota

In addition to the rhizosphere — the below-ground plant-microbe interface — the phyllosphere represents the above-ground counterpart, encompassing all aerial parts of the plant. Globally, leaves constitute one of the largest natural surfaces, covering an estimated area of approximately 508 million km^2 (Woodward and Lomas, 2004). It is estimated that within this ecological niche, between 10^6 and 10^7 bacterial cells inhabit each square centimeter (Lindow and Brandl, 2003). Microbial inhabitants consist of a broad range of taxonomic groups. Overall, bacteria are the most abundant followed by filamentous fungi or single-celled yeasts and other eukaryotes like protists, algae and archea (Vorholt, 2012, Almario et al., 2022). Although not yet extensively studied in the context of microbial communities, viruses and bacteriophages are widely acknowledged to be present and add an additional layer of com-

plexity. Their roles may help shed light on some of the unresolved aspects of host–microbiome interactions (Koskella and Brockhurst, 2014, Debray et al., 2024). Microbes can live on the leaf surface, which we call epiphytes and often aggregate into biofilms (C. E. Morris et al., 1997) compared to endophytes that enter the plant and inhabit its tissues. The plant is able to assemble its microbiome indirectly by different leaf surface properties causing distinct microbial colonization (Hunter et al., 2010). Not only is an indirect assembly possible but it was shown that by jasmonic or gamma-aminobutyric acid signaling the host can directly attract desired microbes (Kniskern et al., 2007, Balint-Kurti et al., 2010). Major taxa include Alphaproteobacteria, which can make up to ∼70% of leaf associated bacteria, followed by Gammaproteobacteria, Bacteroidetes and Actinobacteria (Whipps et al., 2008, Lambais et al., 2006, Vorholt, 2012). Key bacterial groups contain Sphingomonadaceae (mostly epiphytic), Methylobacteriaceae, *Pseudomonas*, *Pantoea* and *Xanthomonas* (Beattie and Marcell, 2002, Vorholt, 2012). Fungal community members often colonize the plant through airborne spores and commonly consist of yeasts, but filamentous fungi like *Alternaria* or *Cladosporium* are also frequently found (Vorholt, 2012).

6.1.3 Environmental and Host Factors Shaping the Phyllosphere Microbiome

The microbial community can be influenced by a multitude of factors including UV radiation, temperature, humidity, precipitation and air quality. While pigmented microbes stand a higher chance of survival on the leaf surface, non-pigmented ones either die, live on the leaf underside or enter the plant to protect themselves leading to the diversification and differentiation of the microbiome (Kadivar and Stapleton, 2003, Vorholt, 2012, Remus-Emsermann et al., 2012). Temperature and humidity mostly go hand in hand, as higher temperatures in general mean a more dry environment, with the exception of equatorial rain forest regions or when rainfall occurs at elevated temperatures. If water aggregates on the leaf surface, the flow of liquid can wash away microbes without the ability to adhere to the plant, for example by formation of biofilms (Noel et al., 2022), or remove the ones not adapted to more humid conditions (Monier and Lindow, 2004). In addition, water flow can move microbes on the leaf and leave them in crevices in which they then accumulate creating “hot-spots” of microbial presence. Another contributing factor to microbiome composition is the plant age. Senescing leaves accumulate different nutrients compared to young ones and therefore provide differ-

ent conditions, which in turn has an impact on the microbial community (Vorholt, 2012). Geographical locations, combining multiple abiotic factor changes at once, also influence microbial community structure and shows that side-specific effects have a greater impact on the microbiome than plant genotype (Finkel et al., 2011, Redford et al., 2010).

6.1.4 Microbial Hubs and Community Assembly

Not only does the host interact with the microbial community, but microbe-microbe interactions are highly important to keep the community composition stable and to provide benefits for the plant and its microbial members. While inter-kingdom interactions in the microbiome are dominated by negative associations, positive correlations make up the majority of intra-kingdom interactions (Agler et al., 2016). Some microbes have a bigger impact on the overall community composition than others. If a microbe is highly interconnected — exhibiting high betweenness and closeness centrality — and has a significant influence on the overall community, it is considered particularly important. We call these microbes hubs (Agler et al., 2016).

6.1.5 Colonization Strategies and Microbial Succession

Primary colonizers, the initial microbes interacting with the plant, support secondary colonizers by shielding them from abiotic stresses such as drought and supplying essential metabolites, thereby enhancing their competitiveness (Poza-Carrion et al., 2013, Roberts and Lindow, 2014). The establishment of secondary colonizers is not solely based on mutually beneficial interactions, as hyperparasitism of primary colonizers has been observed, underscoring the complexity and diversity of microbial interactions (Horner et al., 2012). There are two ways for a plant to be colonized by microbes. The first is vertically, inheriting their microbial partners from the seeds, while horizontal transfer describes the process on how microbes arrive on the plant from the environment (Truyens et al., 2015, Barret et al., 2015, Links et al., 2014, Bulgarelli et al., 2013, Reinhold-Hurek et al., 2015).

6.1.6 Molecular Communication and Functional Interactions

The resulting microbial community is shaped in big parts by interactions happening between the microbes themselves in a dynamic and diverse manner. Molecular communication, such as

quorum sensing, plays a key role in shaping microbial interactions. It was shown that bacteria use quorum sensing molecules to monitor population density, for example by employing N-acyl-l-homoserine lactone (Eberl, 1999). The pathogenic yeast *Candida albicans* uses the signaling compound farnesol to inhibit biofilm formation by regulating the switch from yeast to mycelial growth and increase drug efflux rate of specific transporters (Hornby et al., 2001, Ramage et al., 2002, Sharma and Prasad, 2011). Due to the conserved nature of many sensing molecules, other microbes can interfere with quorum sensing of others leading to a constant struggle between them. Surrounding microbes not only create niches for others, but extend them. This is achieved by making nutrients available through the breakdown of compounds, removal of toxins from the environment or exchanging electrons (Wintermute and Silver, 2010, Harcombe, 2010, Schink, 2002, B. E. Morris et al., 2013). Such beneficial interactions promote more positive interactions between microbes overall and result in increased connectivity (B. E. Morris et al., 2013). On the other hand though, being dependent on others to provide, leads to gene loss over time and full dependency on the provider (Mas et al., 2016, Kemen et al., 2011).

6.1.7 Dispersal, Symbiosis, and Antagonism

Increased microbial dispersal on and within plants represents another context-dependent interaction, with "fungal highways" providing a route for bacteria and other microbes to move along hyphae (Kohlmeier et al., 2005). Other methods of distribution include spore transport by protists or the usage of hyphae and mycelia to colonize in the plant endosphere (Larousse et al., 2017). Speaking of fungi, they were shown to contain a microbiome of their own. These intracellular communities have a low diversity, for example, the arbuscular mycorrhiza fungi *Gigaspora margarita* can host two bacteria of the class Mollicutes and genus *Burkholderia* (Desirò et al., 2014). But not only symbiotic interactions happen in and on the plant host. As discussed earlier, resources are scarce and therefore competition for nutrients is ever-present. Microbes continuously compete for survival, whether by secreting molecules to aid in acquiring essential elements — such as siderophore production for enhanced iron uptake (Wandersman and Delepelaire, 2004, Joshi et al., 2006) — or by outcompeting others through superior speed or efficiency. Another way of securing their place in the niche is the production of antimicrobials. In general, antagonistic interactions are known to be major

drivers to shape and structure the microbial community (Tyc et al., 2014, Maida et al., 2016). Most antimicrobials are secondary metabolites and can be produced by bacteria, fungi and other eukaryotes (Shearer, 1995, Coleman et al., 2011). Some are only synthesized in co-culture, so the presence of multiple microbes might be necessary for compound production (Schroeckh et al., 2009, Netzker et al., 2015). Indirect killing of competitors is not the only way microbes get rid of opposition. By direct contact many microbes use secretion systems to introduce effectors or toxins into their target. Secretion systems are not necessarily used for negative interactions, as it was shown that *Burkholderia rhizoxinica* increases sporulation of *Rhizopus microsporus* in a symbiotic manner (Records, 2011, Lackner et al., 2011).

6.1.8 Pathogenesis and Microbiome Destabilization

Similar to the animal kingdom, predation is also common in the microbial community with bacterial mycophagy, fungal on fungi mycoparasitism or higher eukaryotes grazing on bacteria reshaping the microbial network in plants (De Boer et al., 2004, Barnett, 1963, Flues et al., 2017). As for other living organisms, diseases are not uncommon and plants can be host to a multitude of non-beneficial, even harmful microorganisms. These pathogens have a significant impact on plant health by production of toxins (Tsuge et al., 2013, Howlett, 2006), modification of the host metabolism (Cai et al., 2023, Berger et al., 2007) and altering the host microbial community stability through structural and compositional changes of the microbiome (Agler et al., 2016). Many pathogens usually live as commensals in the plant microbiome. External perturbations like climate, nutrient change or the arrival of a community disturbing actor can change the balance leading to opportunistic pathogens becoming infectious (Charkowski, 2016).

6.2 Importance of Novel Plant-Protective Measures

Agricultural crop production forms the foundation of our food industry, with wheat alone accounting for approximately 20% of global calorie and protein intake (Shiferaw et al., 2013). Evidently, it is imperative that plant protection is a high priority research, not only for environmental protection and climate preservation but crucially to prevent world hunger by securing our food production and making crops more resilient to disease. Nowadays, one of the major plant protection methods is the use of chemical agents, which, more often than not,

have a negative impact on the targeted plant. Additionally, the entire ecosystem including animals and plants not intended as treatment targets or groundwater can be effected (Goulson, 2014, World Health Organization, 1990). As such, the search for alternative treatment options needs to be a top priority. The main alternative in research today is the utilization of naturally occurring microorganisms, which have several advantages: they target pathogens more directly and specifically without too many side or off-target effects, while also being beneficial for the plant health directly (Essiedu et al., 2020).

6.3 *Arabidopsis thaliana* Tübingen Sampling

The baseline data for this study was collected during sampling trips across the city of Tübingen, Baden-Württemberg, Germany. From 2014 onward, *A. thaliana* individuals from populations were collected at six different sites (Agler et al., 2016 supplementary data) two times a year. The first time, they were collected at the beginning of the growing season in fall and the second time at the end of it in spring. During processing, the samples were washed to collect epiphytic microbes and then surface sterilized to get the remaining endophytes. Overall, more than 700 samples were acquired and analyzed with three primer sets for bacteria (16S), fungi (ITS) and other eukaryotes (18S) via amplicon sequencing. Correlation network analysis revealed positive correlations mostly in kingdoms and negative ones predominately between kingdoms (Agler et al., 2016). Further investigation identified the oomycete *Albugo laibachii* and the basidiomycete yeast *Dioszegia hungarica* as major hub taxons in the studied samples (Agler et al., 2016).

6.4 The Oomycete Pathogen *Albugo laibachii*

Surprisingly, *A. laibachii* is not only a hub taxon in the phyllosphere but additionally an obligate biotrophic pathogen and the causal agent of the white rust disease on *A. thaliana* (Kemen et al., 2011), which is one of the major diseases in Brassicaceae (Ploch and Thines, 2011). To fulfill its life cycle, *Albugo* first needs to enter the plant leaf through the stomata, after which it forms intercellular hyphae, penetrating the cell wall to form haustoria used to take up nutrients from the plant cell and secreting effectors into the host to stimulate host reactions to, for example, evade detection (Kemen et al., 2005, Kemen and Jones, 2012, Spanu and Kämper, 2010, Rafiqi et al., 2010). Over time, the pathogen shed several essential

metabolic functions required for independent survival, including thiamine synthesis, nitrate reductase, and the molybdopterin biosynthesis pathway. Conversely, it also acquired new genes, such as CHXC-effectors (Kemen et al., 2011). In addition, effectors in general not only impact the host but shape the microbial community around it as *Albugo* uses released proteins to selectively suppress bacteria and shapes its niche depending on the circumstances, further cementing it as a major player in the *A. thaliana* phyllosphere microbiome (Gómez-Pérez et al., 2023). Interestingly, when taking a deeper look into the genus we can see that there are differences between the species. *A. laibachii* and *A. candida* are both obligate biotrophic organisms but differ in terms of host range. Usually, obligate biotrophs have a very narrow host range, infecting only one host, which is the case for *A. laibachii* infecting *A. thaliana*. In comparison, *A. candida* is able to infect over 200 plant species (McMullan et al., 2015). Even though there are huge differences when it comes to the hosts, both species share very similar genome sizes with 32.77 Mbp for *A. laibachii* and 34.45 Mbp for *A. candida* (McGowan et al., 2019). Comparing genome size, one might suggest the slightly higher number of base pairs correlates to higher number of genes but it was shown that *A. laibachii* has more predicted gene models than *A. candida*. The former having 12567, while the latter has 10698 predicted genes (McGowan et al., 2019). Overall, both *Albugo* species have a small but very dense genome compared to other oomycete pathogens and one of the highest gene density (gene models per Mbp) in the group of obligate biotrophic oomycetes, with *A. laibachii* having more than double the density compared to *Hyaloperonospora arabidopsidis* (adapted from McGowan et al., 2019).

6.5 Microbial Network Structure and Key Species

In general, microbial network analyses help us understand how communities come into existence, evolve over time, and interact with each other (Faust et al., 2015). As previously mentioned, hub microbes have high connectivity compared to non-hubs and therefore greatly influence the community; however, being a hub does not necessarily equate to being a keystone species (Agler et al., 2016). Certain individual Proteobacteria or Actinobacteria have a high potential to act as keystone species, as demonstrated by drop-out experiments conducted by Carlström et al., 2019, even though they may not appear as hub species in correlation-based network analyses.

6.6 Environmental Drivers of Microbial Community Dynamics

Naturally occurring microbial communities are shaped not only by their members but also by abiotic factors that play a major role in sculpting the microbiome. As DNA, RNA, and proteins are sensitive to temperature fluctuations — denaturing at high temperatures — microorganisms must adapt to environmental changes or risk being lost from the community. Temperature stress can alter gene expression, leading to changes in the production of antimicrobial compounds and, consequently, shifts in community composition. Other abiotic stressors include nutrient availability, water supply, and the duration of daylight, which influences UV exposure on leaf surfaces.

A common garden experiment demonstrated that over the growing period of *A. thaliana* from November to March, the microbial network became progressively less complex and diverse (Almario et al., 2022). Despite this, the stability of the community in response to perturbations increased during the same period (Almario et al., 2022). Analysis of alpha diversity — defined as the number of distinct taxa — showed that bacterial communities had the highest diversity, followed by fungi and then oomycetes. Interestingly, fungal and oomycete alpha diversity remained relatively stable throughout the growing season and across multiple years of sampling (Almario et al., 2022).

6.7 Basidiomycete Yeasts in Leaf Microbial Communities

As well adapted, frequent colonizers of the plant leaf surface, basidiomycete yeasts are often known to be a major part of the phyllosphere microbiome (Into et al., 2020). The phyllosphere is a nutrient scarce environment forcing microbes to adapt to harsh and quickly changing conditions and compete for food and space (Gouka, Vogels, et al., 2022). The production of carotenoids protects them from the UV radiation constantly faced on the leaf and additionally are able to construct biofilms using extracellular polysaccharides and surfactants (Noel et al., 2022). Biofilm formation has many advantages. In biofilms, moisture is accumulated compared to the rather dry leaves and it keeps the microbes on the leaf by virtually gluing them to the surface (Gouka, Vogels, et al., 2022). In addition, not only do the pigments produced by the yeasts protect from UV light but the biofilms themselves can act as a barrier for UV radiation and a physical barrier for other microbes to protect the microbial community from invaders, or the host from pathogens (Villa et al., 2017). Being

able to use many different substrates in an otherwise nutrient deficient space as a carbon or nitrogen source, basidiomycetes can utilize glucose, fructose, sucrose and methanol as well as amino acids, ammonium salts or nitrate gives them a competitive edge (Mercier and Lindow, 2000, Żymańczyk-Duda et al., 2017, Moliné et al., 2010, Chi et al., 2015, Shiraishi et al., 2015). Common leaf associated genera include *Sporobolomyces*, *Rhodotorula*, *Cryptococcus* and others that spread through the air using ballistoconidia contributing to their widespread appearance (Noel et al., 2022, Into et al., 2020).

6.7.1 Interactions with Other Microbes in the Phyllosphere

Basidiomycete yeasts can forge and participate in diverse and complex interactions with other microbes present in leaf microbial communities like bacteria, filamentous fungi, other yeasts or other eukaryotes like oomycetes. They often coexist with epiphytic bacterial populations and removing them from the community has a great impact on the composition of the bacterial residents (Noel et al., 2022). As previously shown, yeasts (and specifically basidiomycete yeasts) can have a multitude of interaction types with other microbes. Using network analysis they were observed to directly correlate in a positive and negative manner with a wide range of organisms, for example as shown for *D. hungarica* being directly positively associated with *A. laibachii* (Agler et al., 2016).

6.7.2 Antagonistic Functions Against Pathogens

On the other hand though, negative interactions of basidiomycete yeasts are also described detailing their multifaceted role in communities. A study investigating powdery mildew infections on cucumber plants could show that *Pseudozyma aphidis* hyperparasites the fungus *Podosphaera xanthii* and therefore stop the infection (Gafni et al., 2015). The yeast accomplishes this by overgrowing the fungus, penetrating the hyphae to secrete effectors, which hinder spore germination and results in pathogen inhibition (Gafni et al., 2015). Another very interesting example of negative interactions of basidiomycete yeasts with a pathogen is the example of *Moesziomyces bullatus*, which, in *A. thaliana* leaf microbial network analysis, correlates negatively with *A. laibachii* in contrast to most other basidiomycete yeasts (with the exception of *Cystofilobasidium*) (Döhlemann, Sengupta, Mahmoudi, Kemen unpublished).

6.7.3 GH25 Lysozyme-Mediated Pathogen Suppression

Investigation regarding whether yeast growth is inhibited by the oomycete or the other way around and questioning if the interaction happens in a direct manner revealed an interesting mechanism for pathogen inhibition. *M. bullatus* produces a lysozyme belonging to the family of glycoside hydrolases 25 (GH25), which even in an isolated form reduces pathogen infection rate of *A. thaliana* leaves (Eitzen et al., 2021). Enzymes of the GH25 family specialize on hydrolyzation of β-1,4-glycosidic bonds between N-acetylmuramic acid and N-acetylglucosamine in peptidoglycan (CAZypedia.org, 2025). A unique characteristic of GH25 lysozymes is the ability to degrade the O-acetylation of peptidoglycan at position C6, which is a modification that some bacteria, like *Staphylococcus aureus*, use to be resistant to some lysozymes (Hash and Rothlauf, 1967).

6.7.4 Direct Interactions with the Plant Host

Not only are basidiomycete yeasts able to interact within the microbial community but directly engage with the plant host. Growth stimulating yeasts were found to produce the phytohormone indole-3-acetic acid (IAA), an auxin that increases plant growth (P.-F. Sun et al., 2014). Species, such as *Moesziomyces aphidis* and *Rhodotorula mucilaginosa* can be used as biofertilizers to enhance plant growth in various crops by promoting root growth (Kumla et al., 2020).

6.8 The Basidiomycete Yeast *Cystofilobasidium*

As previously described, the basidiomycete yeast *Cystofilobasidium* was — together with *Moesziomyces* — one of the two basidiomycete yeast genera that were shown to negatively associate with the oomycete pathogen *A. laibachii* (Döhlemann, Sengupta, Mahmoudi, Kemen unpublished). The species belongs to the genus *Cystofilobasidium*, which was differentiated from the genus *Rhodosporium* in 1983 (Oberwinkler et al., 1983). The main difference that led to the distinction is the formation of teliospores, which, compared to basidiospores from *Filobasidium* (a teleomorph of *Cryptococcus neoformans*), are thick-walled resting spores (Oberwinkler et al., 1983, Moore and Rij, 1972). Approximately 20 years after the genus was differentiated, Mrakiaceae was distinguished from Cystofilobasidiaceae, but both families still belong to the order of Cystofilobasidiales (McLaughlin et al., 2001).

6.8.1 Diversity, Ecology, and Field Relevance

Currently, ten species are described within the genus: *C. alribaticum*, *C. bisporidii* (type species), *C. capitatum*, *C. ferigula*, *C. infirmominiatum*, *C. intermedium*, *C. josepaulonis*, *C. lacus-mascardii*, *C. lari-marini*, *C. macerans*, with many having anamorphic states in other genera (H.-Y. Zhu et al., 2023, X.-Z. Liu et al., 2015, Oberwinkler et al., 1983, Fell et al., 1999, Libkind et al., 2009). Generally speaking, the yeasts are known to be able to survive even at freezing temperatures, different pH-values and salinity conditions as *C. bisporidii* was isolated from seawater in the Antarctic Ocean, though they are mainly associated with plants (Sampaio et al., 2001). For example, *C. macerans* and *C. capitatum* were found in *Cineraria* sp. and *Trifolium* sp. respectively (Sampaio et al., 2001). During our *A. thaliana* sampling trips, we could also find yeasts with similar morphology and pigmentation. After further investigation, we identified the isolated microbe as a *Cystofilobasidium* yeast, belonging to the species *C. macerans* and *C. capitatum*, which is important as these two species were used here. This reinforces the results from Almario et al., 2022 that showed Cystofilobasidiales are part of the top 20 most abundant basidiomycete yeast orders and stable over years.

6.9 The Role of *Pseudomonas* in Leaf Microbial Communities

Pseudomonas is another major player in the leaf phyllosphere and is frequently of high ecological significance. As a, often dominant, leaf colonizer it is a core part of the microbial community (Gomila et al., 2015, Long et al., 2021). It can utilize a wide variety of nutrients and is able to adapt to low nutrient conditions in a usually low food quantity environment such as the leaf surface (Sitaraman, 2015, Mercado-Blanco and Bakker, 2007). Additionally, the presence of sophisticated DNA repair systems, like the pSR1 and pSR5 plasmid in *P. syringae*, protects the bacterium from UV radiation faced on leaves (Sundin et al., 1996). High temperatures and low humidity have been shown to decrease the abundance, while higher humidity increased it (Chai et al., 2023). Additionally, humidity can play a big role in pathogenicity, as certain non-pathogenic strains of *P. syringae* do become pathogenic when a specific threshold is reached (Xin et al., 2016).

6.9.1 Metabolic Versatility and Survival Strategies

Showing high metabolic versatility, *Pseudomonas* contributes highly to nutrient cycling through the production of siderophores like pyoverdine, which is used to sequester iron from the environment and modulate the overall microbial composition (Cox and Adams, 1985, Cox and Graham, 1979, Poole et al., 1996). Moreover, some *P. putida* strains display the ability to "clean the air" by reducing the amount of volatile organic compounds (VOC) (De Kempeneer et al., 2004). It was also shown that *Pseudomonas* outcompetes other microbes in terms of growth speed. It is, for example, able to quickly overgrow slow growers like *Sphingomonas* species on the leaf surface (Lundberg et al., 2022). Additional on-leaf strategies for survival include the formation of biofilms and quorum sensing. By exopolysaccharide production (like alginate), *Pseudomonas* is able to better adhere to the plant and be protected from biotic as well as abiotic factors (Helmann et al., 2019). A way to communicate and coordinate the formation of biofilms is quorum sensing, which stimulates many more processes including antibiotic production or the switch from commensalism to pathogenicity in some *Pseudomonas* (Kuiper et al., 2004, Dubern et al., 2006).

6.9.2 Plant-Beneficial Functions and Pathogen Suppression

Specific species are beneficial for the plant host and the microbial community alike. It was shown that *Pseudomonas* can promote plant growth by IAA production and can alter root growth patterns. Exposure to bacteria-secreted 3-oxo-C12-AHL reduced primary root growth, while diketopiperazines enhanced lateral root expansion, again demonstrating the effects *Pseudomonas* can have on the plant (Fett et al., 1987, Ortiz-Castro et al., 2011). Siderophore, quinolines, phenazines and the production of volatiles were all displayed to induce pathogen inhibition (Santos Kron et al., 2020, Yasmin et al., 2017, Chin-A-Woeng et al., 2003, Bailly and Weisskopf, 2017). Some species are also able to inhibit other pathogenic *Pseudomonas* species such as *P. syringae* through direct contact using a type VI secretion system mediated effector transmission (Bernal et al., 2017). Additionally, they can inhibit fungal pathogens like *Botrytis cinerea* and *Rhizoctina solani* by lysis of zoospores (Kruijt et al., 2009). Furthermore, *P. fluorescence* can induce plant growth through a type III secretion system and *P. putida* induces systemic resistance in *A. thaliana*, showing the importance of diverse sets of *Pseudomonas* species in the plant phyllosphere (Preston et al., 2001, Rainey,

1999, Meziane et al., 2005).

6.9.3 Pathogenic *Pseudomonas* and Their Virulence Mechanisms

Unfortunately, the genus does not only comprise of beneficial species, some are pathogenic and can cause potent foliar blights. *P. syringae* infects *A. thaliana* by epiphytic growth, which then enters an endophytic phase to spread inside the leaf tissue (Innerebner et al., 2011, Boureau et al., 2002, Hirano and Upper, 1983). After spreading internally, it produces the effectors syringopeptin and -mycin, which are antimicrobially active and even toxic for plant cells by their pore-forming characteristics (Lavermicocca et al., 1997, Hutchison and Gross, 1997). Overall, the genus is quite abundant in microbial communities with a few dominant species that include detrimental pathogens causing high crop loss worldwide (Lundberg et al., 2022).

6.10 Thesis Aim

This study investigates how cross-kingdom microbial cooperation can enhance antimicrobial activity, with potential implications for managing the obligate biotrophic plant pathogen *A. laibachii*. Our work was motivated by the discovery of a natural *Pseudomonas* strain in *A. thaliana* populations that consistently co-occurs with *Cystofilobasidium* yeasts, suggesting an ecological and functional association. We hypothesize that this co-culture improves bacterial inhibition on the leaf surface, either through increased or more effective antimicrobial production, and through enhanced biofilm formation, which may support microbial competitiveness and stability in the phyllosphere.

To explore this interaction, we used a multi-faceted experimental approach. Confrontation assays with a panel of leaf-associated bacterial strains assessed antagonistic activity in varying microbial contexts. In parallel, biofilm assays evaluated whether the bacterial partner alters yeast biofilm structure or function. To uncover mechanistic insights, we conducted transcriptomic analyses and validated key gene expression patterns with qPCR. Together, these approaches allowed us to characterize both the phenotypic and molecular basis of this cooperative interaction.

7 Results

The goal of this work was to identify the role of basidiomycete yeasts in complex leaf microbial communities. Primary network analysis revealed a negative association between the plant pathogen *Albugo laibachii* and basidiomycete yeasts such as *Moesziomyces bullatus* (MbA) and *Cystofilobasidium*, supporting the role of these yeasts in structuring microbial community composition. Yeast isolation from natural *Arabidopsis thaliana* populations around Tübingen uncovered a consistent co-occurrence of *Cystofilobasidium* species with a *Pseudomonas extremaustralis* strain (subsequently referred to as B2). This interaction exhibited antimicrobial activity against specific leaf-associated bacteria and raised the hypothesis that the yeast - bacterium pairing contributes to pathogen suppression through targeted microbial interactions. To investigate this, we employed co-culture assays and transcriptomic analyses to elucidate the mechanisms of inhibition and to characterize the molecular basis of the yeast – bacterium interaction.

7.1 Glycoside Hydrolases in *Cystofilobasidium*

For the basidiomycete *M. bullatus*, a known *A. laibachii* antagonist, the glycosidic hydrolase 25 (GH25) was identified as the causal enzyme for pathogen inhibition (Eitzen et al., 2021). The first question asked, was whether *Cystofilobasidium* uses the same mechanism to antagonize *A. laibachii*. Therefore, every publicly available *Cystofilobasidium* genome was analyzed for the presence of hydrolases of the family 25 (data provided by Daniel Gómez-Pérez). Pfam domain annotation was performed using InterPro Scan (V 5.73-104.0), and all domains containing a GH domain, a GH catalytic core, or clearly assigned to one of the GH families were identified across the seven publicly available *Cystofilobasidium* genomes (Table S1). The average number of hits per genome was then calculated to illustrate the distribution of GH domains within the genus (Fig. 1).

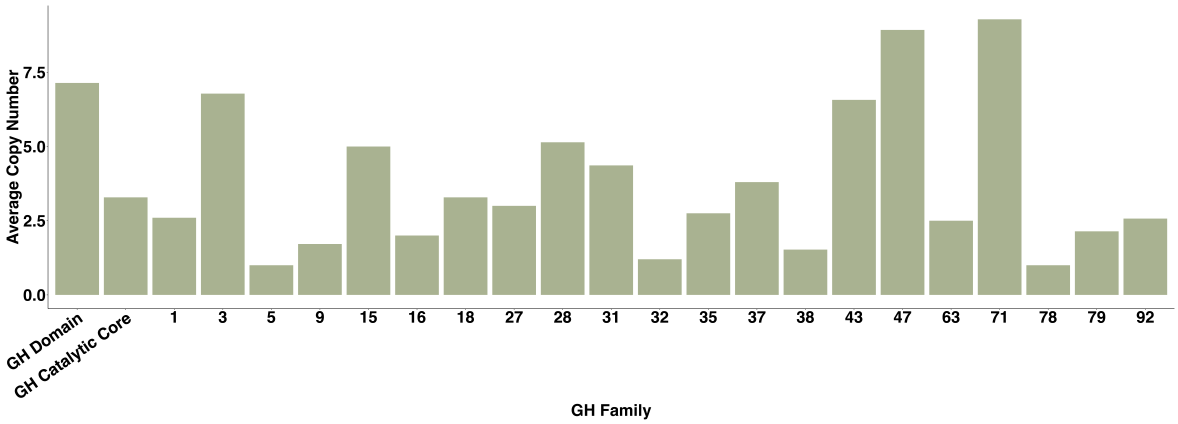

Figure 1: InterPro Scan analysis looking for Pfam domains belonging to GH families on all available *Cystofilobasidium* genomes. Number of hits was divided by the number of available genomes to get the average copy number over all available genomes. GenBank IDs for genomes used can be found in Table S1.

A wide range of GH families with varying average copy number, ranging from one for GH5 to 9.28 for GH20, was detectable, but no hint of a gene belonging to the family 25 was found in the tested *Cystofilobasidium* genomes. The results are corroborated by searching for the GH25 gene from *M. bullatus* in the genomes of the *Cystofilobasidium* yeasts used in this study. By using the local BLAST+ suite (V 2.15.0), no hit for GH25 was found in our genomes, as well as in the predicted genes list. This reinforces the hypothesis that the yeast uses a different method to reduce pathogen infection.

7.2 *Cystofilobasidium* Strain Collection and Phylogeny

In this study, five different yeast strains, isolated over several years through multiple isolation rounds, were used belonging to *Cystofilobasidium capitatum*, *C. macerans*, and *Tausonia pullulans*. To characterize our *Cystofilobasidium* yeasts and build a foundation for later downstream analysis, the genomes of the five yeasts were sequenced (Yeast 1, 2, 3 and 5 were previously sequenced by Vladislav Mokeev) and assembled. In total, three yeasts belonging to *C. macerans* (Yeast 1, 2 and 4), one belonging to *C. capitatum* (Yeast 3) and one yeast of the family Mrakiaceae *T. pullulans* (Yeast 5) add up to the used strain collection. Yeast 1, 2, 3 and 5 sequencing was performed using long-read PacBio and short-read Illumina, while Yeast 4 was done using our in-house Nanopore sequencing system (software: MinKNOW V 23.11.5). Genome assembly was done using the de-novo assembler Canu (V 2.2). Furthermore, AUGUSTUS (V 3.2.3) was used for gene prediction (Table 1).

Assembly statistic	Yeast 1	Yeast 2	Yeast 3	Yeast 4	Yeast 5
Species	*C. macerans*	*C. macerans*	*C. capitatum*	*C. macerans*	*T. pullulans*
Total assembly length (Mbp)	20.7	20.5	20.5	16.3	24.0
N50 contig (kbp)	1040.19	858.11	431.28	40.97	1235.02
Contigs	31	45	80	597	41
GC-content (%)	61.40	65.60	58.67	65.40	58.40
Percentage CDS (%)	61.96	66.30	64.34	65.00	56.18
Average gene size (bp)	2161.8	2230.1	2311.11	2076.77	2255.84
Average gene density (gene/kbp)	0.355	0.362	0.3541	0.3838	0.3239
Protein coding genes	7350	7411	7270	6255	7775
Exons	39864	38253	46085	30954	51899
Introns	32538	30858	38848	24928	44135
Introns/Exon	0.8162	0.8067	0.8430	0.8053	0.8504
Introns/Gene	4.4269	4.1638	5.3436	3.9853	5.6765
Average intron length (kbp)	0.7098	0.7071	0.5896	0.6160	0.6528
Percentage of bases in intergenic regions (%)	23.16	19.35	18.15	20.29	26.93

Table 1: Assembly statistic on the contig-level genome assemblies of *Cystofilobasidium macerans*, *Cystofilobasidium capitatum* and *Tausonia pullulans* (CDS - Coding sequence). Statistics acquired using QUAST (V 5.0.3) and R-packages rtracklayer (V 1.64.0), GenomicRanges (V 1.56.2), Biostrings (V 2.72.1), GenomeInfoDB (V 1.40.1), XVector (V 0.44.0), IRanges (V 2.38.1), S4Vector (V 0.42.1), BiocGenerics (V 0.50.0) and base (V 4.4.1).

Analyzing the assemblies, allowed us to identify key features of the *Cystofilobasidium* genomes. Total length was around 20 Mbp for all but one, as Yeast 4 only assembled up to 16.3 Mbp. Additionally, GC-content of the contig-level assemblies varied between 58.40% and 65.50%. The number of predicted protein coding genes was in the range of 7270 to 7775, with Yeast 4 being the outlier having only 6255 predicted genes, which is correlated to the smaller genome

size. The average gene size for all yeasts was around 2100 bp and therefore very similar. Furthermore, gene density analysis showed that all of them were around 0.35 genes per kbp. Adding to this, the percentage of nucleotides in CDS ranged from 56.18% for Yeast 5 to 66.30% for Yeast 2. Furthermore, the averag intron to exon ratio was 0.8 and the average number of introns per gene reached from 3.9 (Yeast 4) to 5.6 (Yeast 5). Bases in intergenic regions make up 18.15% (Yeast 3) to 26.93% (Yeast 5) of the total genome size. Together, these genome assemblies provide a comprehensive overview of the genetic features of the isolated *Cystofilobasidium* strains. Despite some variation, particularly in Yeast 4, the genomes were largely consistent in size, gene content, and structure.

7.2.1 Whole Genome Alignment of Yeast Assemblies

For comparison of the genomic similarity among the five yeast strains, pairwise genome alignments were performed using progressiveMauve (V snapshot 2015-02-25). The resulting distance matrix and alignment were used to generate both a heatmap of genomic distances and a phylogenetic tree, allowing visualization of divergence patterns and evolutionary relationships (Fig. 2).

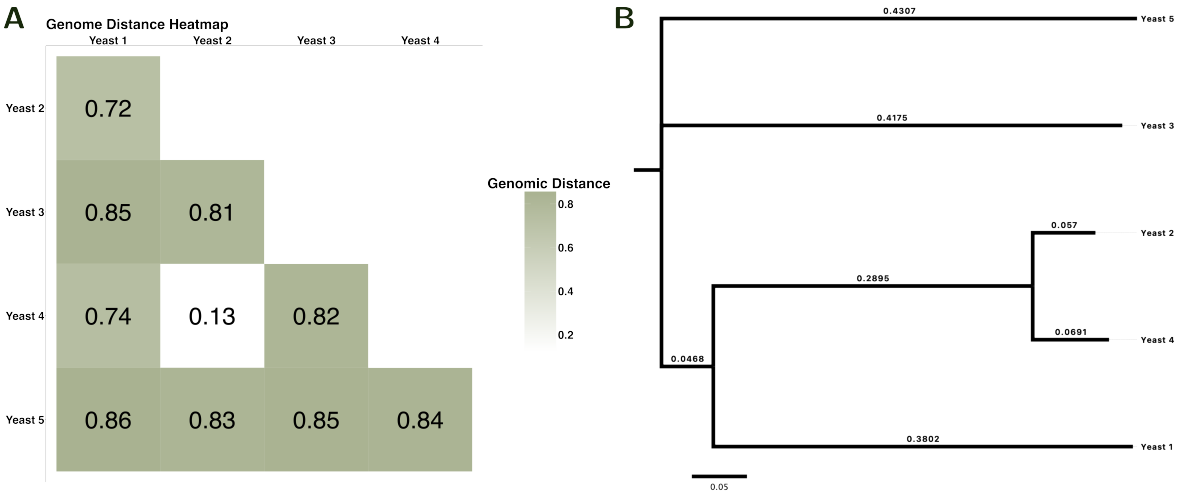

Figure 2: **A**: Heatmap visualizing pairwise genomic distances among Yeast 1–5, based on whole-genome alignment performed with progressiveMauve (V snapshot 2015-02-25). The resulting genomic distance matrix was computed from alignment outputs and visualized in R as a heatmap. Color intensity represents the degree of genomic divergence between strains. **B**: Phylogenetic tree created using progressiveMauve pairwise analysis and visualized with FigTree (V 1.4.4), where branch length corresponds to phylogenetic distance.

The heatmap revealed variation in genomic distance among the yeast strains (Fig. 2 A). The closest relationship was observed between Yeast 2 and Yeast 4 (distance = 0.126), displaying high genome similarity. In contrast, Yeast 1 and Yeast 5 showed the greatest divergence

(distance = 0.857), while Yeast 5 was consistently more distant from the others (average distance = 0.845) followed by Yeast 3 (average distance = 0.8325). The phylogenetic tree based on pairwise sequence alignment revealed the same pattern, with Yeast 5 being the furthest from the other yeasts, and Yeast 2 and 4 clustering the closest (Fig. 2 B).

7.2.2 Genes Tree Inference Supports Phylogenetic Consistency

Using OrthoFinder (V 3.0.1b1), a species tree was inferred to show the phylogenetic relationship between the isolated strains based on protein sequences. The analysis was performed on predicted gene models obtained from AUGUSTUS (V 3.2.3, –species=*Cryptococcus neoformans*) annotation of the individual genomes. Additionally, the genome sequences of *M. bullatus* (provided by the Doehlemann Lab, Universität zu Köln) and *Cryptococcus neoformans* (GenBank ID: GCA_035658335.1) were used as references in the species tree to show distances to related species. A rooted tree was created using the "Species Tree" results from OrthoFinder and visualized with FigTree (V 1.4.4) (Fig. 3).

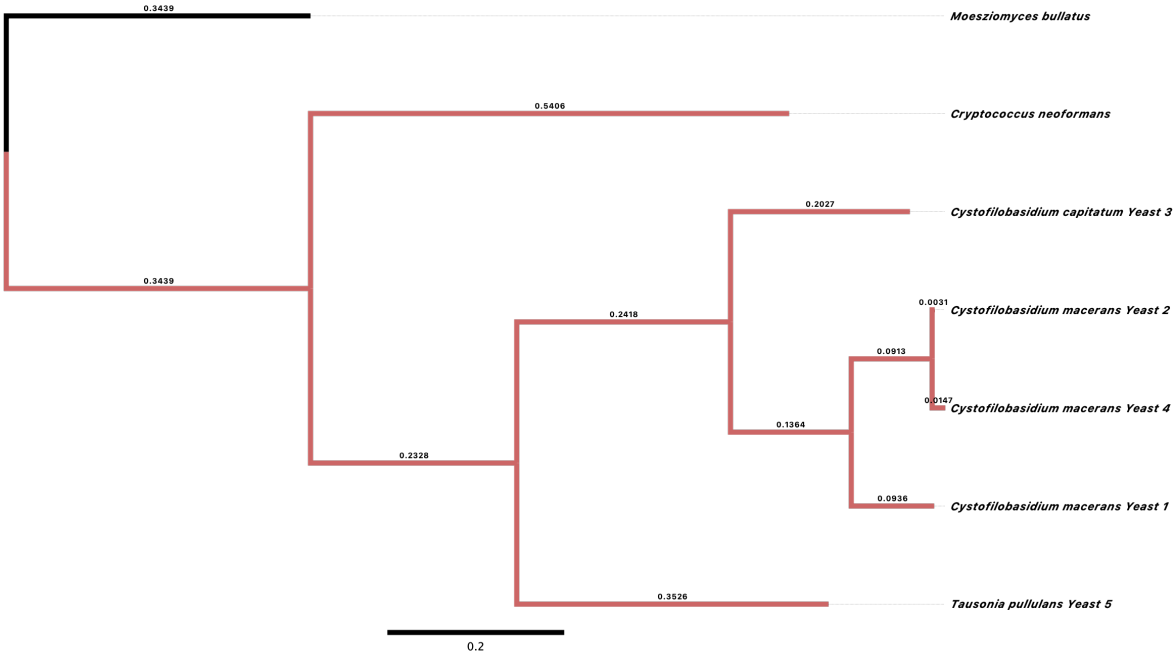

Figure 3: Phylogenetic distances between isolated *Cystofilobasidium* strains. The species tree was generated using OrthoFinder (v3.0.1b1) and visualized with FigTree (v1.4.4). Distances are indicated along the edges between nodes. *C. neoformans* and *M. bullatus* served as reference strains.

Yeast 2 and 4 are closely related to each other, while Yeast 1, which is also a *C. macerans*, clusters nearby. Together with Yeast 3, a *C. capitatum*, they form the monophyletic group for the genus *Cystofilobasidium*. The next closest related species is Yeast 5, a *T. pullulans*. They together form the family of Cystofilobasidiales. The yeast *Cryptococcus neoformans* is closer related to the *Cystofilobasidium* species than *M. bullatus*, which forms the overall outgroup in this tree as it belongs to the class of Ustilaginomycetes. The phylogenetic tree based on gene trees here reflected the same relationships between the yeasts previously obtained

from analysis of the genome assemblies alone (Fig. 2). This agreement between alignment-based and ortholog-based phylogenies supports the reliability of the observed clustering and reinforces the phylogenetic relations inferred from purely nucleotide sequence trees. The consistent clustering patterns highlight the close genetic relatedness of certain strains, while also confirming the distinct separation of others. These results further validate the evolutionary structure within the isolated *Cystofilobasidium* yeast collection.

7.3 Characterization of *Cystofilobasidium* - *Pseudomonas* Interactions

Building on the phylogenetic characterization of the isolated yeasts, we next investigated their interactions with co-isolated microorganisms. During the isolation process, several *Cystofilobasidium* yeasts were repeatedly found in association with bacterial partners. To better understand these interactions, we focused on strains where consistent bacterial co-isolation was observed. This led to the identification and further study of a bacterial partner closely associated with the newly isolated *Cystofilobasidium* strains.

7.3.1 Isolation of Novel *Cystofilobasidium* Revealed Bacterial Partner

Since neither the yeast nor the bacterium showed any signs of inhibited growth in each other's presence, we decided to investigate their relationship in more detail. 16S Sanger sequencing of the bacterial isolate identified it as a *Pseudomonas extremaustralis* strain. When the co-culture was grown on agar plates, an interesting phenotype emerged: the orange yeast formed a central colony while the opaque *Pseudomonas* grew around it. We termed this distinctive growth pattern the "fried-egg" phenotype (Fig. 4).

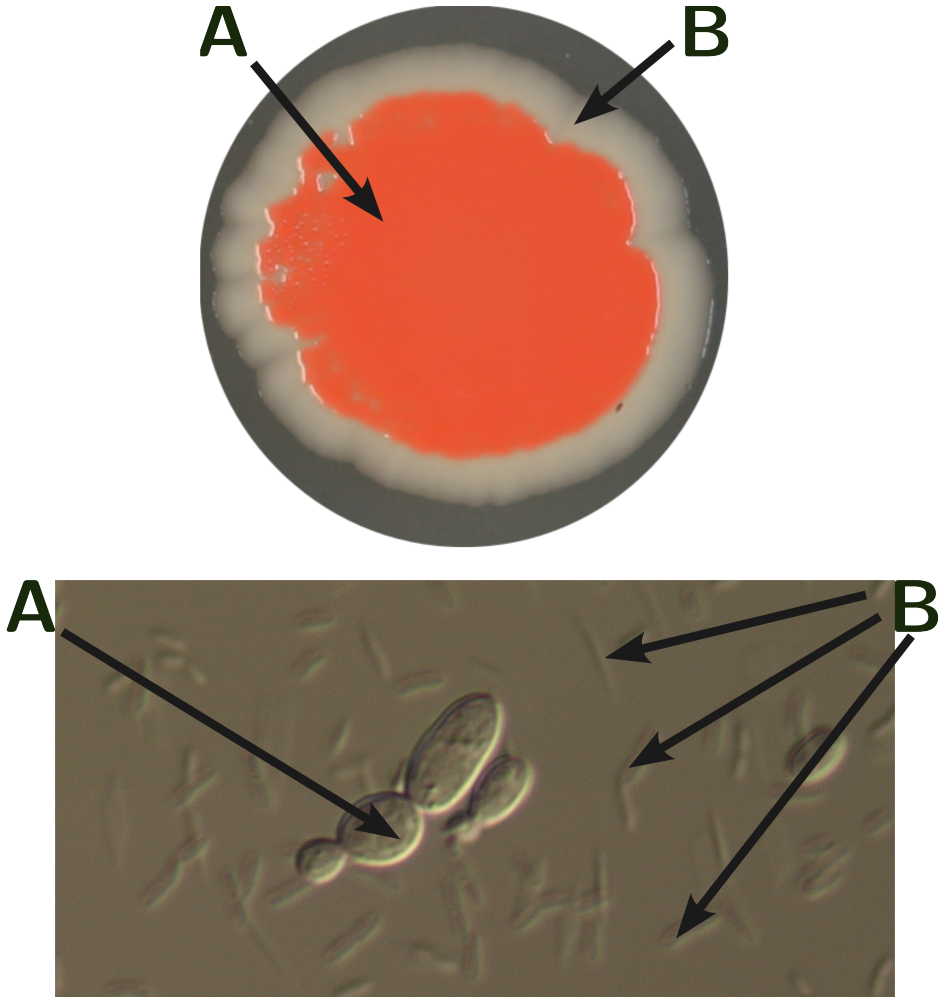

Figure 4: Top: Macroscopic image of 10 µl co-cultured *C. macerans* with *P. extremaustralis* in a 1:1 ratio (OD_{600} = 0.8) on a PDA agar plate. **Bottom**: Microscopic image of the same culture in liquid (before dropping on plate) at 400x magnification. **A** - *C. macerans* Yeast 1; **B** - *P. extremaustralis*.

Microscopic analysis revealed higher bacterial count compared to the yeast (Fig. 4 Bottom). Sometimes, aggregations of *P. extremaustralis* around *Cystofilobasidium* was observed displaying a close interaction. Additionally, when scraping cells off of the co-culture plate (Fig. 4 Top), in the "bacterial" as well as the "yeast" part both partners were observable, which re-

inforces the idea that they are living together and do not antagonize each other.

7.3.2 *A. thaliana* Microbial Network Analysis

The observed association between the isolated yeast and bacterium prompted the question, whether this phenotype is supported by the microbial correlation network analysis. Therefore, a correlation matrix was created from the *Arabidopsis thaliana* Tübingen sampling data over five years to display co-absence or co-presence of microbes belonging to bacteria, yeasts and oomycetes (data provided by Maryam Mahmoudi). The network incorporates only significant co-occurrences ($p - value \leq 0.05$). As we were interested in the interactions of the phyllosphere microbes, the microbial network was analyzed with a focus on bacteria, *Cystofilobasidium* yeasts and oomycete co-occurrences. The resulting network of positive (green) and negative (orange) relations between the corresponding operational taxonomic units (OTUs) revealed that there are two *Cystofilobasidium*, five oomycete and 1909 bacterial OTUs (Fig. 5).

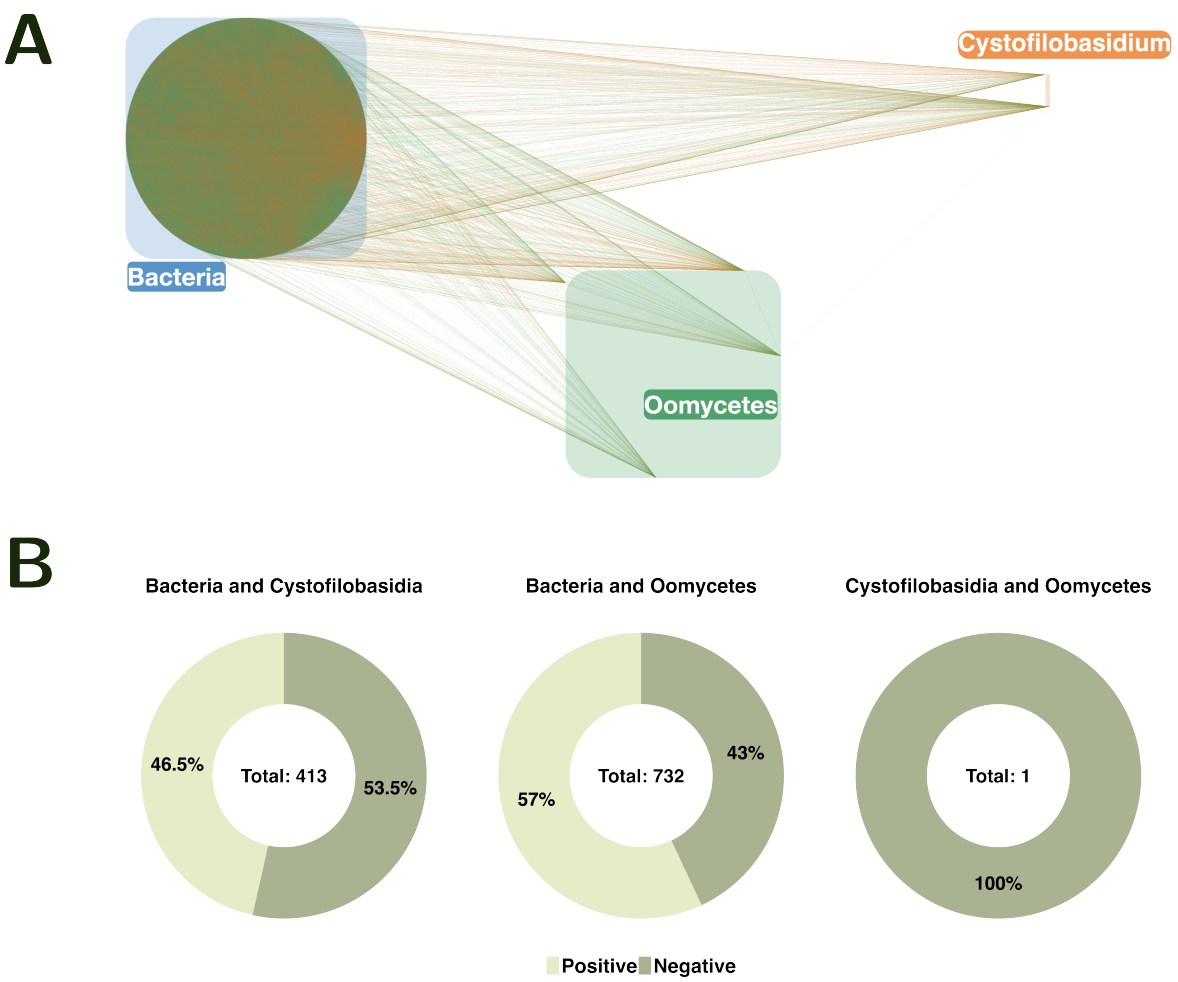

Figure 5: **A**: Network visualization generated in Cytoscape, illustrating co-occurrence relationships among bacterial, *Cystofilobasidium* yeast, and oomycete OTUs. The network was constructed using a matrix filtered at a significance threshold of $p \leq 0.05$ (data provided by Maryam Mahmoudi) and was subset to include only the three organism groups of interest. Green edges represent positive co-occurrences (co-presence), while orange edges indicate negative associations (co-absence). **B**: Pie plot summarizing the total number of co-occurrences between each group, with light green representing co-presence and dark green indicating co-absence as a percentage of the total.

When comparing their direct interactions, most happened between bacteria and oomycetes. Here, in total 732 co-occurrences were found with 57% being classified as co-presence and 43% as co-absence. The second most interactions appeared between bacteria and the yeasts, dominated by co-absence. 53.5% negative and 46.5% positive of a total of 413 correlations were present. The least amount of co-occurrence is reported between *Cystofilobasidium* and the oomycete group with a total of one co-absence (Fig. 5 B). As we were interested in the interaction between *P. extremaustralis* and the yeasts we dived deeper into the network. Therefore, a more detailed analysis looking into the network of *Pseudomonas*, *Cystofilobasidium* and oomycetes was conducted, resulting in a condensed sub-network and redistribution

of co-absence and co-presence interaction counts (Fig. 6).

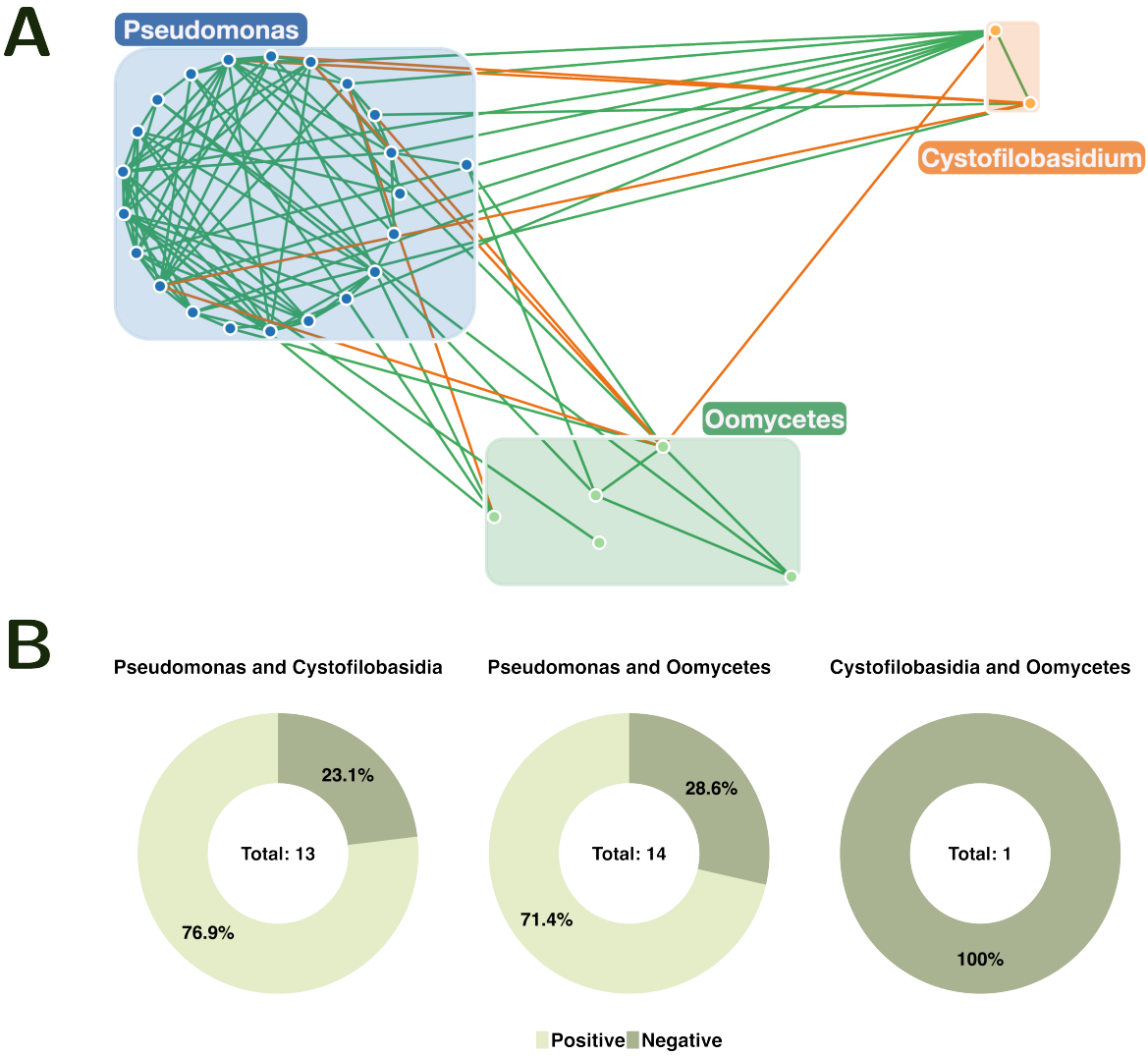

Figure 6: **A**: Network visualization created in Cytoscape, showing co-occurrence relationships specifically between *Pseudomonas* OTUs, *Cystofilobasidium* yeast, and oomycetes. The network was subset from the original co-occurrence matrix (threshold $p \leq 0.05$) to include only nodes associated with *Pseudomonas*. Green edges represent co-presence, and orange edges represent co-absence. **B**: Summary of total co-occurrences among the three groups, with light green indicating co-presence and dark green indicating co-absence, shown as a percentage of all interactions.

In comparison to the primary network (Fig. 5), the bacteria are further filtered to only show members of the genus *Pseudomonas*. The co-presence (green) and co-absence (orange) in the network was further analyzed (Fig. 6 B). *Pseudomonas* and *Cystofilobasidium* have a total of 13 interactions, with 76.9% of them being of positive nature while only 23.1% are negative. A similar trend is seen between *Pseudomonas* and the oomycete group, where 71.4% of the 14 total co-occurrences are co-presence and 28.6% are co-absence, which is in line with our observation of co-culturing the yeasts with our *Pseudomonas* isolate. The one co-

absence relation between oomycetes and the yeasts was still present. As previously reported, *Cystofilobasidium* was shown to inhibit the growth of the oomycete pathogen *A. laibachii*, with this effect being enhanced in the presence of a bacterial community (Kroll, 2018). Building on these findings, we next evaluated the antimicrobial activity of the *Cystofilobasidium* – *P. extremaustralis* co-culture against a leaf-associated bacterial community.

7.3.3 Assessment of Antimicrobial Activity

To assess antimicrobial activity, we tested the yeast isolates and *P. extremaustralis* both individually and in co-culture against a community of leaf-associated bacteria. The background microbes used in this assay were part of the core microbial community of *A. thaliana* and represented commonly encountered bacterial taxa. To determine whether the strains could inhibit the growth of these bacteria, cultures were spotted onto bacterial lawns, and the radius of the resulting inhibition zones was measured (Fig. 7).

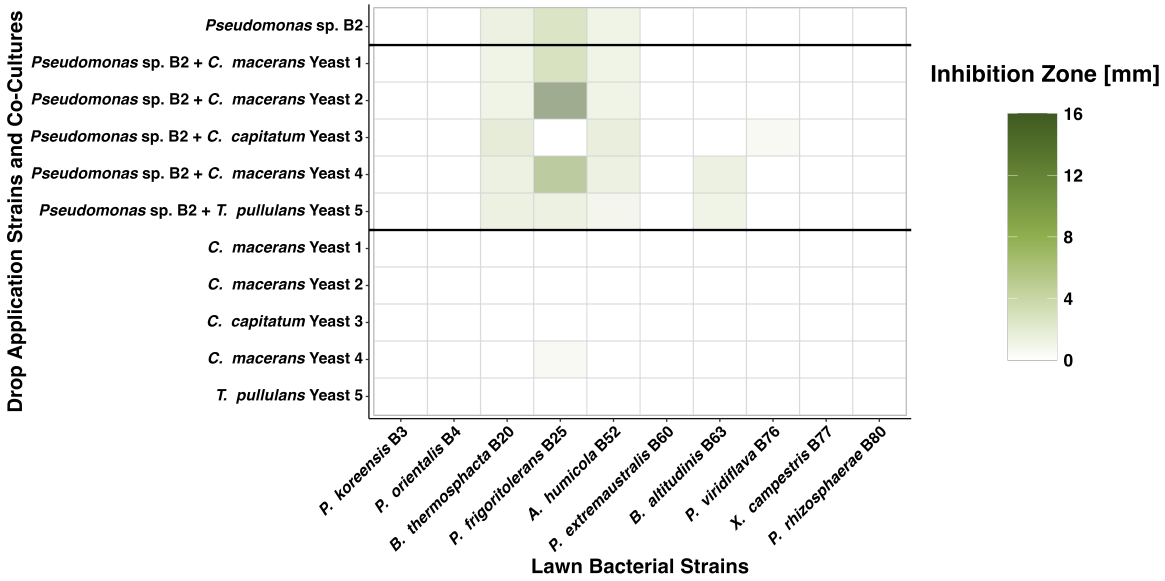

Figure 7: Heatmap illustrating the size of inhibition zones (in mm) formed by Yeast 1–5 (bottom section), B2 (top section), and their respective co-cultures (middle section) against various background bacterial strains shown along the x-axis. Color intensity corresponds to inhibition strength, with darker green shades indicating larger inhibition zones.

When confronting our lawn bacteria solely with the yeast single cultures only Yeast 4 showed a very small inhibition zone with 1 mm radius against *Peribacillus frigoritolerans*. *P. extremaustralis* single culture was able to effectively inhibit three bacteria, *Brochothrix thermosphacta*, *P. frigoritolerans* and *Arthrobacter humicola* with respective inhibition zones of 2.5

mm, 5 mm and 2 mm. Combining the different yeasts with *Pseudomonas* B2, the pattern for inhibition changed. First, the same bacteria previously inhibited by *P. extremaustralis* alone were also inhibited by the co-culture but with bigger inhibition zones. *B. thermosphacta* was inhibited mostly with the same strength, as only the combination with Yeast 3 showed a 40% bigger zone, while the others stayed at around 2.5 mm. Co-culturing had the biggest impact on *P. frigoritolerans*. Here, the 2.5 mm inhibition zone of B2 alone stayed the same for the combination with Yeast 4 but crucially increased for Yeast 1 to 120% and 4-fold for Yeast 4. The biggest change happened with Yeast 2, which displayed a 6.4-fold increase in inhibition zone compared to B2 single culture. Inhibition of *A. humicola* only showed one slight increase and one slight decrease. Yeast 1 and 2 together with B2 stayed at 2 mm, whereas Yeast 4 and Yeast 3 increased to 2.5 mm and 3.5 mm respectively. Only Yeast 5 with B2 displayed a 25% decrease in inhibition zone. Another interesting result was that for two lawn bacteria, where previously no inhibition in either single culture was found, the co-culture showed suppression. For *Bacillus altitudinis* inhibition using a combination of Yeast 4 or Yeast 5 with *P. extremaustralis* showed a 2.5 mm and 2 mm suppression radius respectively. *Pseudomonas viridiflava* on the other hand could only be antagonized by a Yeast 3 - B2 combination and showed an inhibition zone with a 1 mm radius. These findings highlight that the antimicrobial activity of the yeast – *P. extremaustralis* co-cultures often exceeded that of either partner alone, resulting in a synergistic effect in several combinations. Notably, certain interactions led to the emergence of inhibitory activity not observed in single cultures, pointing toward context-dependent enhancement of antimicrobial potential.

7.3.4 Biofilm Formation in Co-Cultures

Since antimicrobial activity is often linked to biofilm formation, we assessed biofilm production in single cultures of Yeast 1 and B2, as well as in their co-culture. To examine the influence of additional microbial interactions, three background lawn bacteria from the previous assay were included: *P. frigoritolerans* (B25), *A. humicola* (B52), and *P. extremaustralis* (B60). Biofilm formation was evaluated using a crystal violet staining assay, with absorbance measured at OD_{595} (Fig. 8).

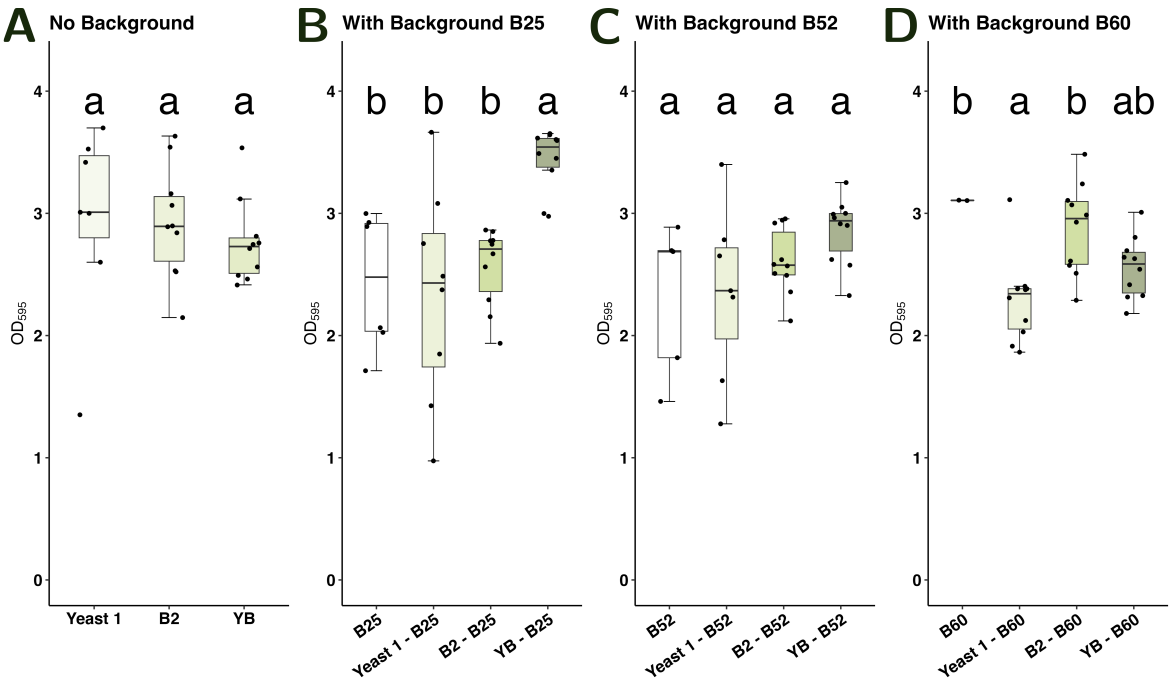

Figure 8: Biofilm formation measured as OD_{595}, with higher values indicating increased biofilm production. **A**: Single cultures of Yeast 1 and B2 along with the Yeast 1–B2 co-culture (YB), without any background bacterium. **B**: Biofilm formation of background control B25, Yeast 1, B2, and YB in the presence of the background bacterium B25. **C**: Biofilm formation of background control B52, Yeast 1, B2, and YB with B52 as background. **D**: Biofilm formation of background control B60, Yeast 1, B2, and YB with B60 as background. Statistical analysis was performed separately for each group (A–D) using a Benjamini–Hochberg adjusted Dunn's Test ($p - value \leq 0.05$) to identify significant differences between conditions.

Single culture controls revealed that B60 exhibited the highest average OD_{595} at 3.11, followed by Yeast 1 at 2.94 (Fig. 8 D and A). The co-culture of Yeast 1 and B2 showed a lower OD_{595} compared to the B2 single culture, with values of 2.76 and 2.92, respectively. The lowest OD_{595} readings were observed for B25 and B52, measuring 2.44 and 2.31 (Fig. 8 B, C). In contrast to the controls, the single cultures of Yeast 1 and B2 displayed reduced, yet not significant ($p - value \geq 0.05$), biofilm formation, with average OD_{595} values of 2.33 and 2.56 respectively when co-inoculated with the background bacterium B25 (Fig. 8 B). However, the co-culture of Yeast 1 and B2 showed significantly higher OD_{595} compared to each single culture with B25 added ($p - value \leq 0.05$). Similarly, biofilm formation with the lawn bacterium B52 did not exhibit statistically significant differences between the samples ($p - value \geq 0.05$). Nevertheless, a trend was observed, with Yeast 1 displaying the lowest OD_{595} at 2.35, followed by B2 at 2.61, while the highest value of 2.86 was seen in the co-culture (Fig. 8 C). Compared to the controls both the yeast and bacterium single cultures demonstrated reduced biofilm formation (2.94 to 2.35 and 2.92 to 2.61, $p - value \geq 0.05$),

whereas the combination culture showed an increase in biofilm formation with the B52 background (2.76 to 2.86, $p - value \geq 0.05$) (Fig. 8 A & C). Differences were also detected with the background bacterium B60. Here, the Yeast 1 and B60 combination exhibited the lowest overall OD_{595} recorded across all samples, at 2.29 (Fig. 8 D), which was significantly lower than the Yeast 1 control ($p - value \leq 0.05$). However, when B2 was combined with B60, the OD_{595} significantly increased to 2.56 compared to the Yeast 1 single culture in combination with the background ($p - value \leq 0.05$). Overall, these results indicated that biofilm formation is influenced by both the presence of background bacteria and the interaction between yeast and bacterial partners. While single cultures showed reduced biofilm production in the presence of additional microbes, co-cultures of Yeast 1 and B2 frequently maintained or enhanced biofilm formation. This showed a synergistic effect between the yeast and bacterial partners when in contact with the B25 or B52 background bacteria and highlighted the dynamic nature of biofilm development in multi-species communities.

7.4 *Cystofilobasidium macerans* Transcriptome Analysis

Genes associated with the phenotype observed in the *Cystofilobasidium* - *P. extremaustralis* interaction were investigated and characterized through a comprehensive transcriptome analysis of the yeast partner. To achieve this, mRNA was extracted from both single and co-culture conditions to capture transcriptional changes resulting from the interaction. The extracted mRNA was subsequently sequenced, generating high-quality transcriptome data for each condition. Differential gene expression analysis was then performed to identify genes that were uniquely upregulated or downregulated in response to the co-culture environment compared to the single culture control (Fig. 9). This approach aimed to pinpoint candidate genes potentially involved in mediating the observed phenotype and antimicrobial activity, providing insights into the molecular mechanisms underlying the yeast - bacterium interaction.

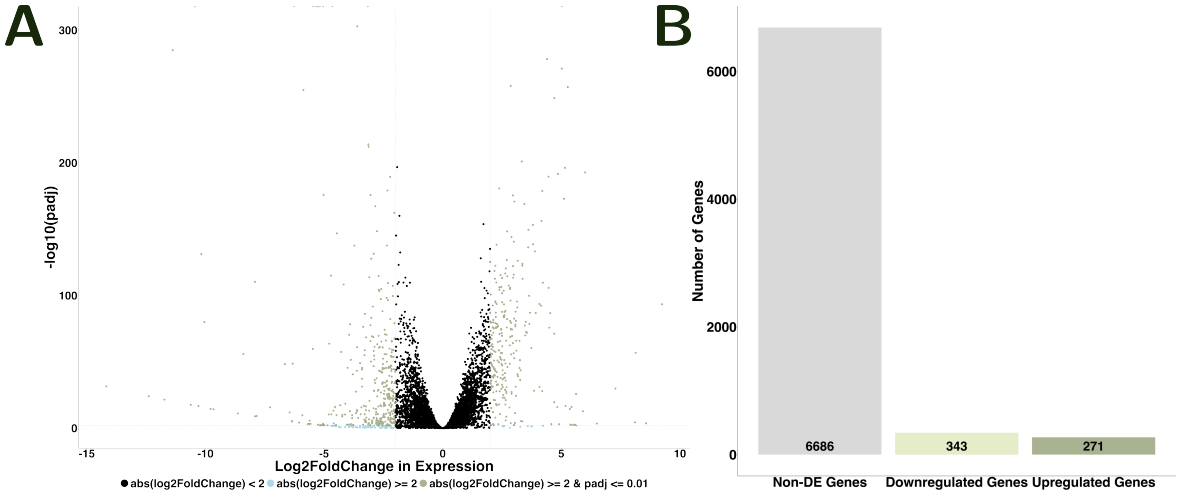

Figure 9: **A**: Volcano plot of differentially expressed genes $-log10(padj)$ plotted against log2FC in expression of yeast mRNA sequencing co-culture compared to single culture. Black: $abs(log2FC) \leq 2$, Lightblue: $abs(log2FC) \geq 2$ & $padj \geq 0.01$, Green: $abs(log2FC) \geq 2$ & $padj \leq 0.01$. **B**: Pie chart showing the percentage of genes being non-differentially expressed (DE; grey), downregulated (darkgreen) and upregulated (upregulated). Plots created from aligned mRNA sequencing reads to assembled Yeast 1 genome, created using HISAT2 (V 2.2.1), reads mapped with R-package Rsubread (V 2.16.1) and differential expression was calculated with DESeq2 (V 1.46.0) using a Wald test for statistical analysis ($p - value \leq 0.01$).

The distribution of genes based on their log2-FoldChange (log2FC) and adjusted p-value (padj) showed three main categories: genes with an absolute log2FC less than 2, genes with a log2FC greater than 2 but a padj greater than 0.01, and genes with a log2FC greater than 2 and a padj below 0.01, the latter representing the differentially expressed genes (Fig. 9 A). Of the 7350 genes analyzed, 91.6% were non-differentially expressed, 4.7% were downregulated,

and 3.7% were upregulated in co-cultures compared to the yeast single culture (Fig. 9 B).

7.4.1 GO-Term Enrichment Analysis

The subsequent step in analyzing the yeast transcriptome involved performing a comprehensive gene ontology (GO) search to gain functional insights into the mRNA sequencing data. For this purpose, all genes were annotated using InterProScan (V 5.73) in conjunction with the InterPro database, generating GO indices that facilitated downstream analysis. The top ten significantly enriched GO terms associated with upregulated and downregulated genes were identified ($p-value \leq 0.01$) through a topGO (V 2.58.0) analysis, providing an overview of enriched biological processes (Fig. 10).

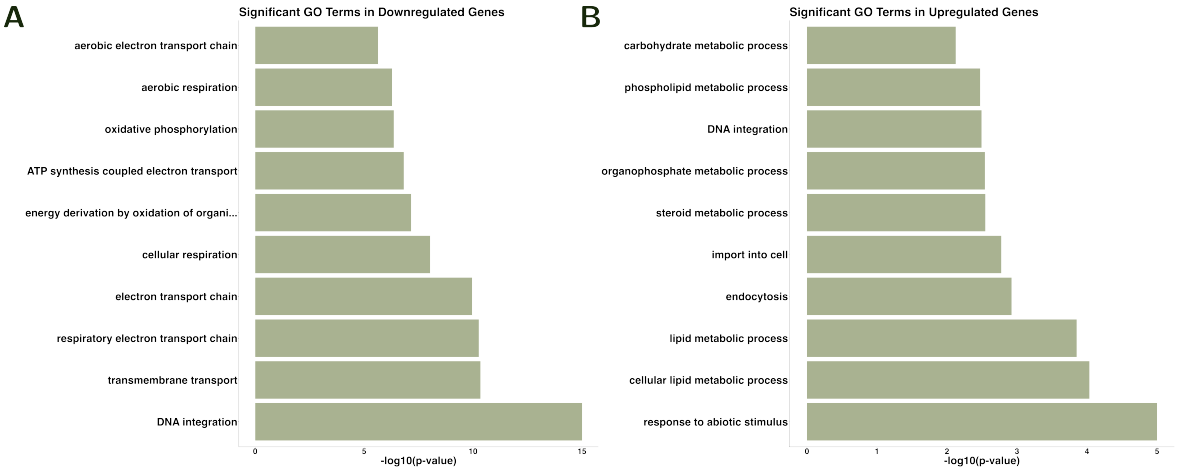

Figure 10: Analysis of GO terms in regards to significant representation within the InterProScan (V 5.73) dataset on transcriptome data (Fisher's Exact Test; $p - value \leq 0.01$) using R-package topGO (V 2.58.0). **A**: Top ten significant GO terms of downregulated genes (sorted by Fisher's Exact Test $-log10(p - value)$ in ascending order). **B**: Top ten significant GO terms of upregulated genes (sorted by Fisher's Exact Test $-log10(p - value)$ in ascending order)

Summarizing the results of the top ten GO terms for downregulated genes, it is evident that the most significantly downregulated biological processes primarily involved energy production, respiratory mechanisms, and transmembrane transport ($p - value \leq 0.01$). The most enriched GO term is DNA integration, with a $-log10(p - value)$ of 15, exceeding transmembrane transport, which has a $-log10(p - value)$ of 10.35 (Fig. 10 A). In contrast, upregulated processes were predominantly associated with metabolic and cellular activities, particularly those related to carbohydrates, lipids, steroids, and organophosphates. Additionally, pathways linked to transport, such as endocytosis and import into cells were significantly enriched ($p - value \leq 0.01$). The most prominent response, however, was directed towards abiotic

stimuli, as shown by a $-log10(p - value)$ of 5, the highest value among the upregulated processes (Fig. 10 B).

7.4.2 Signal Peptide Prediction

To investigate genes responsible for the interaction between *Cystofilobasidium* and *P. extremaustralis*, we looked into secretion signals present in the predicted gene models. To achieve this, we performed a secretion signal analysis using SignalP6 (V 6.0) to identify genes containing secretion signals within their sequences. By integrating this data with gene expression profiles, we present both the number of genes with secretion signals and their expression levels (Fig. 11).

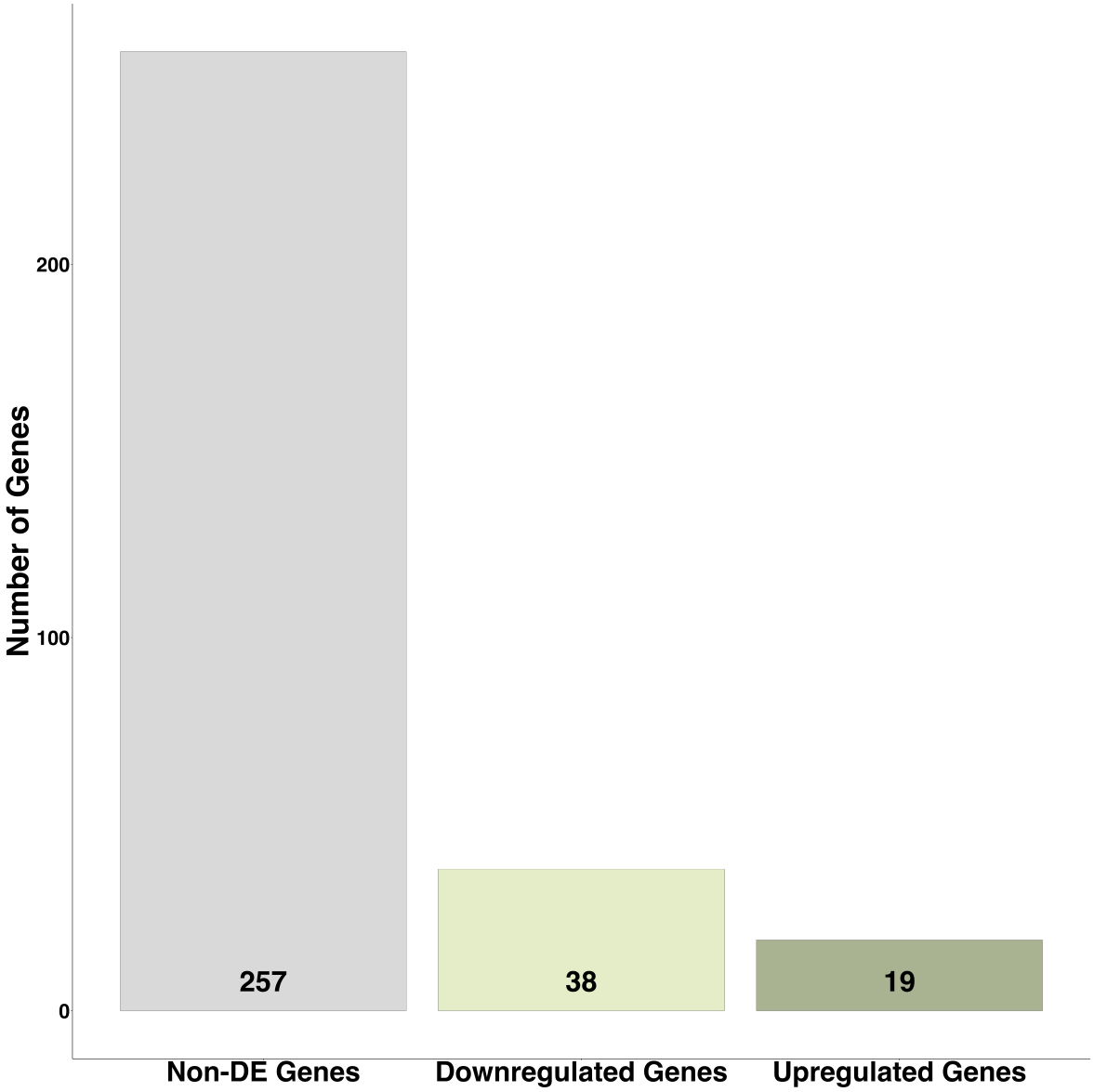

Figure 11: Number of genes with predicted secretion signal annotated using SignalP6 (V 6.0) grouped by either being non-differentially expressed, down- or upregulated. Prediction probability ≥ 0.5 is categorized as containing a secretion signal.

The figure presents the number of genes with a secretion signal predicted by SignalP6 categorized by their expression status. Out of the total identified genes, 257 were classified as non-differentially expressed, representing the largest group. In contrast, a smaller proportion of genes showed differential expression, with 38 genes being downregulated and 19 genes upregulated. This distribution highlights that while the majority of genes containing a secretion signal are not differentially expressed, a subset displayed altered expression levels.

7.4.3 Differential Expression Reveals Genes of Interest

Differential expression analysis provided a comprehensive overview of the expression patterns of the top 100 most differentially expressed genes identified through transcriptome analysis (Fig. 12). The genes were organized into clusters based on their expression profiles, with distinct patterns emerging between single and co-culture conditions. Notably, despite the high variability among these genes, only two exhibit consistent upregulation under co-culture conditions. The color gradient ranged from red to blue, where higher expression levels are represented by red shades, while downregulation is indicated by blue shades.

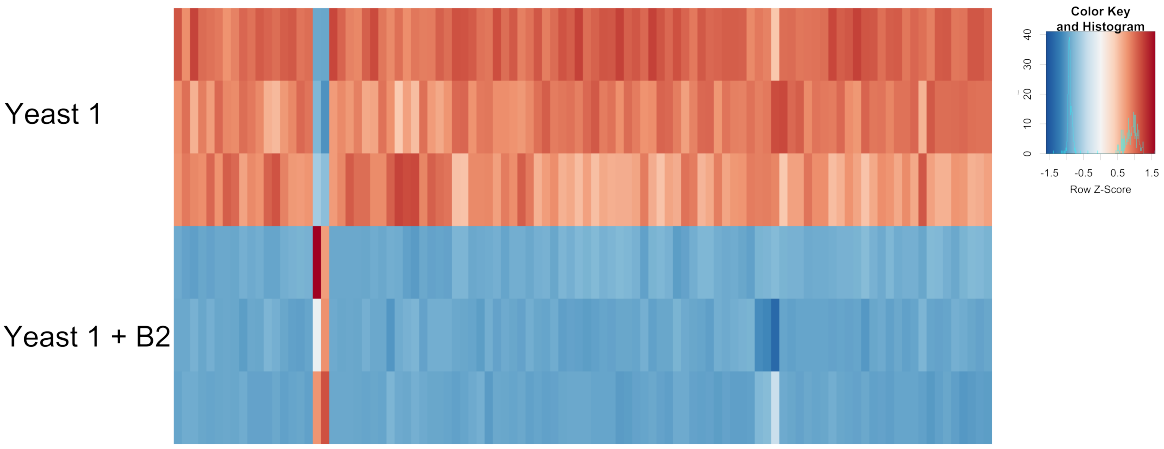

Figure 12: Heatmap displaying the top 100 most highly expressed genes from the RNA sequencing analysis comparing Yeast 1 single culture and the Yeast 1 – B2 co-culture. Differential expression was assessed using DESeq2, applying a Wald test with a significance threshold of $p - value \leq 0.01$. Expression levels are shown as row-wise Z-scores, with red indicating upregulation (higher expression) and blue indicating downregulation (lower expression). Of the 100 genes shown, 98 are upregulated in the single culture, while 2 genes show higher expression in the co-culture condition.

The observation that only two genes are consistently upregulated ($log2FC \geq 2$ and $padj \leq 0.01$) highlighted their importance in mediating the interaction between *Cystofilobasidium* and *P. extremaustralis*. This distinct expression pattern not only underscored their relevance but also showed a targeted response under co-culture conditions. Further investigation into

the functional roles of these genes provided valuable insights into the underlying mechanisms driving this interaction. Additionally, understanding how these genes influence or are influenced by the co-culture environment helped identify potential targets for enhancing beneficial microbial interactions or developing novel antimicrobial strategies.

To explore their potential functions, the two identified genes were labeled as g5886 and g4647. A preliminary analysis using BLASTP (V 2.16.1) against the non-redundant protein database was conducted to gain insight into their roles. The results revealed that g5886 is an ABC-transporter associated with multi-drug transport, while g4647 belongs to the carbohydrate-binding family 13. These findings provided a basis for further investigation into how these genes contribute to the observed phenotype under co-culture conditions.

7.4.4 Candidate Gene Expression Validation

To validate the differential expression of the two identified genes, g5886 and g4647, quantitative real-time PCR (qPCR) was performed using RNA extracted from liquid cultures grown under both single and co-culture conditions. This approach aimed to confirm the transcriptome analysis results and assess whether the observed upregulation of these genes is consistently reproducible under independent experimental conditions. Their expression levels were quantified against the reference gene elongation factor 1 (EF1-α). The qPCR results provide further insights into the expression patterns of g5886 and g4647 during the *Cystofilobasidium - P. extremaustralis* interaction (Fig. 13).

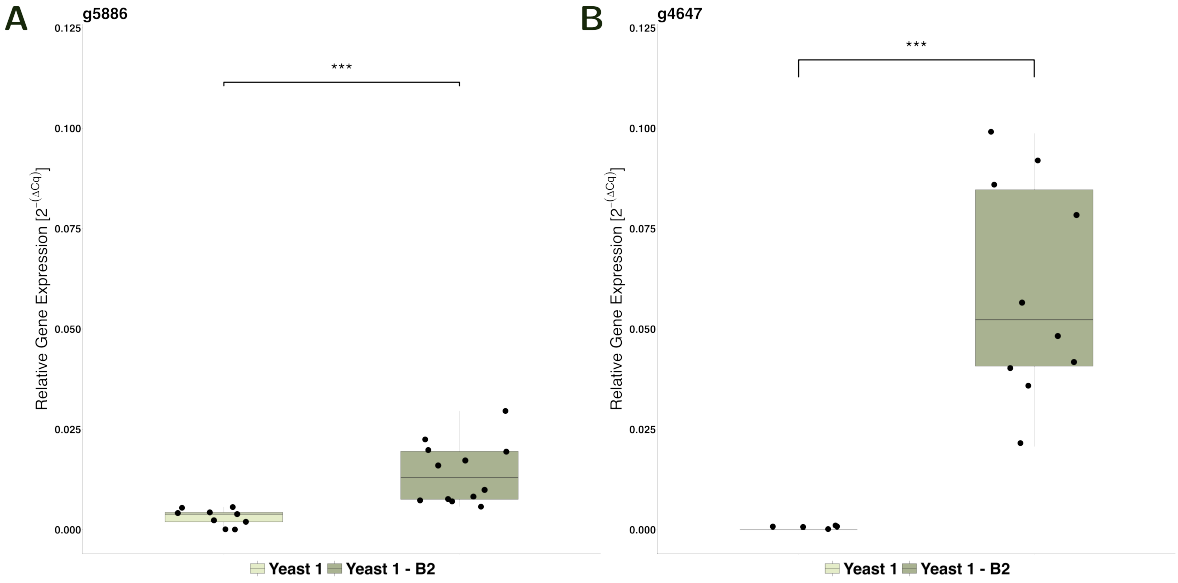

Figure 13: **A**: qPCR comparing g5886 expression to EF1-α shows significantly higher expression in co-culture (Bonferroni adjusted Wilcoxon Test $p-value \leq 0.001$). **B**: qPCR comparing g4647 expression to EF1-α shows significantly higher expression in co-culture (Bonferroni adjusted Wilcoxon Test $p-value \leq 0.001$)

As shown in the qPCR validation results, both genes, g5886 and g4647, exhibited significant upregulation when the yeast culture was co-inoculated with B2, with statistical significance confirmed by a Bonferroni-adjusted Wilcoxon Test ($p-value \leq 0.001$). Notably, the overall relative expression level of g4647 (Fig. 13B) was considerably higher compared to g5886 ($p-value \leq 0.001$, Fig. 13 A). These findings provide robust experimental validation of the transcriptome analysis performed previously, confirming that the differential expression observed was not an artifact of sequencing. The strong upregulation of these genes under co-culture conditions emphasized their relevance and supported their selection as targets for further functional characterization.

After validating the transcriptome analysis by qPCR using RNA extracted from liquid cultures, we sought to confirm the differential expression of g5886 and g4647 under conditions more representative of natural growth, since antimicrobial activity was observed during plate-based cultivation. To this end, RNA was extracted from cultures grown on agar plates either with or without background lawn bacteria, mimicking a more accurate representation of the natural interaction between the yeast and B2. Statistical significance was determined using a Benjamini-Hochberg-adjusted Dunn Test ($p - value \leq 0.05$), performed for each of the background bacteria B25 and B52 separately (Fig. 14).

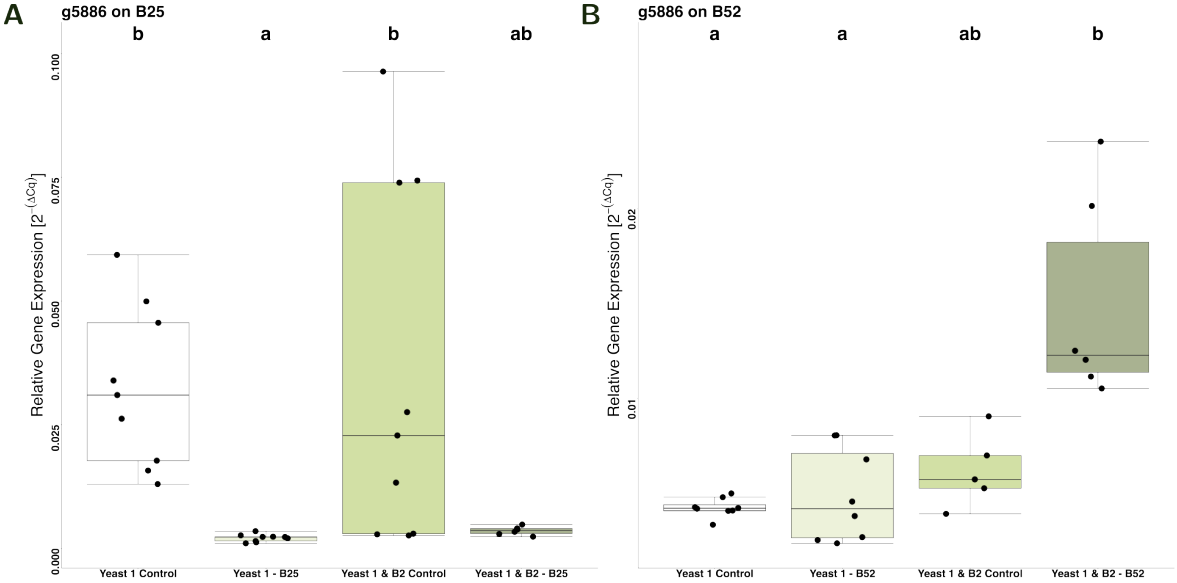

Figure 14: **A**: qPCR comparing g5886 expression in single culture, single culture with B25, co-culture with B2 and all three to EF1-α shows significant differences between groups (Benjamini-Hochberg adjusted Dunn's Test $p - value \leq 0.05$). **B**: qPCR comparing g5886 expression in single culture, single culture with B52, co-culture with B2 and all three to EF1-α shows significant differences between groups (Benjamini-Hochberg adjusted Dunn's Test $p - value \leq 0.05$).

For the B25 background, the Dunn Test grouped the samples as follows: Yeast 1 Control and Yeast 1 & B2 Control both displayed similar expression levels (grouped as "b", $p - value \geq 0.05$). In contrast, co-inoculation of Yeast 1 with B25 resulted in significantly lower expression (grouped as "a", $p - value \leq 0.05$). The combination of Yeast 1 & B2 with B25 exhibited an intermediate, but still low, expression level, classified as "ab" ($p - value \geq 0.05$). Under the B52 background, the Dunn Test revealed a different pattern. Both Yeast 1 Control and Yeast 1 - B52 displayed similar expression levels (grouped as "a", $p - value \geq 0.05$), while the Yeast 1 & B2 Control showed a moderately increased expression level (grouped as "ab", $p - value \geq 0.05$). The highest expression was observed in the co-inoculation of

Yeast 1 & B2 with B52, classified as "b" ($p - value \leq 0.05$). These results showed that the expression of g5886 was significantly influenced by the presence of B2, but its expression patterns were modulated differently depending on whether B25 or B52 was present as a background bacterium.

The qPCR validation results for g4647 under both B25 and B52 background conditions showed, identical to g5886, the expression differences in each background (Fig. 15). Analysis using a Benjamini-Hochberg-adjusted Dunn Test ($p-value \leq 0.05$), applied independently for each background bacterium, was used to identify statistically significant expression changes.

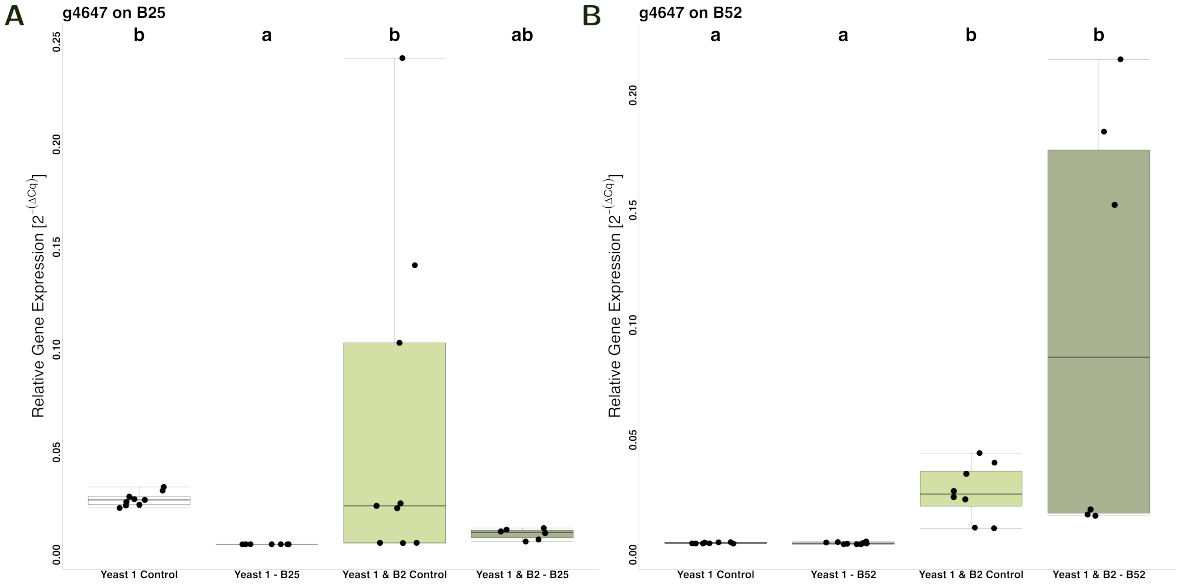

Figure 15: **A**: qPCR comparing g4647 expression in single culture, single culture with B25, co-culture with B2 and all three to EF1-α shows significant differences between groups (Benjamini-Hochberg adjusted Dunn's Test $p - value \leq 0.05$). **B**: qPCR comparing g4647 expression in single culture, single culture with B52, co-culture with B2 and all three to EF1-α shows significant differences between groups (Benjamini-Hochberg adjusted Dunn's Test $p - value \leq 0.05$).

Under the B25 background, Yeast 1 Control and Yeast 1 & B2 Control both exhibited relatively high expression levels (group "b", $p - value \geq 0.05$), while Yeast 1 - B25 showed a significant reduction (group "a", $p - value \leq 0.05$). Co-inoculation with B2 in the presence of B25 (Yeast 1 & B2 - B25) resulted in intermediate expression, classified as group "ab" ($p - value \geq 0.05$). This pattern showed a reduction in g4647 expression in the presence of B25 alone, with partial recovery when co-cultured with B2. In the B52 background, a different expression pattern was observed. Both Yeast 1 Control and Yeast 1 - B52 were grouped as "a", reflecting lower expression levels ($p - value \geq 0.05$). In contrast, both Yeast 1 & B2 Control and Yeast 1 & B2 - B52 were grouped as "b" ($p - value \leq 0.05$), indicating

significantly higher expression. While Yeast 1 & B2 - B52 showed a higher average than Yeast 1 & B2 Control, this difference was not statistically significant ($p - value \geq 0.05$). In summary, the qPCR validation experiments confirm that g5886 and g4647 were significantly and consistently upregulated in response to co-culture with B2, both in liquid and plate-based growth conditions. Moreover, the expression patterns of these genes were modulated by the presence and identity of background bacteria, with distinct responses observed under B25 and B52 conditions. These findings reinforced the reliability of the transcriptome data and underscored the roles of g5886 and g4647 in mediating yeast-bacteria interactions. Together, this evidence supported their selection as promising candidates for future functional studies aimed at uncovering molecular mechanisms underlying microbial interactions.

7.4.5 Gene Orthologs in Yeast 2 - 4

To asses the conservation of the two candidate genes identified through transcriptome and qPCR analysis, an orthology search was conducted using OrthoFinder (V 3.0.1b1) on the AUGUSTUS predicted gene models. This analysis aimed to determine whether the genes are conserved across our related yeast species or unique to the tested strain Yeast 1. The resulting tree was visualized with FigTree (V 1.4.4) and gives a comparative view of the phylogeny of the genes.

The gene tree for g5886 highlights the presence of similar transporter genes across all examined *Cystofilobasidium* yeast strains (Fig. 16). Notably, no homologs were detected in either *M. bullatus* or in the more closely related genus *Cryptococcus*. A second major cluster within the orthogroup consists of P-loop containing nucleoside triphosphate hydrolases, with at least one representative present in each of the tested yeast species. This group is positioned more distant on the tree, showing greater phylogenetic divergence from the clade containing g5886.

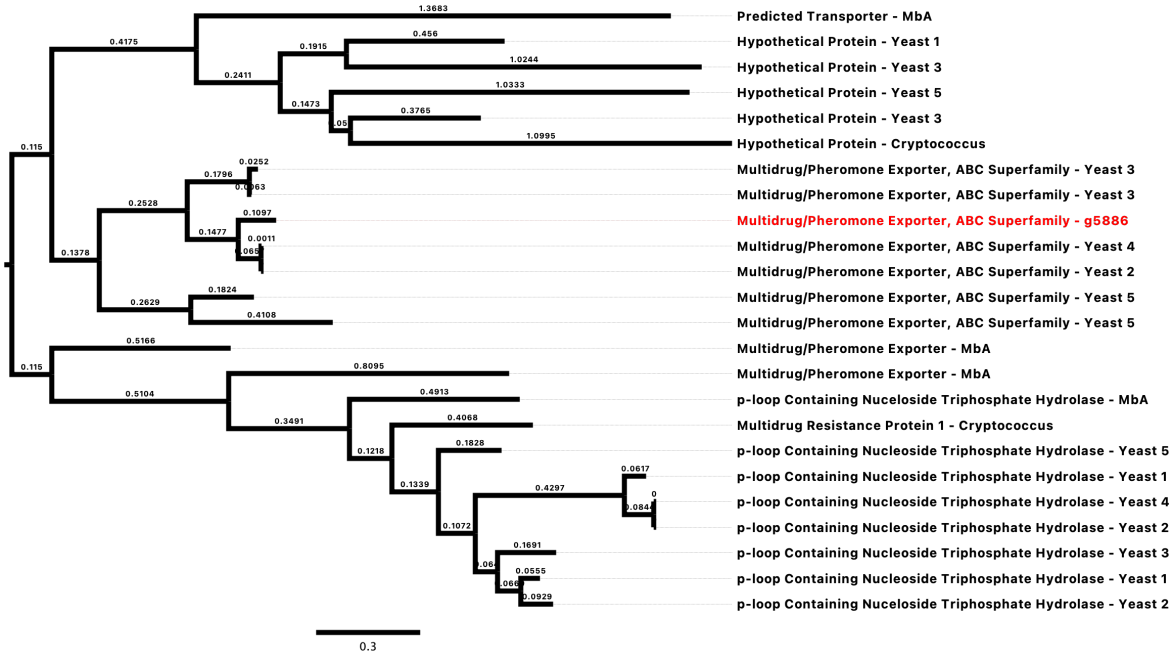

Figure 16: Phylogenetic tree of g5886 gene orthologs from Yeast 1–5, *M. bullatus*, and *Cryptococcus*, identified using OrthoFinder (V 3.0.1b1). The tree was constructed using maximum likelihood analysis and visualized with FigTree (V 1.4.4). Branch lengths indicate evolutionary distances, and numerical values represent branch support.

The orthogroup associated with g4647 was larger and displayed a more complex structure, clustering into several distinct subgroups. The monophyletic clade containing g4647 included only closely related genes from Yeast 1 and Yeast 2, displaying a strain-specific expansion.

Its sister group was associated with signal recognition functions. The largest portion of the orthogroup consisted of multiple subclusters containing genes classified as carbohydrate-binding proteins from family 13, which were functionally more closely related to g4647 than those in the signal recognition clade. Additionally, a distant outgroup included genes with Ricin B lectin domains, present in all yeasts except *M. bullatus* (Fig. 17).

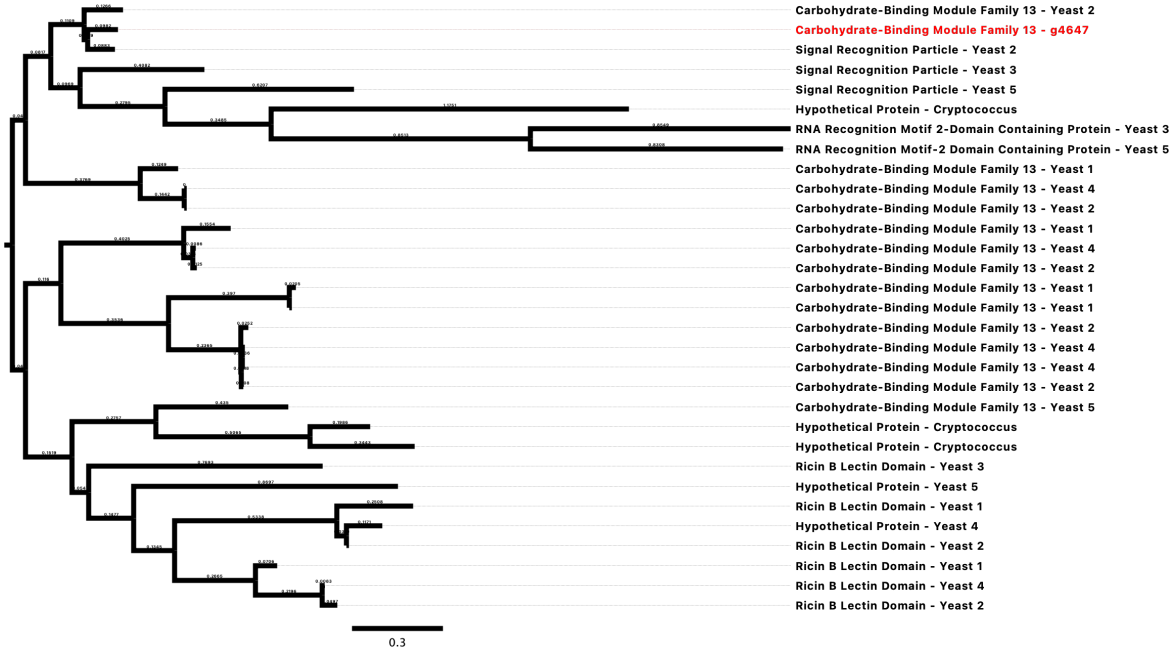

Figure 17: Phylogenetic tree of g4647 gene orthologs from Yeast 1–5, *M. bullatus*, and *Cryptococcus*, identified using OrthoFinder (V 3.0.1b1). The tree was constructed using maximum likelihood analysis and visualized with FigTree (V 1.4.4). Branch lengths indicate evolutionary distances, and numerical values represent branch support.

In summary, ortholog analysis using OrthoFinder combined with visualization in FigTree provided a comparative view of the evolutionary context of both g5886 and g4647. The resulting gene trees revealed distinct orthogroup structures and phylogenetic distributions for each candidate gene, offering insight into their conservation and lineage specificity across the analyzed yeast strains. These results complemented the expression data and served as a foundation for subsequent functional exploration of both genes in the context of the *Cystofilobasidium* - *P. extremaustralis* interaction.

7.4.6 The ABC-Transporter g5886

To gain further insight into the structural features of g5886, a predicted three-dimensional structure was generated using AlphaFold 3 (V 3). The resulting model was visualized in ChimeraX (V 1.9) and colored according to the transmembrane topology predicted by DeepTMHMM (V 1.0). Residue localization was assigned as follows: magenta for intracellular, red for transmembrane, and blue for extracellular regions. This integrative approach enabled the visualization of predicted membrane-spanning segments within the protein's structural context. The AlphaFold model and the corresponding posterior probability plot provided a comprehensive view of the membrane-associated topology of the predicted transporter (Fig. 18).

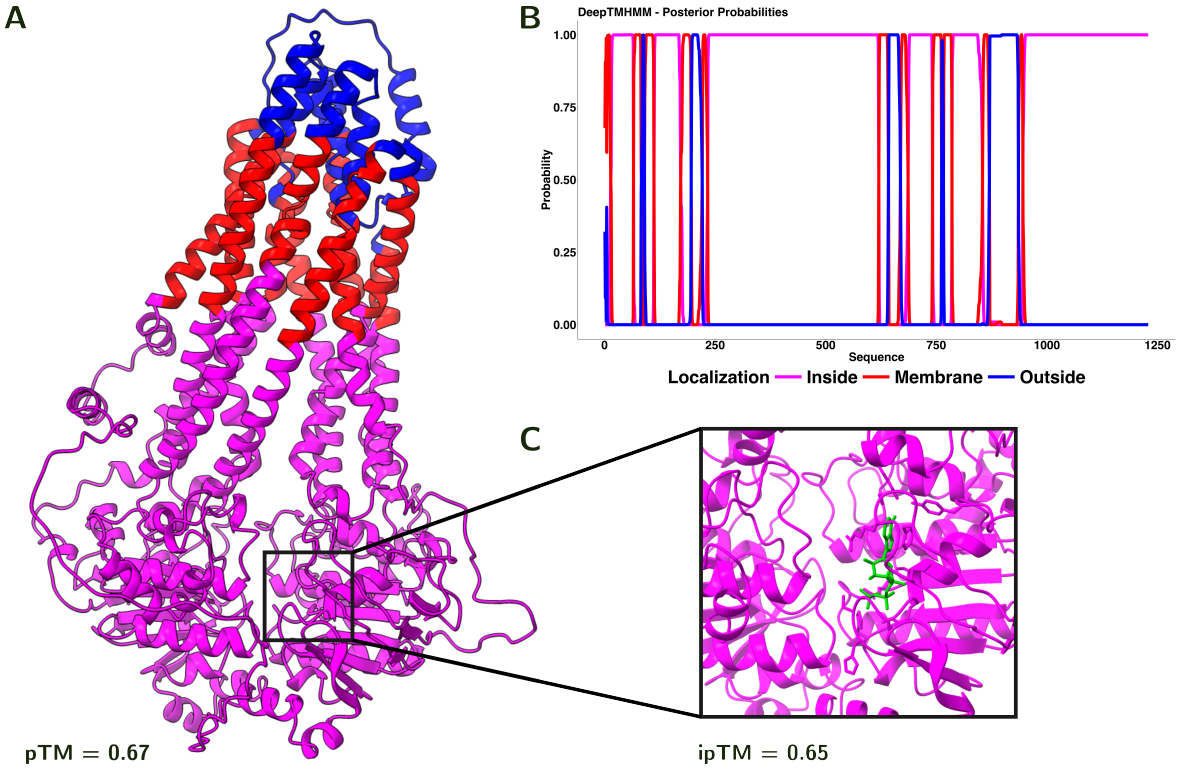

Figure 18: **A**: AlphaFold 3-predicted 3D structure of g5886, visualized in ChimeraX and colored by localization based on DeepTMHMM predictions: magenta indicates intracellular regions, red marks transmembrane helices, and blue highlights extracellular regions. **B**: Posterior probability plot generated by DeepTMHMM showing residue-wise probabilities for intracellular (magenta), membrane (red), and extracellular (blue) localization along the protein sequence. Peaks in red correspond to predicted transmembrane segments, aligned with the helical regions observed in A. **C**: AlphaFold 3 prediction of the ATP binding site (ATP - green) on the intracellular side (magenta). ipTM score = 0.65, pTM score = 0.67.

The DeepTMHMM prediction identified multiple high-confidence transmembrane helices, which aligned well with the AlphaFold structure model (pTM score = 0.67), where membrane-spanning regions were clearly resolved as helical segments embedded within the protein. The

consistent localization of extracellular and intracellular domains further supports the structural model's reliability and that g5886 encoded a membrane-associated transporter. Additionally, AlphaFold 3 predicted an ATP-binding interaction with an ipTM score of 0.65, further supporting the functional relevance of the structural model (Fig. 18 C).

8 Discussion

Plants are exposed to a wide array of stresses throughout their growing season, ranging from abiotic and ecological challenges to biotic stressors like pathogenic organisms. In response, plants employ various adaptive strategies, including transcriptomic adjustments and evolutionary changes (Yokoi et al., 2002, Lasky et al., 2014, Kover and Schaal, 2002). Additionally, they host diverse microbial communities that contribute significantly to their ability to adapt to environmental pressures and defend against pathogens (Newton et al., 2010). The collective system formed by a plant host and its associated microbial partners is referred to as the "holobiont" (Cavalier-Smith, 1992, Simon et al., 2019). Investigating the interactions between microbes, the plant, and other microbial community members reveals numerous insights into how these relationships can either support mutual growth and coexistence or result in antagonistic effects (Newton et al., 2010, Eitzen et al., 2021). A well-studied example of a complex interaction network is the triad involving *Arabidopsis thaliana*, the obligate biotrophic oomycete pathogen *Albugo laibachii*, and the surrounding microbial community. Previous research has demonstrated that *Albugo* infection can be strongly modulated by other microbes: while *Dioszegia hungarica* enhances infection rates, both *Moesziomyces bullatus* (subsequently MbA) and *Cystofilobasidium* have been shown to reduce the number of infected leaves following pathogen exposure (Kroll, 2018). Notably, one key discovery was that *Albugo* relies on a functional bacterial community to successfully colonize the host (Kroll, 2018). In this study, the focus was placed on natural *Cystofilobasidium* yeast isolates and their role in indirectly inhibiting *A. laibachii*. We identified a close interaction of the yeast with a bacterial member of the *A. thaliana* phyllosphere, *Pseudomonas extremaustralis*, which in competition assays displayed increased antimicrobial activity. Furthermore, a transcriptomic based strategy was utilized to unveil yeast genes involved in the interaction. The findings highlight their potential importance in plant defense and suggest novel avenues for managing plant disease through microbiome-based approaches.

8.1 Functional Diversity and Phylogeny of *Cystofilobasidium* Yeasts

The obligate biotrophic oomycete *Albugo laibachii*, the causal agent of the white rust disease, is a pivotal member of the *A. thaliana* phyllosphere microbiome (Agler et al., 2016). It often acts as a "hub" microbe that drastically reduces microbial diversity on infected leaves (Agler et al., 2016). *A. laibachii* presence restructures the leaf microbiome and has earned it the designation of a community "keystone" taxon (Almario et al., 2022). This means that targeting *Albugo* can have cascading, cross-kingdom effects on other microbes. In fact, the identification of such a hub pathogen opened new entry points for targeted disease control, since the disruption of a hub microbe has widespread effects on the community as a whole (Agler et al., 2016). In the case of *A. laibachii*, finding novel ways to inhibit this pathogen is particularly valuable not only for protecting the plant host but also to extrapolate findings in the model system to crop plants and making them more disease resilient. Traditionally chemical control agents are used for pathogen control, which carry high ecological side effects, usually impacting not only the targeted disease but the entire microbial community and the environment (Goulson, 2014, World Health Organization, 1990). Therefore, leveraging naturally antagonistic microbes has emerged as an alternative way that promises to be safer and more sustainable in the future. Targeting *A. laibachii* via its commensal antagonists represents a promising strategy to mitigate the pathogen's effect on plant health and microbiome structure.

A prominent example of a microbial antagonist against *Albugo* is the epiphytic yeast *M. bullatus*, which naturally occurs on *Arabidopsis* leaves. MbA has been shown to significantly reduce pathogen infection on the leaf, acting as an antagonistic member of the community (Eitzen et al., 2021). Recent work has elucidated the mechanism of this antagonism: *M. bullatus* secretes a glycoside hydrolase family 25 (GH25) enzyme with lysozyme activity that directly targets *A. laibachii* (Eitzen et al., 2021). Transcriptomic analyses identified this GH25 hydrolase as a key effector induced during MbA - *Albugo* interactions, and genetic experiments confirmed its importance. Deletion of the GH25-encoding gene in *M. bullatus* abolishes the yeast's ability to suppress the oomycete, demonstrating that the loss of this single enzyme removes its antagonistic effect (Eitzen et al., 2021). Notably, the purified protein alone strongly inhibits *A. laibachii* infection on host leaves, which indicates that the enzyme is both necessary and sufficient to show biocontrol activity. GH25 likely is a lytic

transglycosylase that degrades critical components of the oomycete's cell wall, thereby slowly killing the pathogen. This finding highlights how individual commensal microbes can be leveraged to combat disease.

Given their potent effect on *A. laibachii* infection, it was striking to find no GH25 homologs or other glycoside hydrolases of the family 25 in any of the five tested *Cystofilobasidium* strains. One reason for the absence of GH25 might be its phylogenetic context. Construction of a phylogeny based on OrthoFinder results proved that Yeast 1 - 5 grouped on a different branch than *Moesziomyces* and even farther than *Cryptococcus*, a human pathogen. It appears that the GH25 lysozyme-based antagonism was either retained or gained by *M. bullatus* and is absent in the Tremellomycetes, which include *Cystofilobasidium*, *Tausonia* and *Cryptococcus*. The lack of GH25 genes in these closely related yeasts suggests that the GH25-mediated pathogen suppression is not ubiquitous among phyllosphere yeasts, but rather confined to specific groups. Notably, *Moesziomyces* is related to plant pathogenic smut fungi, such as the Ustilaginaceae smut *Ustilago maydis*, which are known for their antimicrobial enzymes, whereas *Cystofilobasidium* and *Tausonia* belong to a different branch of basidiomycete yeasts (Cortes-Sánchez Alejandro, 2011). If these yeasts antagonize *A. laibachii*, they must do so without usage of the GH25 lysozyme, which is an opportunity to uncover alternative pathogen inhibition mechanisms. In fact, microbe-microbe interactions in natural populations don't occur in a binary manner but in a community context.

Recent research into the impact of *M. bullatus*'s GH25 on the microbiome revealed that the lysozyme does have an active role in shaping the leaf bacterial community elevating the previous findings of a tripartite inter-kingdom interactome (Sorger et al., 2025). In conjunction with the findings regarding *M. bullatus* and its lysozyme effector, previously unpublished preliminary studies performed by us (in collaboration with the Doehlemann Lab, Cologne) revealed an interesting fact. In leaf infection assays, the *A. laibachii* infection rate was significantly increased with the addition of a bacterial community, which overall had no additional significant impact on the disease suppression of *M. bullatus*. If the added bacteria have a positive impact on pathogen infection, one might assume they can at least protect the pathogen and maybe even rescue it from negative interactors. Strikingly though, *Cystofilobasidium* was able to reduce disease symptoms even further with the addition of these microbes, which lead us to hypothesize that these yeasts can utilize the bacterial community

in a way to suppress *A. laibachii* even further than the previously described direct GH25 inhibition.

8.2 Emerging Interactions between *Cystofilobasidium* and *Pseudomonas*

Isolation of novel *Cystofilobasidium* yeasts from natural *A. thaliana* populations revealed a tight association with a bacterium that was identified as *Pseudomonas extremaustralis* (B2). On co-culture plates, the pair displayed a distinctive "fried-egg" phenotype: a central orange yeast colony surrounded by a halo of opaque bacterial growth. This morphology suggests an intimate, possibly mutualistic, relationship. The yeast's orange pigmentation (likely rich in carotenoids) and exudates may create a microenvironment or nutrient niche that encourages B2 to grow around it. Such spatial organization is reminiscent of cooperative cross-feeding or facilitation seen in other microbial pairs, where one organism's metabolites or enzymes support the growth of another (Germerodt et al., 2016, Estrela et al., 2012, Zelezniak et al., 2015). In our system, the *Cystofilobasidium* - *Pseudomonas* pairing appears to establish itself as a structured consortium on the leaf, hinting that these microbes might co-colonize and persist together in nature. This natural co-isolation is a novelty for phyllosphere studies, which have historically focused mostly on bacterial communities while largely overlooking yeasts (Wang et al., 2016). Our finding provides direct evidence that specific yeasts and bacteria form tight partnerships on leaves relevant for community function and disease suppression.

Network analysis of microbial co-occurrence further reinforces the idea that *Cystofilobasidium* yeasts are deeply embedded in bacterial interaction networks while remaining largely antagonistic to oomycetes. In the *A. thaliana* leaf microbial network, the yeasts exhibited high connectivity with diverse bacteria, nearly half of which were positive correlations. This indicates that *Cystofilobasidium* frequently co-occurs with many bacterial taxa. Intriguingly, the yeast had only one direct negative association with oomycetes showing their co-absence and further hinting at an indirect inhibition of the pathogen. As *A. laibachii* is a dominant member of the microbial community, we can assume the network oomycete OTUs (Operational Taxonomic Unit) correspond to the white rust disease germ (Agler et al., 2016). Moreover, when we investigated *Pseudomonas*-related edges in the network, we found that interactions with oomycetes and *Cystofilobasidium* yeasts were mainly of positive nature. Interestingly, some positive interactions flow from the yeasts to a *Pseudomonas* node, which itself is negatively associated with one of the oomycete OTUs. This reinforces our earlier hypothesis, that an inter-kingdom relationship has a negative impact on pathogen spread. It seems though that the interaction between *Pseudomonas* and *Cystofilobasidium* is in the minority,

as most associations of oomycetes and *Pseudomonas* are showing co-occurrence, indicating that many bacterial species benefit from an *Albugo*-infected leaf. In that context, the relationship between *Cystofilobasidium* and *P. extremaustralis* may act as a counterbalance and plant protection mechanism. The yeast - bacterium duo likely represents a beneficial consortium prevalent in healthy leaves that prevents or combats pathogen infection. These findings about an inter-kingdom partnership combating a pathogen is corroborated by a recent study in tomato. Here, it was revealed that a synthetic community consisting of bacteria and fungi was able to decrease *Fusarium* infection (X. Zhou et al., 2022). Our data thus provide community-level evidence that this yeast–bacterium partnership is both naturally occurring and potentially antagonistic to the pathogen.

A central question is whether the close association between *Cystofilobasidium* and B2 merely reflects niche overlap or if it confers functional advantages - particularly in inhibiting other microbes, as our hypothesis states. The confrontation assays address this by testing antimicrobial effects against a panel of leaf-associated background bacteria. Our results reveal a clear synergy in antimicrobial activity when the yeast and B2 are combined. Co-cultivation produced substantially larger inhibition zones against the same three background strains previously lightly inhibited by B2 alone and together they inhibited two additional, previously impervious bacteria. This hints to the fact that the producer of the antimicrobial compound is the bacterial partner of this interaction, which is promoted in its antimicrobial activity by the yeast.

Possible explanations can be manifold and don't have to be mutually exclusive. Metabolic cooperation can play a major role here. The yeast may secrete growth factors or nutrients, for example vitamins, amino acids or carbon sources that boost *Pseudomonas*'s growth or antibiotic production. As implied by the "fried-egg" phenotype, B2 grows more robustly around the yeast and could indicate a higher concentration of the antimicrobial(s) at play, which leads to a stronger inhibition zone. Another possibility is that the yeast produces a complementary antimicrobial compound that by itself is too weak or has no mechanism to cause inhibition. For instance, *Cystofilobasidium* could secrete a metabolite that permeabilizes the target bacteria or weakens their defense, making them more susceptible to B2's inhibitory compound. This phenomenon resembles combination antibiotic therapy in which two agents together overcome a microbe that is resistant to each alone, such as the utilization

of *beta*-lactam antibiotics with *beta*-lactamase inhibitors (Bush, 1988). Additionally, pH or microenvironment modification might change the bacterial antimicrobial in a way to make it more potent (Thomas et al., 2012). Yeast metabolism, such as fermentation, can acidify the local medium or consume oxygen, which in turn could enhance production or activity (Vylkova, 2017). This is supported by the fact that many *Pseudomonas* antibiotics are produced in stationary growth phases or low-oxygen conditions (Xu and Zhong, 2011, Whooley and McLoughlin, 1982).

The net result is a cooperative antagonism whereby the yeast - bacterium pair inhibits a broader array of organisms and to a greater extend than either could alone. This finding is novel in the context of phyllosphere microbiology and provides experimental proof that cross-kingdom interactions can yield emergent antimicrobial activity. In essence, the yeast and bacterium function as a synergistic biocontrol unit. Similar concepts have been explored in agricultural biocontrol, though often with intentionally combined agents. For example, mixing the yeast *Pichia guilermondii* with a *Bacillus mycoides* bacterium resulted in additive suppression of *Botrytis* gray mold, as each partner contributed different anti-pathogen mechanisms (Guetsky et al., 2002). In our case, the synergy arose from a naturally co-occurring pair, underlining the novelty of harnessing inherent microbial relationships.

Beyond direct antagonism on agar plates, we also examined how the yeast - bacterium interaction influences biofilm formation - a key factor in microbial colonization and community resilience (Scher et al., 2005, Lapidot et al., 2006). Biofilms can protect microbes and also modulate antimicrobial production, especially in *Pseudomonas* species (Yan et al., 2003, Recinos et al., 2012). Our biofilm assays, performed with Yeast 1 and B2 in the presence or absence of additional background strains, revealed nuanced, context-dependent effects of their interaction. In simple two-species cultures (Yeast 1 and B2 alone, and Yeast 1 with B2) the yeast monoculture formed the thickest biofilm, whereas B2's biofilm was moderate and the co-culture formed less biofilm than either alone. This outcome suggests a form of competition or interference between the yeast and bacterium in terms of biofilm formation - perhaps each slightly reduces the other's optimal biofilm development. For instance, B2 might produce biosurfactants or enzymes that disrupt the yeast's matrix formation, while the yeast could consume nutrients that B2 would otherwise use in biofilm production. The result is an intermediate biofilm mass when combined, indicating no inherent biofilm synergy

without external stressors.

However, the dynamics shifted when a third-party background bacterium was introduced. Against two of the tested background strains (B25 and B52), the Yeast and B2 co-culture produced more biofilm than either the yeast or B2 alone. This implies that in the face of competition from other microbes, the yeast and B2 cooperate more tightly - possibly co-assembling into mixed biofilms that exclude their antagonist. The presence of B25 or B52 might stimulate the yeast - bacterium pair to fortify their biofilm, whereas alone they did not have that incentive. Notably, in the B25 background condition, the co-culture's biofilm biomass was not just higher in trend but significantly greater, underscoring a genuine synergistic response. These results echo the idea that beneficial interactions often manifest under stress or competition (Piccardi et al., 2019). In low-nutrient or high-competition environments, positive interactions become more pronounced (Hoek et al., 2016). Our findings aligns with a recent report that beneficial cross-kingdom interactions dominate in challenging conditions, whereas richer media can shift interactions toward antagonism (Velez et al., 2018). Thus, the partnership between *Cystofilobasidium* and *P. extremaustralis* is flexible - sometimes neutral when alone, but cooperative when confronting other microbes, enhancing community defensive capacity by building a stronger joint biofilm.

Interestingly, in the case of background strain B60, which was additionally also not inhibited by either Yeast 1, B2 or co-culture in the competition assay, this synergistic pattern was not observed. Our results suggests that the effect of the yeast - bacterium interaction can be antagonistic or neutral in certain conditions. The likely reason for the lack of inhibition and the significantly enhanced biofilm formation observed in the B2 and B60 combination is that both strains belong to the same species, *P. extremaustralis*. With both microbes being the same species (still different strains), it makes sense that they do not interfere with each other as they probably have the ability to neutralize each other's antimicrobial arsenal. Nonetheless, across most conditions tested, the co-culture performed on par with or better than the single strains. This trend indicates that Yeast 1 and B2 together maintain a high performance level across different competitive scenarios, potentially buffering each other against challenges. Such consistency can be valuable in a fluctuating natural community, analogous to how combining biocontrol agents can reduce variability in disease control (Guetsky et al., 2002, Bush, 1988). In summary, the biofilm assays illustrate that the *Cystofilobasidium* -

Pseudomonas relationship can toggle between mild competition and cooperation, with the latter prevailing especially when it's needed to confront competitors. This plasticity may help the pair dominate niches and resist invasion by other microbes, contributing to a more stable community that is adversative to pathogens.

Taken together, these findings support a model in which inter-kingdom microbial interactions bolster antimicrobial activity and thereby shape community composition in ways that favor plant health. The *Cystofilobasidium – P. extremaustralis* synergy appears to enhance the exclusion of certain bacteria. In a natural leaf setting, the targets of this inhibition may include bacterial taxa that are commensals of *A. laibachii* or otherwise promote its infection. Prior studies have shown that *Albugo* infections often coincide with shifts in microbial diversity and composition, likely due to the pathogen's ability to suppress plant defenses and alter the microenvironment through nutrient leakage (Agler et al., 2016, Eitzen et al., 2021, Mahmoudi et al., 2024). By extending antimicrobial activity to bacteria unaffected by B2 alone, the yeast – bacterium pair may help eliminate microbial groups essential for *A. laibachii* or other pathogens to establish on *A. thaliana*.

Unpublished data from our lab (Kroll, Kemen, unpublished) further support this mechanism: *A. laibachii* infection was effectively suppressed only when the *Cystofilobasidium* yeast was established on the leaf surface prior to pathogen exposure. This illustrates a priority effect, where early-arriving microbes can shape community assembly and influence the success of subsequent colonizers (Fukami, 2015, Hess et al., 2019). Such effects may result from early occupants monopolizing resources or altering the niche through compound secretion or biofilm formation. These dynamics can have lasting consequences, leading to divergent community outcomes based on colonization order (Carlström et al., 2019). The presence of our *Cystofilobasidium – P. extremaustralis* partners may exert a similar effect, precluding *A. laibachii* establishment through niche preemption or community reshaping. As a result, the pathogen may be unable to colonize the leaf surface — an essential step in its infection cycle. This mechanism parallels probiotic strategies in the gut microbiome, where beneficial microbes are introduced to outcompete or inhibit pathogens (Vergin, 1954, Lilly and Stillwell, 1965). Additionally, the robust biofilm formed by *Cystofilobasidium* and *P. extremaustralis* may act as both a physical and chemical barrier, obstructing pathogen access and releasing antimicrobials in situ. The net effect is a community less conducive to *A. laibachii* infection.

Indeed, our findings align with field observations showing that the presence of *Cystofilobasidium* in natural leaf communities correlates with approximately 73% lower *Albugo* levels (Mahmoudi et al., 2024). The partnership with *P. extremaustralis* may be a key driver of this pronounced anti-pathogen effect.

8.3 Genomic Insights into Yeast - Bacterium Symbiosis

Understanding genomics is foundational and crucial for interpreting the interaction between *Cystofilobasidium* and *P. extremaustralis*. Therefore, we sequenced and assembled the genomes of our five yeast strains. These assemblies surpass the quality of currently available *Cystofilobasidium* genomes, offering greater completeness, higher sequencing depth, and improved contiguity. To our knowledge, this represents the most comprehensive genomic dataset for this genus to date. Here we discuss the key assembly-derived characteristics of these genomes, compare intra-group similarities and subtle differences, and consider the implications for downstream transcriptomic analyses.

The five *Cystofilobasidium* yeast isolates show remarkably consistent genome features, reflecting their close taxonomic relations. All five genomes roughly range from 20 to 40 Mb in size, with GC contents around 49 to 50%, which is typical for Tremellomycete yeasts (Loftus et al., 2005, Floudas et al., 2012, Janbon et al., 2014, Kourist et al., 2015, S. Sun et al., 2017, Jarrige et al., 2022). Minor deviations in the *C. macerans* and *C. capitatum* assemblies are most likely attributed to sequencing variation or small lineage-specific elements rather than fundamental differences. All yeast assemblies show reasonable contiguity, with contig counts ranging from a few dozen to just over a hundred and N50 values between $10^5 - 10^6$ bp, indicating successful assembly of large chromosomal segments. Notably, the *T. pullulans* assembly was the most contiguous, with N50 in the megabase range, consistent with long-read sequencing achieving near chromosome-level scaffolds (Wright et al., 2024). Overall, the similarity in these metrics underscores that the genomes of these yeast isolates share a conserved structure, with subtle differences likely due to technical factors or the presence of particular regions rather than major genomic differences.

Importantly, all five yeast genomes exhibit the general characteristics of basidiomycete genome structure. They have a high gene count in the order of 6000 - 7500 genes, consistent with other Tremellomycete yeasts. Coding sequence density in these fungal genomes is moderate, with about 50% of the genomic bases are protein-coding and the rest being either intronic or intergenic. This is in contrast to compact yeasts genomes like the Ascomycete *Saccharomyces* and reflects the intron-rich gene structures characteristic of basidiomycetous yeasts (Janbon et al., 2014). Nearly every predicted gene in our isolates contains multiple introns, as typical for this clade. For example, the pathogenic basidiomycete yeast *C. neoformans* is noted to

have introns in 99.5% of its genes, averaging around 5 to 6 per gene (Janbon et al., 2014). While our environmental isolates are different species, their gene models likewise contain numerous introns and many genes span multiple exons. In practical terms, the average number of exons per gene we observed closely mirror those reported in other basidiomycete genomes (Janbon et al., 2014). This means that a typical gene in these yeasts is broken into many short coding exons by introns, a feature that can expand the genome size and regulatory complexity without increasing gene number. The prevalence of introns in basidiomycetes has functional implications, by which introns are known to modulate gene expression and enable alternative splicing in fungi, and our isolates likely share these regulatory attribute (Heyn et al., 2015, Shaul, 2017, Kelemen et al., 2013, Fan and Lin, 2020, Goebels et al., 2013). Additionally, the intergenic regions make up a substantial fraction of the yeast genomes. These sequences include promotors, terminators and possibly repetitive elements (Jubin et al., 2014, Kämper et al., 2006). Their proportion further highlights the more expansive, less gene-dense genome organization of the yeasts compared to microbes like bacteria. In summary, the yeast isolates' assemblies consistently reveal a genome architecture of moderate gene density with intron-rich genes - a pattern in line with other basidiomycetous yeasts. The subtle differences among them likely reflect its distinct genus lineage but do not obscure the overall intra-group genomic coherence.

A significant outcome of obtaining high-quality genomes is the ability to perform robust phylogenetic analysis. In the case of our yeast isolates we constructed an alignment-based phylogenetic tree from their whole-genome sequences, and importantly, this genome-based tree was congruent with the gene-based tree we had inferred using OrthoFinder on shared orthologous genes. The agreement between these two approaches increases the confidence in the evolutionary relationships of theses isolates. All analyses indicate that the three *C. macerans* strains from a tight clade, with *C. capitatum* grouping just outside and *T. pullulans* as a more distant outgroup within the broader Cystofilobasidiales order. This topology matches classical expectations based on taxonomy and confirms our assemblies have captured the phylogenetic signal without artifact. The OrthoFinder species tree, which was derived from hundreds of single-copy gene alignments, was in complete agreement with the alignment-based tree, illustrating that when sufficient genomic data is analyzed, the inferred species relationships are robust and reproducible. In fact, large-scale fungal phylogenetic studies

have shown that using genome-scale data yields highly resolved and congruent phylogenies in which the majority of branches are consistently supported (Y. Li et al., 2021).

These findings validate that our genome assemblies and annotations are accurate. If there were major misassemblies or missing genes, the phylogenetic trees might have conflicted. The lack of conflict suggests that the set of orthologous genes identified is complete and correctly assembled for each yeast, and that alignment of conserved genomic regions is meaningful. The placement of *Cystofilobasidium* and *Tausonia* in the trees agrees with published phylogenies of Tremellomycete yeasts (Millanes et al., 2011, Wright et al., 2024). Thus, our alignment-based tree essentially recapitulates known relationships, providing an independent confirmation using whole-genome data. This is noteworthy because sometimes gene tree methods can disagree due to horizontal gene transfer or gene family biases, but in this case the OrthoFinder approach was sound and no conflicting information arose (Galtier and Daubin, 2008, Slot and Rokas, 2011, Fitzpatrick, 2012).

Beyond comparative genomics and phylogeny, the ultimate purpose of assembling these genomes was to enable downstream functional analyses, notably transcriptomics in the context of inter-kingdom interactions between the yeasts and *P. extremaustralis* isolate B2. Having high-quality, annotated genomes for each organism is vital to these next steps. With the genome sequences in hand, we can now interpret transcriptomic data with great resolution and confidence.

8.4 Transcriptomic Shifts in *Cystofilobasidium macerans*

The co-culture of *C. macerans* Yeast 1 and *P. extremaustralis* B2 elicited a focused transcriptomic response. Only roughly 8.4% of the yeast's genes were differentially expressed (DE), with 3.7% being upregulated and 4.7% downregulated, while the vast majority remained unchanged. This modest proportion of DE genes suggests that Yeast 1 mounts a targeted adaption to B2 rather than a large scale rewiring of its transcriptome. Similar observations have been reported in other inter-species interactions, such as the yeast-like fungus *Aureobasidium pullulans*, which altered expression of only 79 genes when confronting a competitor (Rueda-Mejia et al., 2021). Such limited yet strategic transcriptional plasticity implies that specific pathways are modulated to facilitate coexistence or competition, while core cellular functions remain stable. In our system, the enriched functional categories among differentially expressed genes provide clues to the nature of the yeast - bacterium interaction.

Upregulated genes in Yeast 1 during co-culture showed significant gene ontology enrichment in carbohydrate metabolism, lipid metabolism, DNA integration and endocytosis. These suggest an enhanced metabolic engagement with the environment and possible genome or protein turnover events in the presence of B2. Elevated carbohydrate and lipid metabolism indicates the yeast may be leveraging available substrates or energy stores - potentially consuming bacterial exudates or mobilizing its own reserves to adapt to new conditions. Increased endocytosis could reflect increased uptake of nutrients or signaling molecules released by B2. Additionally, this can indicate active internalization of extracellular material for remodeling the cell's surface and membranes to cope with bacterial presence. Another idea is that the yeast cell can take up the antimicrobial compound produced by B2 to modify and release it back into the environment making it more potent in the process. Interestingly, the upregulation of DNA integration-related processes might point to transposable element activation or virus-related function, which are sometimes triggered by stress or inter-kingdom interactions (Capy et al., 2000, Makarevitch et al., 2015, Gusa et al., 2023). In contrast, oxidative phosphorylation and aerobic respiration were enriched among the downregulated genes, alongside a broad repression of many transmembrane transporters. This downregulation hints that Yeast 1 may be shifting its energy metabolism, possibly due to oxygen limitation or altered redox conditions imposed by *P. extremaustralis* presence. If B2 rapidly consumes oxygen or produces respiratory inhibitors, *C. macerans* might suppress its own mitochondrial activity

and rely more on fermentative metabolism, a common adjustment in mixed cultures (Filkins et al., 2015, N. Zhou et al., 2017). The reduction in certain transport processes could mean the yeast is conserving energy and minimizing nutrient uptake pathways that are less needed or already supplemented by the bacterial partner. Overall, this pattern suggests *C. macerans* is reallocating its metabolic priorities in response to the presence of *P. extremaustralis* B2.
A notable aspect of the co-culture response is the change in the yeast's secretome. SignalP6 analysis predicted secretion signals in 19 up- and 38 downregulated genes. The induction of nearly 20 secreted or cell-surface targeted proteins in co-culture indicates an adjustment of the yeast's outward facing arsenal. Many of the upregulated genes with secretion signal peptides likely encode enzymes and effectors that act in the extracellular space. For instance, hydrolases involved in nutrient breakdown or molecules that mediate communication or defense. Indeed, studies of microbial consortia often find that organisms modulate their secreted enzyme profiles when a partner is present. In the previously mentioned co-culture study, *Aureobasidium pullulans* specifically upregulated a number of secreted hydrolases and secondary metabolites during competition with a fungus (Rueda-Mejia et al., 2021).

8.4.1 ABC Transporter g5886: Detoxification and Inter-Kingdom Signaling

Among the most strongly upregulated genes in co-culture was g5886, annotated as an ABC multidrug transporter. qPCR validation confirmed its robust induction specifically with *P. extremaustralis* B2. The prominence of this transporter suggests it plays a critical role in the yeast's strategy for dealing with bacterial partners. Members of the ATP-Binding Cassette transporter family are well known for mediating antimicrobial efflux and drug resistance in fungi (Winski et al., 2022). In host-pathogen contexts, fungal ABC pumps reduce intracellular accumulation of toxic compounds and can even affect interaction outcomes. For example, the plant pathogen *Botrytis cinerea* upregulates its ABC transporter BcatrB in response to antibiotics like phenazines produced by *Pseudomonas*, enabling the fungus to pump out these bacterial toxins (Schoonbeek et al., 2002). Deletion of BcatrB renders *B. cinerea* hypersensitive to *Pseudomonas* phenazines and other antimicrobials, highlighting the importance of efflux pumps in microbial interactions. By analogy, the induction of g5886 in *C. macerans* likely serves a detoxification function, safeguarding the yeast from inhibitory metabolites that B2 may secrete. *P. extremaustralis*, like many pseudomonads, secretes antibacterial or anti-

fungal compounds, which make the presence of an effective detoxification system even more important. This interpretation aligns with broader findings that microbial efflux systems are often the front line defense in inter-species competition. In a recent co-culture study, a rumen bacterium exposed to antagonistic fungi likewise upregulated multiple drug efflux pump genes to protect itself from fungal toxins, underscoring the universal importance of transporters (Swift et al., 2021).

Beyond detoxification, g5886 might also contribute to inter-kingdom metabolite exchange or signaling. ABC transporters are versatile, while some secrete toxins, others are known to transport signaling molecules or nutrients. In bacteria, for instance, multidrug efflux pumps can secrete quorum-sensing autoinducers and other communication signals (Dawan et al., 2022). We speculate that Yeast 1's transporter could similarly handle small molecules that mediate cross-talk with B2. If *P. extremaustralis* produces a diffusible quorum sensing molecule — such as an acyl-homoserine lactone (AHL) or another signal compound — the yeast may detect or modulate this signal via the g5886 gene, potentially by mimicking or importing the bacterial molecule. While import of such signals by ABC transporters in fungi is relatively uncommon, the export of signaling compounds is more plausible. Given that quorum sensing is a cell density–dependent system, the addition of the yeast might raise the local concentration of signaling molecules above the threshold required to trigger enhanced antimicrobial production in the bacterium.

Notably, inter-kingdom quorum sensing enables bacteria and fungi to influence each other's physiology in mixed communities. For example, *Pseudomonas aeruginosa* secretes 3-oxo-C12-homoserine lactone (3OC12-HSL), a quorum signal that can be sensed by fungal cells. This molecule has been shown to inhibit filamentation in *Candida albicans* without affecting its overall growth (Hogan et al., 2004). *Candida*, in turn, produces its own quorum sensing molecule, farnesol, which not only regulates its own morphology but also modulates bacterial behavior. Farnesol can disrupt bacterial quorum sensing pathways and, strikingly, stimulate phenazine toxin production in *P. aeruginosa* even when its main quorum regulator LasR is inactive (Cugini et al., 2010). In this way, fungal signals can restore or amplify bacterial secondary metabolite production, potentially increasing antimicrobial output.

Conversely, bacterial quorum signals can also interfere with fungal signaling. For instance, 3OC12-HSL inhibits fungal hyphal growth in a manner similar to *Candida*'s own farnesol-

mediated repression of filamentation (Hogan et al., 2004). These reciprocal interactions highlight a sophisticated chemical dialogue between bacteria and fungi. Even in basidiomycete yeasts such as *Cryptococcus*, quorum sensing systems have been described. These systems utilize molecules like pantothenic acid and Qsp1 for signaling, suggesting that basidiomycete-derived signals could also engage in cross-kingdom communication with bacterial quorum systems (Pruitt et al., 2025). In summary, quorum sensing serves as a molecular language for inter-kingdom communication, enabling coordination between yeasts and bacteria in processes such as biofilm formation and antimicrobial compound production.

Another possible role is the export of yeast-derived metabolites that influence the bacteria and surrounding microbiome. Yeasts are known to influence microbial communities through the secretion of organic acids and other metabolites, which can either inhibit or promote the growth of neighboring bacteria. An upregulated efflux pump may support the export of such compounds. Overall, g5886 appears to enhance the capacity of *C. macerans* Yeast 1 to engage in chemical interactions with B2, primarily through efflux-based detoxification of antimicrobial compounds and possibly by contributing to inter-species signaling.

Its protein structure, as predicted by AlphaFold 3 and DeepTMHMM, revealed a prominent intracellular nucleotide binding domain, consistent with ATP-dependent transport activity and multiple transmembrane regions for substrate translocation. The structure is typical of PDR-type (pleiotropic drug resistance) fungal ABC transporters, supporting the hypothesis that g5886 functions as an active efflux pump (Winski et al., 2022). This interpretation is further supported by the AlphaFold 3 prediction of ATP binding, which yielded an ipTM score above 0.60 — generally considered indicative of a reliable structural fit. Notably, orthologs of g5886 were found in our closely related species Yeast 2 - 4 but not in more distantly related *M. bullatus* or *C. neoformans*. This phylogenic distribution suggests g5886 is a lineage-specific adaption, possibly evolved in *Cystofilobasidium* and its near relatives to interact with *P. extremaustralis* B2. Its clustering with P-loop nucleoside triphosphate hydrolases confirms it belongs to the classic ABC ATPase superfamily and its conservation in the *Cystofilobasidium* yeasts hints at a conserved function.

In the context of yeast - bacterium interactions, the induction of g5886 is therefore a strong indicator that *C. macerans* Yeast 1 actively manages chemical stress and communication when dealing with bacteria. By pumping out unwanted molecules, like antimicrobials, toxic

byproducts or signaling molecules, the yeast likely maintains cellular homeostasis and can persist alongside B2. Such transporters may also enable the yeast to tolerate antimicrobial compounds and thus modulate bacterial community dynamics, as was seen in plant-associated environments where fungal ABC transporters helped fungi survive in the presence of bacteria (Schoonbeek et al., 2002).

8.4.2 Glycoside Hydrolase g4647: Uptake and Interaction

The second gene of interest, g4647, encodes a putative glycoside hydrolase of family 13 (GH13) and was also strongly upregulated in the presence of B2 and validated by qPCR. GH13 enzymes typically include α-amylases and related starch-degrading enzymes, which act on α-linked polysaccharides (Svensson, 1994, Janecek, 1997). The upregulation of a GH13 suggests that Yeast 1 may be boosting its capacity to degrade complex carbohydrates during co-culture. One straightforward explanation is nutrient acquisition: the yeast could be breaking down extracellular polysaccharides into simple sugars that it can absorb. In a mixed culture, such polysaccharides might come from various sources, such as remnants of growth medium, plant material if present or even polymers produced by other microbes, like biofilms formed by B2. In fact, microbial partnerships often involve cross-feeding on complex substrates. Research on anaerobic fungal - bacterial consortia has shown that fungi will ramp up carbohydrate-active enzymes in co-culture, benefiting both partners. For instance, one study found a gut fungus upregulated over 100 CAZyme genes (about 12% of its CAZyme repertoire) when grown with a bacterium, presumably to break down plant fiber more efficiently for mutual gain (Swift et al., 2021). Drawing a parallel, g4647 might help Yeast 1 and B2 access additional carbon sources that neither could fully utilize alone. The presence of background bacteria was also found to induce g4647, though less consistently than B2 did, which implies that this gene responds to a general cue of nearby bacteria and possible competition for nutrients. Cross-feeding could thus be a factor by secretion of g4647 by *C. macerans* and subsequent liberation of sugars from polysaccharides, some of which the yeast consumes and some might become available to B2. This cooperative aspect would enhance growth in both organisms in the co-culture and is one way the yeast could modulate the microbiome, by increasing the pool of readily available nutrients through enzymatic digestion.

It is also worth noting that g4647 forms a monophyletic group limited to Yeast 1 and Yeast

2, according to ortholog analysis. This restricted distribution suggests that it is a relatively novel or unique enzyme, possibly evolved for a niche function shared by these two yeasts. Intriguingly, it is sister to proteins involved in signal recognition and carbohydrate binding, hinting that it might have dual functionality - perhaps binding to specific cell surfaces or sugars as a recognition mechanism before hydrolysis. One could speculate that g4647 has adapted to recognize particular glycans associated with the plant or certain bacteria and hydrolyze them. Its induction specifically by bacterial co-culture supports the idea that its natural role is tied to the presence of other microbes. In contrast, g4647 likely does not encode a secreted enzyme, as SignalP6 analysis revealed no secretion signal in the amino acid sequence, indicating an intracellular role.

In summary, g4647 appears to equip Yeast 1 with an enhanced capability to alter the carbohydrate landscape of its environment on the presence of bacteria. Whether that is primarily to harvest additional nutrients or to degrade bacterial protective layers is an open question. As GH13 contains no secretion signal, its intracellular activity remains elusive. We speculate that one possibility is that similar to other antimicrobial compounds, the agent produced by B2 is taken up by the yeast, a sugar residue is cleaved off and the resulting product is secreted again displaying increased antimicrobial activity.

8.5 Yeast – Bacterium Relations and Microbiome Modulation

The interaction between *Cystofilobasidium* and *P. extremaustralis* B2 appears to be mutualistic, with important consequences for the leaf microbiome and pathogen suppression. Rather than a one-sided antagonism, this yeast - bacterium partnership benefits both microbes and the host plant. Taken together, the yeast is able to enhance B2's antimicrobial activity against other leaf-associated bacteria, an effect that likely reshapes the microbial community to the detriment of pathogens. Notably, the oomycete pathogen *Albugo laibachii*, which normally infects more effectively in the presence of a supportive community, may be indirectly suppressed by this pairing (Kroll, 2018). In essence, *Cystofilobasidium* yeast and *P. extremaustralis* form a cooperative alliance that excludes competitors and deprives the pathogen of potentially crucial infection promoting bacteria.

8.5.1 Mutualistic Partnership Enhances Antimicrobial Activity

Our findings indicate that when *Cystofilobasidium* yeasts and *P. extremaustralis* B2 co-exist, the production or efficacy of antimicrobial compounds is increased, leading to stronger inhibition of other phyllosphere bacteria. This contrasts with typical cross-kingdom interactions on leaves, which are often antagonistic in nature (Agler et al., 2016). Here, the yeast - bacterium cooperation deviates from the norm, by instead of inhibiting each other, they work together to target third-party microbes. This synergy likely benefits both partners. B2 gains a competitive edge in the leaf environment, by more efficiently eliminating rival bacteria, while *Cystofilobasidium* benefits from *P. extremaustralis*'s suppression of potential antagonists. The net result is a pruned microbial community dominated by mutualists and lacking other bacteria. Such community modulation can directly impact *A. laibachii*, a pathogen known to exploit the microbial community on *A. thaliana* leaves (Agler et al., 2016, Muller et al., 2018, Trivedi et al., 2020). As a hub microbe, it decreases the bacterial diversity and stabilizes the community composition in its favor (Agler et al., 2016). It effectively creates a supportive network suppressing or tolerating certain bacteria while excluding others (Gómez-Pérez et al., 2023). The combination of *Cystofilobasidium* yeast and *Pseudomonas* B2 may counter this by preemptively inhibiting a range of leaf microbes, thereby preventing *Albugo* from assembling its normally supportive community. In preliminary plant infection experiments (Fig. S2), we could see an indication of reduced *A. laibachii* infection supporting

our in-vitro findings and conclusions.

This concept aligns with broader principles of microbiome-mediated pathogen suppression. Cooperative interactions between different microbes can yield emergent antimicrobial capabilities that surpass what single species achieve alone. For example, in plant roots, cross-kingdom synthetic communities containing both bacteria and fungi were far more effective at suppressing *Fusarium* wilt disease, a soil-borne pathogen, than either bacterial or fungal communities alone (X. Zhou et al., 2022). In our *A. thaliana* leaf system, the presence of *Cystofilobasidium* yeasts and *P. extremaustralis* B2 together similarly creates a heightened defensive effect. The yeasts might directly stimulate the antimicrobial compound production of B2 or create conditions in which the bacterium is able to increase their antagonism towards other microbes. Additionally, through the breakdown of other microbes, *P. extremaustralis* releases nutrients, which *Cystofilobasidium* can use to promote its growth, reinforcing the partnership. Importantly, this positive feedback stands in contrast to purely competitive outcomes and highlights how mutualism can shape community structure and be a driving force in community assembly. This is consistent with observations in *A. thaliana* microbial networks, which are typically dominated by positive interactions (Agler et al., 2016). Such mutualistic dynamics are thought to contribute to community stability and host health.

The *Cystofilobasidium* - *P. extremaustralis* interaction demonstrates this principle in a novel way, uncovering a previously undescribed cross-kingdom mutualism that not only enhances partner fitness but also contributes to pathogen suppression. This expands the current understanding of beneficial microbial interactions by showing how a yeast – bacterium consortium can coordinate metabolic and ecological functions to promote host protection. Instead of acting independently, they create a hostile microenvironment for pathogens on the leaves. This supports the idea that emergent properties like pathogen resistance arise from multi-microbe interactions. While individual microbes can promote health, microbial consortia often have stronger, more stable effects. Ecologically, the cross-kingdom relationship of yeast and bacterium likely shifts the phyllosphere toward a lower-diversity, more pathogen resilient state. Like pathogenic hubs that restructure communities, this beneficial pair may reduce diversity in a way that favors plant health. Their presence might suppress pathogen-beneficial microbes, offering a strategy for biological control at the community level. This reflects a growing trend in plant protection - using consortia rather than single agents to outcom-

pete pathogens (Martins et al., 2023). Multi-species treatments are more resistant under environmental stresses, with different members compensating for each other.

Cross-kingdom microbial mutualism, like the one we observed in this work, are widespread in nature. In cheese rinds, yeasts and bacteria cooperate metabolically to create stable, protective communities (Mayo et al., 2021). In the gut, cross-feeding between bacteria enhances productivity and pathogen resistance (Berkhout et al., 2022). On leaves, microbes like *M. bullatus* protect plants by targeting specific pathogens like *A. laibachii* or a set of different microbes (Eitzen et al., 2021, Sorger et al., 2025). Such examples show how microbial symbiosis can result in emergent benefits and reinforces the impact of microbial partnerships promoting plant health. Genomic analyses reveal that key microbial genes are often activated only in co-culture. Genes like g5886 and g4647 may seem non-essential in isolation but are crucial in interaction with a bacterial partner. This highlights many functional traits, such as secondary metabolites or stress responses, emerge in the context of microbial communities. Co-cultivation frequently uncovers hidden genes and novel metabolites. Understanding these genetic interactions is vital for designing effective microbiome-based solutions for biocontrol.

In conclusion, the *Cystofilobasidium* - *P. extremaustralis* mutualism serves as a model for microbiome engineering through cooperation. Their partnership boosts antimicrobial activity and alters the microbiome in a way that disfavors pathogens. Genes like g5886 and g4647 underpin this interaction, linking molecular mechanisms to ecological outcomes. Studying such interactions expands our view of plant microbiomes from isolated species to interconnected networks. By uncovering how these relationships suppress disease, we can develop innovative agricultural strategies — deploying synergistic microbial communities as living therapeutics to promote sustainable plant health.

8.6 Functional Innovation through Cross-Kingdom Cooperation

This work uncovered a novel cross-kingdom interaction in the phyllosphere, where a leaf-associated *Cystofilobasidium* yeast is partnering with a *Pseudomonas* bacterium. Together they posses emergent antimicrobial and biofilm-forming capabilities, not seen in either microbe alone. Phyllosphere yeasts haven been historically understudied, and little is known about their ecological functions (Gouka, Raaijmakers, and Cordovez, 2022). Identifying a cooperative yeast - bacterium consortium on leaf surfaces is therefore highly novel. While microbial interactions in the phyllosphere often focus on bacteria - bacteria or pathogen antagonism, our findings highlight synergistic cross-kingdom cooperation. Such inter-kingdom synergy has few precedents in plant systems. Notably, analogous phenomena have been described in medical contexts. For example, mixed biofilms of a *Candida* yeast and *Pseudomonas* on lung tissues are far more extensive than single-species biofilms (Phuengmaung et al., 2022). By drawing a parallel, our study suggests that beneficial microbes too can form enhanced mixed biofilms on plant surfaces, potentially fortifying their survival and antagonistic capabilities. This presents a significant advance in phyllosphere biology, demonstrating cooperation - not just competition - between vastly different microbes can drive important functional outcomes. Indeed, recent synthetic community experiments support that combining microbes often yields superior plant protection than single inoculants (Ali et al., 2021, Z. Li et al., 2021). Our discovery provides a concrete example of this principle in the phyllosphere, marking a new understanding that multi-species and multi-kingdom alliances on leaves can produce heightened biocontrol effects.

From an applied perspective, these findings are especially important given current gaps in plant disease management, particularly for obligate biotrophic pathogens like *Albugo laibachii*. Obligate biotrophs are challenging to control and study as they cannot be cultured outside their hosts and often evade conventional biocontrol agents. Our yeast - bacterium partners offer a promising microbe-based strategy to reduce disease susceptibility in this context. In preliminary in planta infection assays, *A. thaliana* plants treated with the co-culture showed lower *Albugo* infection levels compared to untreated single-inoculant plants (Fig. S2). This suggests an entirely new approach, where instead of trying to kill the pathogen with chemicals, we enlist naturally occurring epiphytes to create an inhospitable environment or directly attack the pathogen or its necessary bacterial partners. Notably, *A.*

laibachii and other foliar biotrophs have an infection stage on the surface before penetrating the leaf, which could be targeted by antagonistic microbes. The synergistic biofilm of *Cystofilobasidium* and *Pseudomonas* might form a physical and chemical barrier on the leaf, preventing pathogen establishment, or the partners might jointly produce antimicrobials and lytic enzymes to destroy the incoming pathogen. This fills a critical gap: current biocontrol efforts for leaf pathogens often focus on single bacteria (e.g. *Bacillus* or *Pseudomonas* strains) with inconsistent success and very few target obligate biotrophic oomycetes. By contrast, our findings point to a community solution, leveraging a natural *Cystofilobasidium* - *Pseudomonas* partnership to achieve what neither can do alone. The importance of this is underscored by recent research identifying *Cystofilobasidium* as a key health-associated taxon in wild *A. thaliana* populations (Kemen et al., 2025). Given the urgent need for sustainable crop protection, especially against pathogens that are hard to manage, this work provides a proof of concept for harnessing native microbiome interactions. It addresses a current gap by showing that even understudied players in the phyllosphere like *Cystofilobasidium* yeasts can be pivotal when combined appropriately, expanding the arsenal of biocontrol strategies beyond the well-trodden soil bacteria and signaling a shift towards targeting foliar pathogens with tailored cross-kingdom microbial consortia.

8.7 Prospects and Possibilities

Building on the promising findings of this work, several avenues for future research can deepen our understanding of the yeast - bacterium symbiosis and its role in microbiome-mediated suppression of the oomycete pathogen *A. laibachii*. To increase our knowledge, several integrated research directions should be pursued. First, proteomic and metabolomic approaches are essential to bridge the gap between transcriptional responses and functional phenotypes. Proteomics will validate the production and secretion of key proteins such as the ABC-transporter g5886 and the glycoside hydrolase g4647 under co-culture conditions, and may uncover additional interaction-specific proteins not evident at the transcript level. Untargeted metabolomics applied to co-culture supernatants and plant-microbe microcosms allows the identification of secreted compounds or metabolite modifications associated with increased antimicrobial activity. These datasets will clarify whether the yeast modulates or enhances the bioactivity of bacterial antimicrobials through enzymatic or metabolic cooperation.

To causally link gene function to phenotype, the development of gene knock-out mutants in *C. macerans* Yeast 1 is a critical next step. Deletion of our genes of interest will reveal their role in the interaction with *P. extremaustralis* B2. Equally important is deeper exploration of the bacterial side of the interaction, as we postulate that the antimicrobial compound is produced by the bacterial partner. While B2 exhibits antimicrobial activity independently, the co-culture significantly amplifies its effects, suggesting that compound production may be modulated by yeast-derived cues. Future work should focus on bioassay-guided fractionation and comparative metabolomics of B2 mono- versus co-culture conditions to identify specific antimicrobial compounds responsible for the observed inhibition. Genome mining tools such as antiSMASH or PRISM could be used to predict biosynthetic gene clusters (BGCs) in B2's genome, guiding the search for candidate metabolites such as phenazines, lipopeptides, or siderophores. Expression analysis of BGCs in co-culture will reveal whether the presence of the yeast activates otherwise silent or lowly expressed pathways — a phenomenon often seen in microbe–microbe interactions. This may ultimately allow identification of novel bioactive compounds or synergistic activities enhanced by yeast–bacteria cross-talk.

Additionally, expanding co-culture assays to include microbial strains more closely related to *Albugo laibachii* or known to facilitate its infection will help determine whether the

Cystofilobasidium - *P. extremaustralis* interaction selectively inhibits *Albugo*-supportive microbes or exerts broader suppressive effects. This is key to understanding the specificity and ecological relevance of the observed pathogen suppression. Finally, screening additional environmental *Cystofilobasidium* and *Pseudomonas* isolates for similar interaction traits will clarify whether the mutualism observed here is conserved or strain-specific. Such insights will be foundational for designing microbial consortia with enhanced stability and biocontrol potential, leveraging natural mutualisms to reshape host-associated microbiomes in favor of plant health.

9 Material and Methods

9.1 Reagents

A complete list of reagents, chemicals, and materials used throughout the experimental procedures is provided, including supplier information (Table 2). Reagents included in commercial kits are specified in the corresponding kit protocols.

Reagents	Company
Nuclease Free Water	Sigma-Aldrich
$MgCl_2$	Carl Roth GmbH
NaOH	Carl Roth GmbH
Potassium Acetate	Carl Roth GmbH
Sodium Acetate	Carl Roth GmbH
Potato Dextrose Broth	Carl Roth GmbH
Potato Dextrose Agar	Carl Roth GmbH
King's B Broth	Carl Roth GmbH
King's B Agar	Carl Roth GmbH
Ethanol	Carl Roth GmbH
Isopropanol	Carl Roth GmbH
Tris	Carl Roth GmbH
EDTA	Carl Roth GmbH
Crystal Violet	Merck
Phenol:Chloroform:Isoamylalcohol	Carl Roth GmbH
RNase A	Carl Roth GmbH
dNTPs	Genaxxon
Oligo(dT) Primer	Merck
SYBR Green Supermix	Bio Rad
Bovine Serum Albumin	Merck
Zirconia Beads	Carl Roth GmbH
SpeedBead Magnetic Carboxylate Modified Particles	Cytiva

Table 2: List of reagents and materials used in this study along with their respective suppliers.

9.2 Kits

The following commercial kits were used for DNA and RNA extraction, reverse transcription, and library preparation during the study (Table 3).

Kit	Company
Quick-DNA Fungal/Bacterial Miniprep Kit	Zymo Research
Native Barcoding Kit 24 V14 (SQK-NBD114.24)	Oxford Nanopore Technologies
RNeasy MiniKit from Yeast	Qiagen
RNeasy Plant MiniKit	Qiagen
TURBO DNA-free Kit	Thermo Fischer
SuperScript IV Reverse Transcriptase	Invitrogen

Table 3: List of molecular biology kits used in this study and their corresponding manufacturers.

9.3 Instruments

The instruments and equipment used for sample processing, quantification, and molecular analyses are listed below along with their manufacturers (Table 4).

Machine	Company
NanoDrop 2000C Spectrophotometer	Thermo Fischer
Infors HT Ecotron	Infors AG
Tecan Spark Plate Reader	Tecan
Centrifuge 5425R	Eppendorf
Sorvall RC 6+ Centrifuge	Thermo Fischer
Precellys Evolution	Bertin Technologies
Cryolys	Bertin Technologies
Thermomixer C	Eppendorf
Mixer Uzusio VTX-3000	LMS
CFX Connect Real-Time PCR Detection System	Bio Rad
MinION Flow Cell R10 (FLO-MIN114)	Oxford Nanopore Technologies

Table 4: Laboratory equipment and analytical instruments used in this study, with corresponding manufacturers.

9.4 Primer List

Primers were designed and used for amplification of the fungal ITS region, bacterial 16S rRNA gene, and selected candidate genes for qPCR analysis, including two genes of interest and the EF1-α reference gene (Table 5).

Amplicon	Direction	Name	Sequence
ITS	Forward	ITS1	TCCGTAGGTGAACCTGCGG
	Reverse	ITS4	TCCTCCGCTTATTGATATGC
16S	Forward	27F	AGRGTTYGATYMTGGCTCAG
	Reverse	1492R	TACGGYTACCTTGTTACGACTT
g5886	Forward	Q099	TGGCACCTTTCTCGCCCTGTCT
	Reverse	Q100	TGGATCGCCTGACTCAGCGTGA
g4647	Forward	Q117	TTCTGGCGGTCCCGATGAAAGC
	Reverse	Q118	AACTGGAGACACAGGGCGAGCA
EF1-α	Forward	Q071	GCGGCTACAACCCCAAGACC
	Reverse	Q072	GTCGATGGCCTCAAGGAGGG

Table 5: Sequences and annotations of primers used for ITS and 16S rRNA gene sequencing, as well as for quantitative PCR targeting two candidate genes (g5886, g4647) and the EF1-α reference gene.

9.5 Microbe Isolation from Natural *A. thaliana* Populations

Epiphytic microbes from natural *A. thaliana* populations were isolated by collecting plants in sterile tubes using disinfected tweezers at designated field sites Agler et al., 2016, Supplementary Data. Roots were removed, and visible debris or senescent tissue was cleaned off prior to storage. For processing, 5 mL of 10 mM $MgCl_2$ was added to each plant to dislodge epiphytic microorganisms. The resulting wash was serially diluted and plated on 0.2x PDA agar to select for yeasts. Colonies were subsequently transferred to 1x PDA for cultivation.

9.6 Crude DNA Extraction from Liquid Culture

Genomic DNA for colony PCR was extracted from overnight cultures using a rapid alkaline lysis method. A 50 µL aliquot of overnight culture was transferred to a 1.5 mL microcentrifuge tube and centrifuged at 15.000 rcf for 1 minute. The supernatant was discarded, and the pellet was resuspended in 50 µL of 20 mM NaOH. The suspension was frozen at –80°C for at least 30 minutes and subsequently boiled at 98°C for 10 minutes. The lysate was used directly as PCR template without further purification.

9.7 ITS and 16S Sequencing

DNA sequencing for colony PCR was performed by LGC Genomics using their Ready2 Run service. Therefore 10 µL sample DNA and 4 µL forward primer (Table 5) were added to a 1.5 mL test tube according to instructions (Table 6).

Sample DNA	200 - 500 bp	10 ng/µL
	500 - 1.000 bp	20 ng/µL
	1.000 - 2.000 bp	40 ng/µL

Table 6: Recommended DNA concentrations for Sanger sequencing using LGC Genomics Ready2Run service, based on amplicon size. A total volume of 10 µL DNA at the specified concentration was submitted per sample.

9.8 Co-Culture Microscopy

Single colonies of *C. macerans* Yeast 1 and *P. extremaustralis* B2 were individually inoculated into 5 mL of Potato Dextrose Broth (PDB) and cultured overnight at 22°C with shaking at 180 rpm. The following day, the OD_{600} was adjusted to 0.8 for each culture, and the two cultures were combined in a 1:1 ratio. After an additional incubation period of 3 hours at 22°C and 180 rpm, the OD_{600} of the co-culture was readjusted to 0.8. Subsequently, 10 µL of the co-culture was placed on a microscopy slide, and images were captured using a Zeiss Axiophot microscope at 400× magnification, equipped with a Zeiss Axiocam 512 color camera and Zeiss Zen lite 2.3 software.

9.9 Confrontation Assay

Single colonies of yeast and bacteria strains were revived from cryogenic stocks by plating onto Potato Dextrose Agar (PDA) and King's B agar, respectively, and incubated at 22°C for 24 hours. Subsequently, a single colony from each was inoculated into 10 mL of their corresponding media and incubated for 24 hours at 22°C with shaking at 180 rpm. The OD_{600} of each culture was then adjusted to 0.4 in its respective medium, after which each yeast culture was combined with the *P. extremaustralis* B2 strain at a 1:1 ratio. Additionally, single cultures of yeast and B2 were refilled to their original volumes following the combination step. The cultures were incubated for an additional 3 to 4 hours at 22°C and 180 rpm, after which their OD_{600} was adjusted to 0.8 using their respective media (for yeast–bacteria co-cultures, a 1:1 medium mixture was used). Next, 100 µL of background bacteria culture was spread onto fresh PDA plates and allowed to dry for 5 minutes. Subsequently, 10 µL of yeast, B2, or co-culture suspension was spotted onto the center of each plate and allowed to dry for an additional 5 minutes. Plates were incubated for 3 days at 22°C, and inhibition zone radii were measured from the edge of the central colony to the beginning of the bacterial lawn.

9.10 Biofilm Formation Assessment

Single colonies of yeast and bacterial strains were revived from cryogenic stocks by streaking onto Potato Dextrose Agar (PDA) and King's B agar plates, respectively, followed by incubation at 22°C for 24 hours. Afterwards, a single colony from each strain was inoculated into 10 mL of its corresponding medium and cultured for 24 hours at 22°C with shaking at 180 rpm. Each culture was then adjusted to an OD_{600} of 0.4 in its respective medium, and yeast cultures were combined individually with the *P. extremaustralis* B2 strain in a 1:1 ratio. Single cultures of yeast and B2 were refilled to their original volumes following combination. After an additional incubation of 3 to 4 hours at 22°C and 180 rpm, each culture's OD_{600} was set to 0.2 in their respective media (for yeast–bacteria co-cultures, a 1:1 medium mixture was used).

Next, 200 µL of the appropriate medium (a 1:1 mixture of media for yeast–bacteria combinations) was dispensed into each well of a 96-well plate. Subsequently, either 20 µL or 40 µL of medium was removed, depending on the intended treatment: 20 µL was removed from wells designated to receive yeast, B2, co-culture, or background culture alone, and 40 µL was removed from wells receiving yeast, B2, or co-culture combined with background bacteria. Wells were then inoculated accordingly: some received 20 µL of yeast, B2, co-culture, or background single culture individually, whereas others received 20 µL of yeast, B2, or co-culture along with an additional 20 µL of background bacterial culture.

The plate was incubated undisturbed at 22°C for 3 days. Following incubation, cultures were removed from the wells, and 200 µL of a 10% Crystal Violet (CV) solution was added and incubated for 15 minutes at room temperature. Wells were subsequently washed three times with 200 µL MilliQ water, after which the plate was firmly tapped onto an absorbent cloth to remove residual water and CV. Next, the stained biofilms were solubilized by adding 200 µL of 95% ethanol to each well, followed by mixing at 500 rpm for 15 minutes. Finally, absorbance at 595 nm (OD_{595}) was measured using a Tecan Spark plate reader equipped with SPARKCONTROL software.

9.11 High Molecular Weight DNA Extraction

Fresh cultures were streaked from cryogenic stocks onto potato dextrose agar (PDA) plates and incubated at 22°C for 2–3 days. A single colony was inoculated into 10 mL of potato

dextrose broth (PDB) and grown overnight at 22°C with shaking at 180 rpm. The overnight culture was then transferred to 740 mL of PDB in a sterile Erlenmeyer flask and incubated overnight at 22°C with shaking at 120 rpm.

9.11.1 Cell Harvesting and Mechanical Lysis

Cells were harvested by centrifugation at 4,000 rcf for 20 minutes. The pellet was transferred to a sterile mortar using a spatula and ground in the presence of 20 g of 0.1 mm zirconia beads. Liquid nitrogen was added intermittently during grinding to aid in cell disruption and preserve DNA integrity.

9.11.2 Chemical Lysis and Protein Precipitation

An equal volume (17.5 mL) of Genomic Lysis Buffer (Quick-DNA™ Fungal/Bacterial Miniprep Kit, Zymo Research) was added to 17.5 mL of ground cell material. The mixture was incubated at 37°C for 30 minutes with inversion every 5 minutes. After incubation, the lysate was chilled on ice for 5 minutes before adding 3.5 mL of 5 M potassium acetate (pH 7.5). The solution was mixed by inversion and incubated on ice for another 5 minutes. Debris was pelleted by centrifugation at 5,000 rcf for 12 minutes at 4°C.

9.11.3 Organic Extraction and RNA Removal

The clarified supernatant was transferred to a fresh tube containing 17.5 mL of phenol : chloroform : isoamyl alcohol (PCI, 25:24:1), mixed by inversion for 2 minutes, and centrifuged at 4,000 rcf for 10 minutes at 4°C. The aqueous phase was transferred to a new tube containing a second volume of PCI, mixed, and centrifuged again under the same conditions. The final supernatant was treated with 5 µL RNase A and incubated at room temperature for 30 minutes.

9.11.4 DNA Precipitation

To precipitate genomic DNA, 1.8 mL of 3 M sodium acetate (pH 5.2) and 18 mL of 100% isopropanol were added to the sample, mixed gently by inversion, and incubated at room temperature for 10 minutes. The DNA was pelleted by centrifugation at 10,000 rcf for 30 minutes at 4°C. The supernatant was carefully discarded, leaving 2 mL, and the pellet was

transferred to a 1.5 mL tube. Remaining liquid was removed by centrifugation at 6,000 rcf for 5 minutes at 4°C.

9.11.5 Ethanol Wash and Initial Resuspension

The DNA pellet was washed three times with 1.5 mL of 70% ethanol, each followed by centrifugation at 6,000 rcf for 5 minutes at 4°C. After the final wash, the pellet was air-dried for 10 minutes and resuspended in 200 µL of 10 mM Tris-HCl (pH 9). The sample was incubated for 3 hours at room temperature. Subsequently, 200 µL of TE buffer (1 % Tris base, 0.2% EDTA) was added and the solution was incubated overnight at room temperature. An additional 100 µL of TE buffer was added the next day to ensure full dissolution of the DNA pellet.

9.11.6 Magnetic Bead Clean-Up

To purify the DNA, 0.8x volume of self-prepared magnetic beads was added to the DNA solution in a 1.5 mL tube. The mixture was incubated at 400 rpm for 5 minutes, then allowed to rest at room temperature for another 5 minutes. Tubes were placed on a magnetic stand for 15 minutes to pellet the beads, and the supernatant was removed. Beads were washed three times with 1 mL of 80% ethanol, with each wash followed by a 15-minute incubation on the magnetic stand.

9.11.7 Final Elution

Beads were air-dried for at least 15 minutes on the magnetic stand. DNA was eluted in 70 µL of 10 mM Tris-HCl (pH 8) by incubating on a thermomixer at room temperature and 400 rpm for a minimum of 20 minutes. After separation on a magnetic stand for 5 minutes, the eluate containing purified high molecular weight DNA was transferred to a fresh 1.5 mL tube and stored for downstream applications.

9.12 Nanopore Sequencing

Nanopore sequencing run was prepared according to Oxford Nanopore Technologies Native Barcoding Kit 24 V14 (SQK-NBD114.24) protocol.

9.12.1 DNA Repair and End-Preparation

AMPure XP Beads (AXP) and the DNA Control Sample (DCS) were thawed at room temperature (RT) and mixed by vortexing. AXP was kept at RT, and DCS was stored on ice. NEBNext FFPE DNA Repair Mix and NEBNext Ultra II End Repair/dA-Tailing reagents were thawed on ice, mixed by gentle inversion, and briefly centrifuged. DNA input was adjusted to 400 ng per sample (for >4 barcodes) or 1000 ng per sample (for ≤4 barcodes) in a 0.2 mL PCR tube. The volume was brought to 12 µL using nuclease-free water (Table 7).

Component	Volume [µL]
DNA sample (adjusted to 400 or 1000 ng)	12
NEBNext FFPE DNA Repair Buffer	0.875
Ultra II End-prep Reaction Buffer	0.875
Ultra II End-prep Enzyme Mix	0.75
NEBNext FFPE DNA Repair Mix	0.5

Table 7: Reaction mix for DNA repair and end-prep.

Samples were mixed by pipetting, spun down, and incubated at 20°C for 5 minutes followed by 65°C for 5 minutes. Each sample was transferred to a 1.5 mL DNA LoBind tube and purified using 15 µL AXP beads. After 5 minutes of incubation on a rotator, beads were pelleted on a magnetic rack, washed twice with 200 µL 80% ethanol, and air-dried. DNA was eluted in 10 µL nuclease-free water.

9.12.2 Native Barcoding Ligation

NEB Blunt/TA Ligase Master Mix, Clear Cap EDTA, and Native Barcodes (NB01–NB24) were thawed, mixed, and kept on ice. Each sample was ligated to a unique barcode in a 0.2 mL PCR tube (Table 8).

Component	Volume [µL]
End-prepped DNA	7.5
Native Barcode (NB01–NB24)	2.5
Blunt/TA Ligase Master Mix	10

Table 8: Reaction mix for native barcode ligation.

Samples were incubated at RT for 20 minutes, followed by the addition of 2 µL EDTA. All barcoded samples were pooled and purified using 0.4× AXP beads. After bead binding and

washing twice with 700 µL 80% ethanol, DNA was eluted in 35 µL nuclease-free water after a 10-minute incubation at 37°C with intermittent flicking. Beads were pelleted, and the eluate was retained.

9.12.3 Adapter Ligation and Cleanup

NEBNext Quick Ligation reagents, Native Adapter (NA), and Quick T4 DNA Ligase were thawed and mixed. In a 1.5 mL DNA LoBind tube, adapter ligation was performed (Table 9).

Component	**Volume (µL)**
Pooled barcoded DNA	30
Native Adapter (NA)	5
Quick Ligation Reaction Buffer (5×)	10
Quick T4 DNA Ligase	5

Table 9: Reaction mix for adapter ligation.

The reaction was incubated at RT for 20 minutes and purified with 20 µL AXP beads. Beads were washed twice with 125 µL Long Fragment Buffer (LFB), and DNA was eluted in 15 µL Elution Buffer (EB) following a 10-minute incubation at 37°C. Beads were pelleted and 15 µL eluate was retained.

9.12.4 Flow Cell Priming and Library Loading

Sequencing Buffer (SB), Library Beads (LIB), Flow Cell Tether (FCT), and Flow Cell Flush (FCF) were thawed, mixed, and placed on ice. The priming mix was prepared by combining 1170 µL FCF, 5 µL 50 mg/mL BSA, and 30 µL FCT. A MinION flow cell was mounted and primed by withdrawing 20–30 µL from the priming port and loading 800 µL of priming mix. After 5 minutes, a library mix was prepared (Table 10).

Component	Volume [µL]
Sequencing Buffer (SB)	37.5
Library Beads (LIB)	25.5
DNA Library	12

Table 10: Final library mix prepared for SpotON flow cell loading.

Following the addition of 200 µL priming mix to the priming port, 75 µL of the prepared library was loaded dropwise into the SpotON sample port. The flow cell was closed, and

sequencing was initiated using MinKNOW v23.11.5.

9.13 RNA Extraction and cDNA Synthesis

9.13.1 Culture Preparation and Cell Lysis

Single colonies of yeast and bacterial strains were revived from cryogenic stocks by streaking onto Potato Dextrose Agar (PDA) and King's B agar plates, respectively, followed by incubation at 22°C for 24 hours. Afterwards, a single colony from each strain was inoculated into 10 mL of its corresponding medium and cultured for 24 hours at 22°C with shaking at 180 rpm. Each culture was then adjusted to an OD_{600} of 0.4 in its respective medium, and yeast cultures were combined individually with the *P. extremaustralis* B2 strain in a 1:1 ratio. Single cultures of yeast and B2 were refilled to their original volumes following combination. After an additional incubation of 3 to 4 hours at 22°C and 180 rpm, each culture's OD_{600} was set to 0.8 in their respective media (for yeast–bacteria co-cultures, a 1:1 medium mixture was used). The samples were then further used in two ways: firstly, they were centrifuged at 19150 rcf at 4°C for 5 minutes and subsequently the pellet was frozen in liquid nitrogen to gather RNA from liquid cultures. Secondly, background bacteria were prepared identical to the confrontation assay culture preparation, the lawn was plated and the treatment dropped onto the plate. After 3 days of incubation, the yeast or yeast - bacterium culture in the center was scraped off the plate, frozen in liquid nitrogen and used for RNA extraction.

9.13.2 RNA Extraction

These samples were then processed using the Qiagen RNeasy MiniKit from Yeast and therefore the pellets were loosened by flicking the tube and 600 µL Buffer RLT was added and vortexed. Next, the samples were added to acid washed Zirconia beads (mixture of 0.1 mm, 0.5 mm and 2.3 mm diameter beads) and the cells were lysed using a Bertin Technologies Precellys Evolution cell lyser with added Bertin Technologies Cryolys advanced temperature controller. Therefore, the machine was pre-cooled to at least -15°C and the samples were lysed according to protocol (Table 11).

Tube	2 mL	Cryo	Off
Speed	6300 rpm	Temp	0°C
Cycle	2x 40 sec	Mode	Normal
Pause	15 sec		

Table 11: Cell lysis settings used with the Precellys Evolution tissue homogenizer (Bertin Technologies). Parameters include tube volume, speed, cycle duration, and cooling settings used for effective disruption of microbial cells.

The tubes were removed from the homogenizer and briefly allowed to settle, after which the lysate was transferred to fresh tubes. The samples were then centrifuged at 19150 rcf for 2 minutes, and the resulting supernatant was transferred to new tubes. One volume of 70% ethanol was added to the lysate and mixed thoroughly by pipetting. Subsequent steps followed the protocol outlined in the Qiagen RNeasy Plant Mini Kit manual. Briefly, each sample was transferred to an RNeasy spin column placed within a 2 mL collection tube and centrifuged at 19150 rcf for 20 seconds. The flow-through was discarded, and 700 µL of Buffer RW1 was added, followed by centrifugation under the same conditions. After discarding the flow-through again, 500 µL Buffer RPE was added, and the columns were centrifuged at 19150 rcf for another 20 seconds. Following removal of the flow-through, a second 500 µL aliquot of Buffer RPE was added, and columns were centrifuged for 2 minutes at 19150 rcf. Next, each spin column was placed in a new collection tube, centrifuged at 19150 rcf for 1 minute to remove residual ethanol, and finally transferred to a clean 1.5 mL tube. RNA was eluted by adding 30 µL of RNase-free water directly onto each spin column membrane, followed by centrifugation at 19150 rcf for 1 minute.

9.13.3 DNase Treatment

Next, DNase treatment was carried out to eliminate any remaining DNA from the RNA samples, using the Thermo Fisher TURBO DNA-free kit. To each RNA sample, 0.1 volume of 10x TURBO DNase Buffer and 1 µL TURBO DNase enzyme were added, and the mixture was gently mixed. The samples were incubated at 37°C for 25 minutes. Afterward, the DNase Inactivation Reagent was thoroughly resuspended, and 2 µL was added to each sample and mixed carefully. The tubes were incubated at room temperature for 5 minutes, occasionally flicked to ensure proper mixing, and then centrifuged at 10000 rcf for 90 seconds. Finally, the supernatant containing the purified RNA was transferred to fresh tubes.

9.13.4 cDNA Synthesis

cDNA synthesis was performed following the Invitrogen SuperScript IV Reverse Transcriptase protocol. The RNA-primer mixture was prepared by combining the components listed in Table 12 in a reaction tube.

Component	Volume for 20 µL reaction [µL]
Oligo(dT) Primer	1
10 mM dNTP Mix	1
Template RNA	11
Nuclease Free Water	7

Table 12: Preparation of the RNA-primer mix for a 20 µL reverse transcription reaction using the Invitrogen SuperScript IV Reverse Transcriptase protocol. The mix includes template RNA, oligo(dT) primers, dNTPs, and nuclease-free water prior to denaturation and primer annealing.

The RNA-primer mix was heated to 65°C for 5 minutes, followed by an incubation on ice for at least 1 minute. Next, the Reverse Transcriptase reaction mix (RT reaction mix) was prepared by combining the following agents in Table 13.

Component	Volume for 7 µL reaction [µL]
5x SSIV Buffer	4
100mM DTT	1
RNaseOUT Recombinant RNase Inhibitor	1
SuperScript IV Reverse Transcriptase (200 U/µL)	1

Table 13: Composition of the reverse transcription reaction mix for a 7 µL reaction using SuperScript IV Reverse Transcriptase (Invitrogen). The mix was prepared according to the manufacturer's protocol and used for first-strand cDNA synthesis.

After mixing the RNA-primer mixture and the RT reaction mix in a 1:1 ratio, the sample was incubated initially at 53°C for 10 minutes, followed by a second incubation at 80°C for 10 minutes. Additionally, a step not included in the original Invitrogen protocol was performed by adding 1 µL of RNase A to each sample, followed by incubation at 37°C for 20 minutes to degrade any residual RNA.

9.13.5 Magnetic Bead Clean-Up

Following cDNA synthesis, a bead-based clean-up was performed to improve cDNA purity. Magnetic beads (SpeedBead Magnetic Carboxylate Modified Particles, Cytiva) were first resuspended by vortexing. In a 1.5 mL tube, 20 µL of cDNA was mixed with 1.8 volumes

of beads by pipetting. After incubating the mixture at room temperature for 5 minutes, the tubes were placed on a magnetic rack for at least 2 minutes to separate the beads. The supernatant was carefully removed, leaving behind approximately 5 µL. While keeping the tubes on the rack, 200 µL of 70% ethanol was gently added without disturbing the pellet, incubated for 30 seconds, and then removed. This ethanol wash was repeated a total of three times. The samples were then air-dried for 15 minutes, removed from the magnetic rack, and resuspended in 50 µL of nuclease-free water. After thorough mixing by pipetting, the samples were incubated with shaking at 500 rpm for at least one hour. Finally, the tubes were returned to the magnetic rack, incubated for at least one minute, and the supernatant containing the purified cDNA was transferred to a fresh tube.

9.14 RNA Sequencing

The purified and cleaned cDNA samples were send to BMKGENE for sequencing. Samples were prepared according to the sequencing company's instructions (Table 14). Sequencing was carried out on the Illumina NovaSeq 6000 platform (PE150), generating approximately 9Gb of data per sample.

Concentration	$\geq$ 100 ng/µL
Volume	20 µL

Table 14: Sample quality and quantity requirements for RNA sequencing submission to BMKGENE. Each RNA sample was required to have a concentration of at least 100 ng/µL and a total volume of 20 µL.

9.15 qPCR Validation of Candidate Genes

To validate the expression data gathered from RNA sequencing analysis, Real-Time qPCR was performed. Therefore, 10 µL qPCR Master Mix (Table 15) and 5 µL cDNA template was added to a 96-well PCR plate (Hard-Shell PCR Plates 96-well, thin-well, Bio Rad). The plates were then spun down for a few seconds and put into a CFX Connect Real-Time PCR Detection System (Bio Rad).

Component	Volume for 10 µL reaction [µL]
SYBR Green Supermix	7.5
Nuclease Free Water	1.9
10 µM Primer Forward	0.3
10 µM Primer Reverse	0.3

Table 15: Composition of the quantitative PCR (qPCR) master mix for a 10 µL reaction volume. The reaction was prepared using SsoAdvanced Universal SYBR Green Supermix (Bio-Rad), with final primer (Table 5) concentrations of 300 nM each.

Using the CFX Maestro Software (Bio Rad), the qPCR was run on reactions with a sample volume of 20 µL (Table 16).

Step	Temperature [°C]	Time [s]	Cycles
1	95.0	10	39
2	60.0	30	
3	65.0 - 95.0 in 0.5 steps	20 per step	1

Table 16: Thermal cycling protocol used for quantitative PCR on the CFX Connect Real-Time PCR Detection System. The protocol includes 39 amplification cycles (steps 1 and 2) followed by a melt curve analysis (step 3) with temperature increments of 0.5°C.

9.16 Computational Analyses

All computational analysis were performed either on a de.NBI sourced virtual machine or the BinAC Server Cluster.

Acknowledgement:

The authors acknowledge support by the High Performance and Cloud Computing Group at the Zentrum für Datenverarbeitung of the University of Tübingen, the state of Baden-Württemberg through bwHPC and the German Research Foundation (DFG) through grant no INST 37/935-1 FUGG.

Code available on GitHub: https://github.com/SamQu25

10 Supplementary Data

10.1 Genbank Accession Numbers for GH-Family Search

GenBank ID	Species Name
GCA_014825545.1	*Cystofilobasidium capitatum*
GCA_014825535.1	*Cystofilobasidium bisporidii*
GCA_014825765.1	*Cystofilobasidium macerans*
GCA_014825675.1	*Cystofilobasidium ferigula*
GCA_014825555.1	*Cystofilobasidium bisporidii*
GCA_014825745.1	*Cystofilobasidium macerans*
GCA_014825955.1	*Cystofilobasidium ferigula*

Table S1: GenBank accession numbers and corresponding species names for genome assemblies used in GH family analysis.

10.2 Genome Assembly Statistics

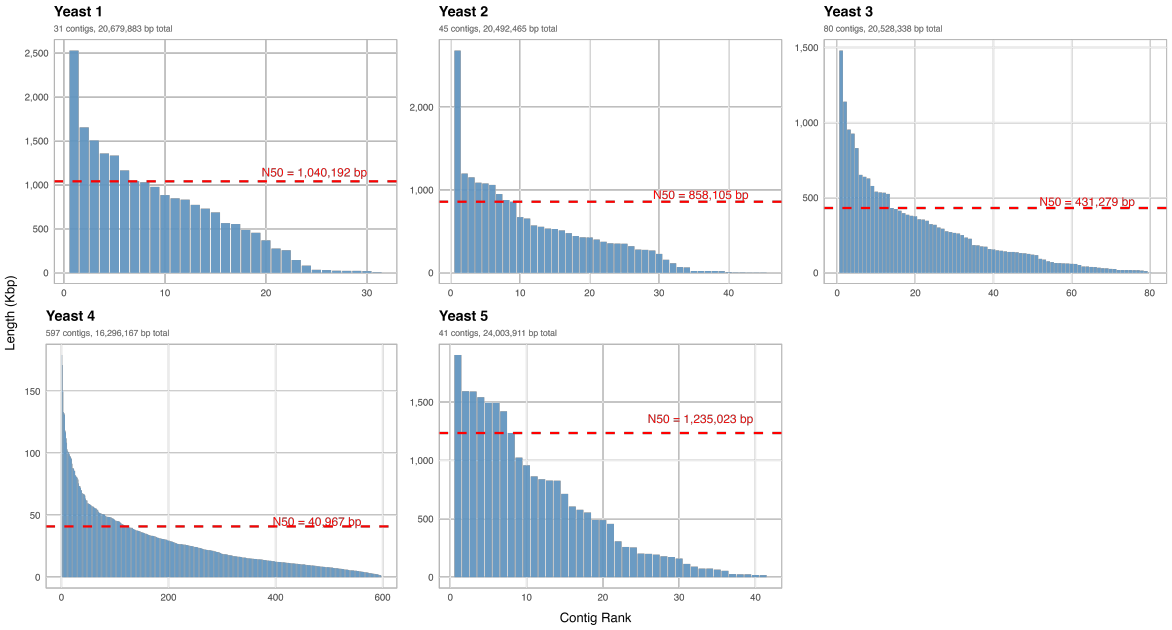

Figure S1: Summarized plots for the contig-level yeast genome assemblies displaying length per contig, contig number, N50 and total assembly length.

10.3 Preliminary Infection Assay

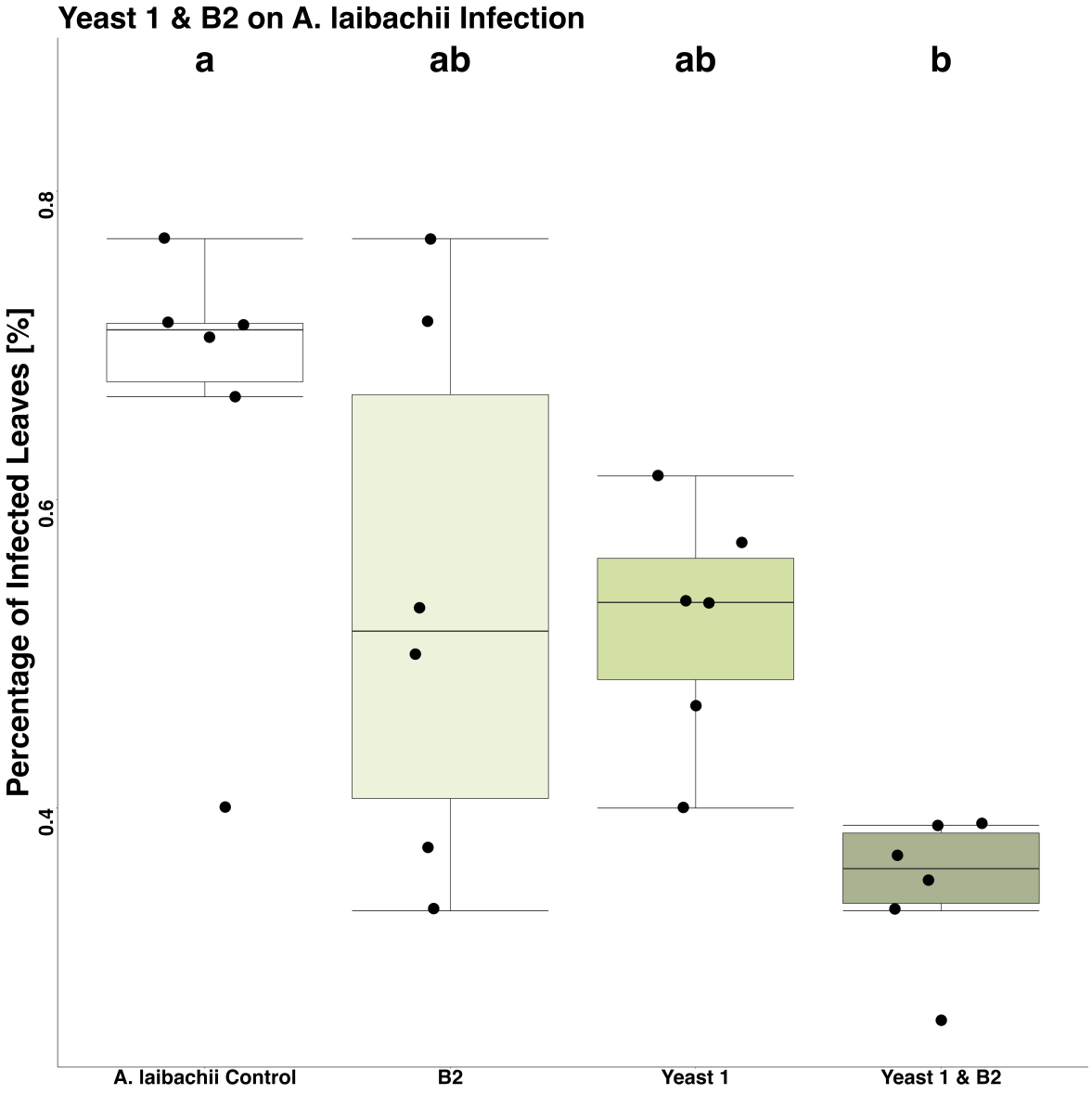

Figure S2: Preliminary infection assay results of *A. laibachii* infection of non-sterile *A. thaliana* plants. Percentage of infected leaves plotted for each Treatment. Significance test and grouping performed using a Benjamini-Hochberg adjusted Dunn's Test $p - value \leq 0.01$.

11 References

Agler, M. T., Ruhe, J., Kroll, S., Morhenn, C., Kim, S.-T., Weigel, D., & Kemen, E. M. (2016). Microbial hub taxa link host and abiotic factors to plant microbiome variation (M. K. Waldor, Ed.). *PLOS Biology*, *14*(1), e1002352. https://doi.org/10.1371/journal.pbio.1002352

Ali, M., Ahmad, Z., Ashraf, M. F., & Dong, W. (2021). Maize endophytic microbial-communities revealed by removing PCR and 16s rRNA sequencing and their synthetic applications to suppress maize banded leaf and sheath blight. *Microbiological Research*, *242*, 126639. https://doi.org/10.1016/j.micres.2020.126639

Almario, J., Mahmoudi, M., Kroll, S., Agler, M., Placzek, A., Mari, A., & Kemen, E. (2022). The leaf microbiome of *Arabidopsis* displays reproducible dynamics and patterns throughout the growing season (D. S. Guttman, Ed.). *mBio*, *13*(3), e02825–21. https://doi.org/10.1128/mbio.02825-21

Backer, R., Rokem, J. S., Ilangumaran, G., Lamont, J., Praslickova, D., Ricci, E., Subramanian, S., & Smith, D. L. (2018). Plant growth-promoting rhizobacteria: Context, mechanisms of action, and roadmap to commercialization of biostimulants for sustainable agriculture. *Frontiers in Plant Science*, *9*, 1473. https://doi.org/10.3389/fpls.2018.01473

Bailly, A., & Weisskopf, L. (2017). Mining the volatilomes of plant-associated microbiota for new biocontrol solutions. *Frontiers in Microbiology*, *8*, 1638. https://doi.org/10.3389/fmicb.2017.01638

Bakker, M. G., Schlatter, D. C., Otto-Hanson, L., & Kinkel, L. L. (2014). Diffuse symbioses: Roles of plant–plant, plant–microbe and microbe–microbe interactions in structuring the soil microbiome. *Molecular Ecology*, *23*(6), 1571–1583. https://doi.org/10.1111/mec.12571

Balint-Kurti, P., Simmons, S. J., Blum, J. E., Ballaré, C. L., & Stapleton, A. E. (2010). Maize leaf epiphytic bacteria diversity patterns are genetically correlated with resistance to fungal pathogen infection. *Molecular Plant-Microbe Interactions®*, *23*(4), 473–484. https://doi.org/10.1094/MPMI-23-4-0473

Barnett, H. L. (1963). The nature of mycoparasitism by fungi. *Annual Review of Microbiology*, *17*(1), 1–14. https://doi.org/10.1146/annurev.mi.17.100163.000245

Barret, M., Briand, M., Bonneau, S., Préveaux, A., Valière, S., Bouchez, O., Hunault, G., Simoneau, P., & Jacques, M.-A. (2015). Emergence shapes the structure of the seed microbiota (H. L. Drake, Ed.). *Applied and Environmental Microbiology*, *81*(4), 1257–1266. https://doi.org/10.1128/AEM.03722-14

Beattie, G. A., & Marcell, L. M. (2002). Comparative dynamics of adherent and nonadherent bacterial populations on maize leaves. *Phytopathology®*, *92*(9), 1015–1023. https://doi.org/10.1094/PHYTO.2002.92.9.1015

Berger, S., Sinha, A. K., & Roitsch, T. (2007). Plant physiology meets phytopathology: Plant primary metabolism and plant pathogen interactions. *Journal of Experimental Botany*, *58*(15), 4019–4026. https://doi.org/10.1093/jxb/erm298

Berkhout, M. D., Plugge, C. M., & Belzer, C. (2022). How microbial glycosyl hydrolase activity in the gut mucosa initiates microbial cross-feeding. *Glycobiology*, *32*(3), 182–200. https://doi.org/10.1093/glycob/cwab105

Bernal, P., Allsopp, L. P., Filloux, A., & Llamas, M. A. (2017). The *Pseudomonas putida* t6ss is a plant warden against phytopathogens. *The ISME Journal*, *11*(4), 972–987. https://doi.org/10.1038/ismej.2016.169

Bienhold, C., Zinger, L., Boetius, A., & Ramette, A. (2016). Diversity and biogeography of bathyal and abyssal seafloor bacteria (C. A. Kellogg, Ed.). *PLOS ONE*, *11*(1), e0148016. https://doi.org/10.1371/journal.pone.0148016

Boureau, T., Routtu, J., Roine, E., Taira, S., & Romantschuk, M. (2002). Localization of *hrpA* -induced *Pseudomonas syringae* pv. *tomato* DC3000 in infected tomato leaves. *Molecular Plant Pathology*, *3*(6), 451–460. https://doi.org/10.1046/j.1364-3703.2002.00139.x

Bulgarelli, D., Schlaeppi, K., Spaepen, S., Van Themaat, E. V. L., & Schulze-Lefert, P. (2013). Structure and functions of the bacterial microbiota of plants. *Annual Review of Plant Biology*, *64*(1), 807–838. https://doi.org/10.1146/annurev-arplant-050312-120106

Bush, K. (1988). Beta-lactamase inhibitors from laboratory to clinic. *Clinical Microbiology Reviews*, *1*(1), 109–123. https://doi.org/10.1128/CMR.1.1.109

Cai, J., Jiang, Y., Ritchie, E. S., Macho, A. P., Yu, F., & Wu, D. (2023). Manipulation of plant metabolism by pathogen effectors: More than just food. *FEMS Microbiology Reviews*, *47*(2), fuad007. https://doi.org/10.1093/femsre/fuad007

Capy, P., Gasperi, G., Biémont, C., & Bazin, C. (2000). Stress and transposable elements: Co-evolution or useful parasites? *Heredity*, *85*(2), 101–106. https://doi.org/10.1046/j.1365-2540.2000.00751.x

Carlström, C. I., Field, C. M., Bortfeld-Miller, M., Müller, B., Sunagawa, S., & Vorholt, J. A. (2019). Synthetic microbiota reveal priority effects and keystone strains in the arabidopsis phyllosphere. *Nature Ecology & Evolution*, *3*(10), 1445–1454. https://doi.org/10.1038/s41559-019-0994-z

Cavalier-Smith, T. (1992). Symbiosis as a source of evolutionary innovation: Speciation and morphogenesis. *7*(12), 422–423.

CAZypedia.org. (2025, April 3). *Glycoside hydrolase family 25*. Retrieved March 4, 2025, from https://www.cazypedia.org/index.php/Glycoside_Hydrolase_Family_25#:~:text=Glycoside%20hydrolases%20%20of%20family,The%20activity%20of%20GH25%20enzymes

Chai, A., Yuan, L., Li, X., Li, L., Shi, Y., Xie, X., & Li, B. (2023). Effect of temperature and humidity on dynamics and transmission of pseudomonas amygdali pv. lachrymans aerosols. *Frontiers in Plant Science*, *14*, 1087496. https://doi.org/10.3389/fpls.2023.1087496

Charkowski, A. O. (2016). Opportunistic pathogens of terrestrial plants [Series Title: Advances in Environmental Microbiology]. In C. J. Hurst (Ed.), *The rasputin effect: When commensals and symbionts become parasitic* (pp. 147–168, Vol. 3). Springer International Publishing. https://doi.org/10.1007/978-3-319-28170-4_7

Chi, M., Li, G., Liu, Y., Liu, G., Li, M., Zhang, X., Sun, Z., Sui, Y., & Liu, J. (2015). Increase in antioxidant enzyme activity, stress tolerance and biocontrol efficacy of pichia kudriavzevii with the transition from a yeast-like to biofilm morphology. *Biological Control*, *90*, 113–119. https://doi.org/10.1016/j.biocontrol.2015.06.006

Chin-A-Woeng, T. F. C., Bloemberg, G. V., & Lugtenberg, B. J. J. (2003). Phenazines and their role in biocontrol by *Pseudomonas* bacteria. *New Phytologist*, *157*(3), 503–523. https://doi.org/10.1046/j.1469-8137.2003.00686.x

Coleman, J. J., Ghosh, S., Okoli, I., & Mylonakis, E. (2011). Antifungal activity of microbial secondary metabolites (V. Chaturvedi, Ed.). *PLoS ONE*, *6*(9), e25321. https://doi.org/10.1371/journal.pone.0025321

Cortes-Sánchez Alejandro. (2011). Production of glycolipids with antimicrobial activity by ustilago maydis FBD12 in submerged culture. *African Journal of Microbiology Research*, *5*(17). https://doi.org/10.5897/AJMR10.814

Cox, C. D., & Adams, P. (1985). Siderophore activity of pyoverdin for pseudomonas aeruginosa. *Infection and Immunity*, *48*(1), 130–138. https://doi.org/10.1128/iai.48.1.130-138.1985

Cox, C. D., & Graham, R. (1979). Isolation of an iron-binding compound from pseudomonas aeruginosa. *Journal of Bacteriology*, *137*(1), 357–364. https://doi.org/10.1128/jb.137.1.357-364.1979

Cugini, C., Morales, D. K., & Hogan, D. A. (2010). Candida albicans-produced farnesol stimulates pseudomonas quinolone signal production in LasR-defective pseudomonas aeruginosa strains. *Microbiology*, *156*(10), 3096–3107. https://doi.org/10.1099/mic.0.037911-0

Dawan, J., Li, Y., Lu, F., He, X., & Ahn, J. (2022). Role of efflux pump-mediated antibiotic resistance in quorum sensing-regulated biofilm formation by salmonella typhimurium. *Pathogens*, *11*(2), 147. https://doi.org/10.3390/pathogens11020147

De Boer, W., Leveau, J. H. J., Kowalchuk, G. A., Gunnewiek, P. J. A. K., Abeln, E. C. A., Figge, M. J., Sjollema, K., Janse, J. D., & Van Veen, J. A. (2004). Collimonas fungivorans gen. nov., sp. nov., a chitinolytic soil bacterium with the ability to grow on living fungal hyphae. *International Journal of Systematic and Evolutionary Microbiology*, *54*(3), 857–864. https://doi.org/10.1099/ijs.0.02920-0

De Kempeneer, L., Sercu, B., Vanbrabant, W., Van Langenhove, H., & Verstraete, W. (2004). Bioaugmentation of the phyllosphere for the removal of toluene from indoor air. *Applied Microbiology and Biotechnology*, *64*(2), 284–288. https://doi.org/10.1007/s00253-003-1415-3

Debray, R., Conover, A., & Koskella, B. (2024, April 23). Phages indirectly maintain plant pathogen defense through regulation of the commensal microbiome. https://doi.org/10.1101/2024.04.23.590639

Desirò, A., Salvioli, A., Ngonkeu, E. L., Mondo, S. J., Epis, S., Faccio, A., Kaech, A., Pawlowska, T. E., & Bonfante, P. (2014). Detection of a novel intracellular microbiome hosted in arbuscular mycorrhizal fungi. *The ISME Journal*, *8*(2), 257–270. https://doi.org/10.1038/ismej.2013.151

Dubern, J.-F., Lugtenberg, B. J. J., & Bloemberg, G. V. (2006). The *ppuI-rsaL-ppuR* quorum-sensing system regulates biofilm formation of *Pseudomonas putida* PCL1445 by controlling biosynthesis of the cyclic lipopeptides putisolvins i and II. *Journal of Bacteriology*, *188*(8), 2898–2906. https://doi.org/10.1128/JB.188.8.2898-2906.2006

Eberl, L. (1999). N-acyl homoserinelactone-mediated gene regulation in gram-negative bacteria. *Systematic and Applied Microbiology*, *22*(4), 493–506. https://doi.org/10.1016/S0723-2020(99)80001-0

Edwards, J., Johnson, C., Santos-Medellín, C., Lurie, E., Podishetty, N. K., Bhatnagar, S., Eisen, J. A., & Sundaresan, V. (2015). Structure, variation, and assembly of the root-associated microbiomes of rice. *Proceedings of the National Academy of Sciences*, *112*(8). https://doi.org/10.1073/pnas.1414592112

Eitzen, K., Sengupta, P., Kroll, S., Kemen, E., & Doehlemann, G. (2021). A fungal member of the arabidopsis thaliana phyllosphere antagonizes albugo laibachii via a GH25 lysozyme. *eLife*, *10*, e65306. https://doi.org/10.7554/eLife.65306

Essiedu, J. A., Adepoju, F. O., & Ivantsova, M. N. (2020). Benefits and limitations in using biopesticides: A review, 080002. https://doi.org/10.1063/5.0032223

Estrela, S., Trisos, C. H., & Brown, S. P. (2012). From metabolism to ecology: Cross-feeding interactions shape the balance between polymicrobial conflict and mutualism. *The American Naturalist*, *180*(5), 566–576. https://doi.org/10.1086/667887

Fan, Y., & Lin, X. (2020). An intergenic "safe haven" region in cryptococcus neoformans serotype d genomes. *Fungal Genetics and Biology*, *144*, 103464. https://doi.org/10.1016/j.fgb.2020.103464

Faust, K., Lahti, L., Gonze, D., De Vos, W. M., & Raes, J. (2015). Metagenomics meets time series analysis: Unraveling microbial community dynamics. *Current Opinion in Microbiology*, *25*, 56–66. https://doi.org/10.1016/j.mib.2015.04.004

Fell, J. W., Roeijmans, H., & Boekhout, T. (1999). Cystofilobasidiales, a new order of basidiomycetous yeasts. *International Journal of Systematic and Evolutionary Microbiology*, *49*(2), 907–913. https://doi.org/10.1099/00207713-49-2-907

Fett, W. F., Osman, S. F., & Dunn, M. F. (1987). Auxin production by plant-pathogenic pseudomonads and xanthomonads. *Applied and Environmental Microbiology*, *53*(8), 1839–1845. https://doi.org/10.1128/aem.53.8.1839-1845.1987

Filkins, L. M., Graber, J. A., Olson, D. G., Dolben, E. L., Lynd, L. R., Bhuju, S., & O'Toole, G. A. (2015). Coculture of staphylococcus aureus with pseudomonas aeruginosa drives s. aureus towards fermentative metabolism and reduced viability in a cystic fibrosis model (V. J. DiRita, Ed.). *Journal of Bacteriology*, *197*(14), 2252–2264. https://doi.org/10.1128/JB.00059-15

Finkel, O. M., Burch, A. Y., Lindow, S. E., Post, A. F., & Belkin, S. (2011). Geographical location determines the population structure in phyllosphere microbial communities of a salt-excreting desert tree. *Applied and Environmental Microbiology*, *77*(21), 7647–7655. https://doi.org/10.1128/AEM.05565-11

Fitzpatrick, D. A. (2012). Horizontal gene transfer in fungi. *FEMS Microbiology Letters*, *329*(1), 1–8. https://doi.org/10.1111/j.1574-6968.2011.02465.x

Floudas, D., Binder, M., Riley, R., Barry, K., Blanchette, R. A., Henrissat, B., Martínez, A. T., Otillar, R., Spatafora, J. W., Yadav, J. S., Aerts, A., Benoit, I., Boyd, A., Carlson, A., Copeland, A., Coutinho, P. M., De Vries, R. P., Ferreira, P., Findley, K., ... Hibbett, D. S. (2012). The paleozoic origin of enzymatic lignin decomposition reconstructed from 31 fungal genomes. *Science*, *336*(6089), 1715–1719. https://doi.org/10.1126/science.1221748

Flues, S., Bass, D., & Bonkowski, M. (2017). Grazing of leaf-associated cercomonads (protists: Rhizaria: Cercozoa) structures bacterial community composition and function. *Environmental Microbiology*, *19*(8), 3297–3309. https://doi.org/10.1111/1462-2920.13824

Fukami, T. (2015). Historical contingency in community assembly: Integrating niches, species pools, and priority effects. *Annual Review of Ecology, Evolution, and Systematics*, *46*(1), 1–23. https://doi.org/10.1146/annurev-ecolsys-110411-160340

Gafni, A., Calderon, C. E., Harris, R., Buxdorf, K., Dafa-Berger, A., Zeilinger-Reichert, E., & Levy, M. (2015). Biological control of the cucurbit powdery mildew pathogen podosphaera xanthii by means of the epiphytic fungus pseudozyma aphidis and parasitism as a mode of action. *Frontiers in Plant Science*, *6*. https://doi.org/10.3389/fpls.2015.00132

Galtier, N., & Daubin, V. (2008). Dealing with incongruence in phylogenomic analyses. *Philosophical Transactions of the Royal Society B: Biological Sciences*, *363*(1512), 4023–4029. https://doi.org/10.1098/rstb.2008.0144

Gehring, C. A., Sthultz, C. M., Flores-Rentería, L., Whipple, A. V., & Whitham, T. G. (2017). Tree genetics defines fungal partner communities that may confer drought tolerance. *Proceedings of the National Academy of Sciences*, *114*(42), 11169–11174. https://doi.org/10.1073/pnas.1704022114

Germerodt, S., Bohl, K., Lück, A., Pande, S., Schröter, A., Kaleta, C., Schuster, S., & Kost, C. (2016). Pervasive selection for cooperative cross-feeding in bacterial communities (O. A. Igoshin, Ed.). *PLOS Computational Biology*, *12*(6), e1004986. https://doi.org/10.1371/journal.pcbi.1004986

Goebels, C., Thonn, A., Gonzalez-Hilarion, S., Rolland, O., Moyrand, F., Beilharz, T. H., & Janbon, G. (2013). Introns regulate gene expression in cryptococcus neoformans in a pab2p dependent pathway (H. D. Madhani, Ed.). *PLoS Genetics*, *9*(8), e1003686. https://doi.org/10.1371/journal.pgen.1003686

Gómez-Pérez, D., Schmid, M., Chaudhry, V., Hu, Y., Velic, A., Maček, B., Ruhe, J., Kemen, A., & Kemen, E. (2023). Proteins released into the plant apoplast by the obligate parasitic protist *Albugo* selectively repress phyllosphere-associated bacteria. *New Phytologist*, *239*(6), 2320–2334. https://doi.org/10.1111/nph.18995

Gomila, M., PeÃ±a, A., Mulet, M., Lalucat, J., & GarcÃa-ValdÃ©s, E. (2015). Phylogenomics and systematics in pseudomonas. *Frontiers in Microbiology*, *6*. https://doi.org/10.3389/fmicb.2015.00214

Gouda, S., Kerry, R. G., Das, G., Paramithiotis, S., Shin, H.-S., & Patra, J. K. (2018). Revitalization of plant growth promoting rhizobacteria for sustainable development in agriculture. *Microbiological Research*, *206*, 131–140. https://doi.org/10.1016/j.micres.2017.08.016

Gouka, L., Raaijmakers, J. M., & Cordovez, V. (2022). Ecology and functional potential of phyllosphere yeasts. *Trends in Plant Science*, *27*(11), 1109–1123. https://doi.org/10.1016/j.tplants.2022.06.007

Gouka, L., Vogels, C., Hansen, L. H., Raaijmakers, J. M., & Cordovez, V. (2022). Genetic, phenotypic and metabolic diversity of yeasts from wheat flag leaves. *Frontiers in Plant Science*, *13*, 908628. https://doi.org/10.3389/fpls.2022.908628

Goulson, D. (2014). Pesticides linked to bird declines. *Nature*, *511*(7509), 295–296. https://doi.org/10.1038/nature13642

Guetsky, R., Shtienberg, D., Elad, Y., Fischer, E., & Dinoor, A. (2002). Improving biological control by combining biocontrol agents each with several mechanisms of disease suppression. *Phytopathology®*, *92*(9), 976–985. https://doi.org/10.1094/PHYTO.2002.92.9.976

Gusa, A., Yadav, V., Roth, C., Williams, J. D., Shouse, E. M., Magwene, P., Heitman, J., & Jinks-Robertson, S. (2023). Genome-wide analysis of heat stress-stimulated transposon mobility in the human fungal pathogen *Cryptococcus deneoformans*. *Proceedings of the National Academy of Sciences*, *120*(4), e2209831120. https://doi.org/10.1073/pnas.2209831120

Harcombe, W. (2010). NOVEL COOPERATION EXPERIMENTALLY EVOLVED BETWEEN SPECIES. *Evolution*. https://doi.org/10.1111/j.1558-5646.2010.00959.x

Hash, J. H., & Rothlauf, M. V. (1967). The n,o-diacetylmuramidase of chalaropsis species. i. purification and crystallization. *The Journal of Biological Chemistry*, *242*(23), 5586–5590.

Helmann, T. C., Deutschbauer, A. M., & Lindow, S. E. (2019). Genome-wide identification of *Pseudomonas syringae* genes required for fitness during colonization of the leaf surface and apoplast. *Proceedings of the National Academy of Sciences*, *116*(38), 18900–18910. https://doi.org/10.1073/pnas.1908858116

Hess, M. C., Mesléard, F., & Buisson, E. (2019). Priority effects: Emerging principles for invasive plant species management. *Ecological Engineering*, *127*, 48–57. https://doi.org/10.1016/j.ecoleng.2018.11.011

Heyn, P., Kalinka, A. T., Tomancak, P., & Neugebauer, K. M. (2015). Introns and gene expression: Cellular constraints, transcriptional regulation, and evolutionary consequences. *BioEssays*, *37*(2), 148–154. https://doi.org/10.1002/bies.201400138

Hirano, S. S., & Upper, C. D. (1983). Ecology and epidemiology of foliar bacterial plant pathogens. *Annual Review of Phytopathology*, *21*(1), 243–270. https://doi.org/10.1146/annurev.py.21.090183.001331

Hoek, T. A., Axelrod, K., Biancalani, T., Yurtsev, E. A., Liu, J., & Gore, J. (2016). Resource availability modulates the cooperative and competitive nature of a microbial cross-feeding mutualism (N. Balaban, Ed.). *PLOS Biology*, *14*(8), e1002540. https://doi.org/10.1371/journal.pbio.1002540

Hogan, D. A., Vik, Å., & Kolter, R. (2004). A *Pseudomonas aeruginosa* quorum-sensing molecule influences *Candida albicans* morphology. *Molecular Microbiology*, *54*(5), 1212–1223. https://doi.org/10.1111/j.1365-2958.2004.04349.x

Hornby, J. M., Jensen, E. C., Lisec, A. D., Tasto, J. J., Jahnke, B., Shoemaker, R., Dussault, P., & Nickerson, K. W. (2001). Quorum sensing in the dimorphic fungus *Candida albicans* is mediated by farnesol. *Applied and Environmental Microbiology*, *67*(7), 2982–2992. https://doi.org/10.1128/AEM.67.7.2982-2992.2001

Horner, N. R., Grenville-Briggs, L. J., & Van West, P. (2012). The oomycete pythium oligandrum expresses putative effectors during mycoparasitism of phytophthora infestans and is amenable to transformation. *Fungal Biology*, *116*(1), 24–41. https://doi.org/10.1016/j.funbio.2011.09.004

Howlett, B. J. (2006). Secondary metabolite toxins and nutrition of plant pathogenic fungi. *Current Opinion in Plant Biology*, *9*(4), 371–375. https://doi.org/10.1016/j.pbi.2006.05.004

Hu, L., Robert, C. A. M., Cadot, S., Zhang, X., Ye, M., Li, B., Manzo, D., Chervet, N., Steinger, T., Van Der Heijden, M. G. A., Schlaeppi, K., & Erb, M. (2018). Root exudate metabolites drive plant-soil feedbacks on growth and defense by shaping the rhizosphere microbiota. *Nature Communications*, *9*(1), 2738. https://doi.org/10.1038/s41467-018-05122-7

Hunter, P. J., Hand, P., Pink, D., Whipps, J. M., & Bending, G. D. (2010). Both leaf properties and microbe-microbe interactions influence within-species variation in bacterial population diversity and structure in the lettuce (*Lactuca* species) phyllosphere. *Applied and Environmental Microbiology*, *76*(24), 8117–8125. https://doi.org/10.1128/AEM.01321-10

Hutchison, M. L., & Gross, D. C. (1997). Lipopeptide phytotoxins produced by *Pseudomonas syringae* pv. *syringae* : Comparison of the biosurfactant and ion channel-forming activities of syringopeptin and syringomycin. *Molecular Plant-Microbe Interactions®*, *10*(3), 347–354. https://doi.org/10.1094/MPMI.1997.10.3.347

Innerebner, G., Knief, C., & Vorholt, J. A. (2011). Protection of arabidopsis thaliana against leaf-pathogenic pseudomonas syringae by sphingomonas strains in a controlled model system. *Applied and Environmental Microbiology*, *77*(10), 3202–3210. https://doi.org/10.1128/AEM.00133-11

Into, P., Pontes, A., Sampaio, J. P., & Limtong, S. (2020). Yeast diversity associated with the phylloplane of corn plants cultivated in thailand. *Microorganisms*, *8*(1), 80. https://doi.org/10.3390/microorganisms8010080

Janbon, G., Ormerod, K. L., Paulet, D., Byrnes, E. J., Yadav, V., Chatterjee, G., Mullapudi, N., Hon, C.-C., Billmyre, R. B., Brunel, F., Bahn, Y.-S., Chen, W., Chen, Y., Chow, E. W. L., Coppée, J.-Y., Floyd-Averette, A., Gaillardin, C., Gerik, K. J., Goldberg, J., ... Dietrich, F. S. (2014). Analysis of the genome and transcriptome of cryptococcus neoformans var. grubii reveals complex RNA expression and microevolution leading to virulence attenuation (M. Freitag, Ed.). *PLoS Genetics*, *10*(4), e1004261. https://doi.org/10.1371/journal.pgen.1004261

Janecek, S. (1997). Alpha-amylase family: Molecular biology and evolution. *Progress in Biophysics and Molecular Biology*, *67*(1), 67–97. https://doi.org/10.1016/S0079-6107(97)00015-1

Jarrige, D., Haridas, S., Bleykasten-Grosshans, C., Joly, M., Nadalig, T., Sancelme, M., Vuilleumier, S., Grigoriev, I. V., Amato, P., & Bringel, F. (2022). High-quality genome of the basidiomycete yeast *Dioszegia hungarica* PDD-24b-2 isolated from cloud water (J. Heitman, Ed.). *G3*, *12*(12), jkac282. https://doi.org/10.1093/g3journal/jkac282

Joshi, F., Archana, G., & Desai, A. (2006). Siderophore cross-utilization amongst rhizospheric bacteria and the role of their differential affinities for fe3+ on growth stimulation under iron-limited conditions. *Current Microbiology*, *53*(2), 141–147. https://doi.org/10.1007/s00284-005-0400-8

Jubin, C., Serero, A., Loeillet, S., Barillot, E., & Nicolas, A. (2014). Sequence profiling of the *Saccharomyces cerevisiae* genome permits deconvolution of unique and multialigned reads for variant detection. *G3 Genes—Genomes—Genetics*, *4*(4), 707–715. https://doi.org/10.1534/g3.113.009464

Kadivar, H., & Stapleton, A. (2003). Ultraviolet radiation alters maize phyllosphere bacterial diversity. *Microbial Ecology*, *45*(4), 353–361. https://doi.org/10.1007/s00248-002-1065-5

Kämper, J., Kahmann, R., Bölker, M., Ma, L.-J., Brefort, T., Saville, B. J., Banuett, F., Kronstad, J. W., Gold, S. E., Müller, O., Perlin, M. H., Wösten, H. A. B., De Vries, R., Ruiz-Herrera, J., Reynaga-Peña, C. G., Snetselaar, K., McCann, M., Pérez-Martín, J., Feldbrügge, M., … Birren, B. W. (2006). Insights from the genome of the biotrophic fungal plant pathogen ustilago maydis. *Nature*, *444*(7115), 97–101. https://doi.org/10.1038/nature05248

Kelemen, O., Convertini, P., Zhang, Z., Wen, Y., Shen, M., Falaleeva, M., & Stamm, S. (2013). Function of alternative splicing. *Gene*, *514*(1), 1–30. https://doi.org/10.1016/j.gene.2012.07.083

Kemen, E., Gardiner, A., Schultz-Larsen, T., Kemen, A. C., Balmuth, A. L., Robert-Seilaniantz, A., Bailey, K., Holub, E., Studholme, D. J., MacLean, D., & Jones, J. D. G. (2011). Gene gain and loss during evolution of obligate parasitism in the white rust pathogen of arabidopsis thaliana (F. M. Ausubel, Ed.). *PLoS Biology*, *9*(7), e1001094. https://doi.org/10.1371/journal.pbio.1001094

Kemen, E., & Jones, J. D. (2012). Obligate biotroph parasitism: Can we link genomes to lifestyles? *Trends in Plant Science*, *17*(8), 448–457. https://doi.org/10.1016/j.tplants.2012.04.005

Kemen, E., Kemen, A. C., Rafiqi, M., Hempel, U., Mendgen, K., Hahn, M., & Voegele, R. T. (2005). Identification of a protein from rust fungi transferred from haustoria into infected plant cells. *Molecular Plant-Microbe Interactions®*, *18*(11), 1130–1139. https://doi.org/10.1094/MPMI-18-1130

Kemen, E., Mahmoudi, M., Hu, Y., Almario, J., Stincone, P., Tenzer, L.-M., Chaudhry, V., & Nieselt, K. (2025, March 14). Machine learning reveals biocontrol agents shaping disease protection in natural arabidopsis populations and synthetic communities. https://doi.org/10.21203/rs.3.rs-6130404/v1

Kniskern, J. M., Traw, M. B., & Bergelson, J. (2007). Salicylic acid and jasmonic acid signaling defense pathways reduce natural bacterial diversity on *Arabidopsis thaliana*. *Molecular Plant-Microbe Interactions®*, *20*(12), 1512–1522. https://doi.org/10.1094/MPMI-20-12-1512

Kohlmeier, S., Smits, T. H. M., Ford, R. M., Keel, C., Harms, H., & Wick, L. Y. (2005). Taking the fungal highway: Mobilization of pollutant-degrading bacteria by fungi. *Environmental Science & Technology*, *39*(12), 4640–4646. https://doi.org/10.1021/es047979z

Koskella, B., & Brockhurst, M. A. (2014). Bacteria–phage coevolution as a driver of ecological and evolutionary processes in microbial communities. *FEMS Microbiology Reviews*, *38*(5), 916–931. https://doi.org/10.1111/1574-6976.12072

Kourist, R., Bracharz, F., Lorenzen, J., Kracht, O. N., Chovatia, M., Daum, C., Deshpande, S., Lipzen, A., Nolan, M., Ohm, R. A., Grigoriev, I. V., Sun, S., Heitman, J., Brück, T., & Nowrousian, M. (2015). Genomics and transcriptomics analyses of the oil-accumulating basidiomycete yeast *Trichosporon oleaginosus* : Insights into substrate utilization and alternative evolutionary trajectories of fungal mating systems (B. G. Turgeon, Ed.). *mBio*, *6*(4), e00918–15. https://doi.org/10.1128/mBio.00918-15

Kover, P. X., & Schaal, B. A. (2002). Genetic variation for disease resistance and tolerance among *Arabidopsis thaliana* accessions. *Proceedings of the National Academy of Sciences*, *99*(17), 11270–11274. https://doi.org/10.1073/pnas.102288999

Kroll, S. (2018). *Microbial colonisation is steered by host-microbe and microbe-microbe interactions in the phyllosphere of arabidopsis thaliana* [Doctoral dissertation, Universität zu Köln].

Kruijt, M., Tran, H., & Raaijmakers, J. M. (2009). Functional, genetic and chemical characterization of biosurfactants produced by plant growth-promoting *Pseudomonas putida* 267. *Journal of Applied Microbiology*, *107*(2), 546–556. https://doi.org/10.1111/j.1365-2672.2009.04244.x

Kuiper, I., Lagendijk, E. L., Pickford, R., Derrick, J. P., Lamers, G. E. M., Thomas-Oates, J. E., Lugtenberg, B. J. J., & Bloemberg, G. V. (2004). Characterization of two *Pseudomonas putida* lipopeptide biosurfactants, putisolvin i and II, which inhibit biofilm formation and break down existing biofilms. *Molecular Microbiology*, *51*(1), 97–113. https://doi.org/10.1046/j.1365-2958.2003.03751.x

Kumla, J., Nundaeng, S., Suwannarach, N., & Lumyong, S. (2020). Evaluation of multifarious plant growth promoting trials of yeast isolated from the soil of assam tea (camellia sinensis var. assamica) plantations in northern thailand. *Microorganisms*, *8*(8), 1168. https://doi.org/10.3390/microorganisms8081168

Lackner, G., Moebius, N., & Hertweck, C. (2011). Endofungal bacterium controls its host by an *hrp* type III secretion system. *The ISME Journal*, *5*(2), 252–261. https://doi.org/10.1038/ismej.2010.126

Lambais, M. R., Crowley, D. E., Cury, J. C., Büll, R. C., & Rodrigues, R. R. (2006). Bacterial diversity in tree canopies of the atlantic forest. *Science*, *312*(5782), 1917–1917. https://doi.org/10.1126/science.1124696

Lapidot, A., Romling, U., & Yaron, S. (2006). Biofilm formation and the survival of salmonella typhimurium on parsley. *International Journal of Food Microbiology*, *109*(3), 229–233. https://doi.org/10.1016/j.ijfoodmicro.2006.01.012

Larousse, M., Rancurel, C., Syska, C., Palero, F., Etienne, C., Industri, B., Nesme, X., Bardin, M., & Galiana, E. (2017). Tomato root microbiota and phytophthora parasitica-associated disease. *Microbiome*, *5*(1), 56. https://doi.org/10.1186/s40168-017-0273-7

Lasky, J. R., Des Marais, D. L., Lowry, D. B., Povolotskaya, I., McKay, J. K., Richards, J. H., Keitt, T. H., & Juenger, T. E. (2014). Natural variation in abiotic stress responsive gene expression and local adaptation to climate in arabidopsis thaliana. *Molecular Biology and Evolution*, *31*(9), 2283–2296. https://doi.org/10.1093/molbev/msu170

Lau, J. A., & Lennon, J. T. (2012). Rapid responses of soil microorganisms improve plant fitness in novel environments. *Proceedings of the National Academy of Sciences*, *109*(35), 14058–14062. https://doi.org/10.1073/pnas.1202319109

Lavermicocca, P., Iacobellis, N. S., & Simmaco, M. (1997). Comparison of biological activities of pseudomonas syringae pv. syringae toxins [Series Title: Developments in Plant Pathology]. In K. Rudolph, T. J. Burr, J. W. Mansfield, D. Stead, A. Vivian, & J. Von Kietzell (Eds.), *Pseudomonas syringae pathovars and related pathogens* (pp. 176–181, Vol. 9). Springer Netherlands. https://doi.org/10.1007/978-94-011-5472-7_31

Li, Y., Steenwyk, J. L., Chang, Y., Wang, Y., James, T. Y., Stajich, J. E., Spatafora, J. W., Groenewald, M., Dunn, C. W., Hittinger, C. T., Shen, X.-X., & Rokas, A. (2021). A genome-scale phylogeny of the kingdom fungi. *Current Biology*, *31*(8), 1653–1665.e5. https://doi.org/10.1016/j.cub.2021.01.074

Li, Z., Bai, X., Jiao, S., Li, Y., Li, P., Yang, Y., Zhang, H., & Wei, G. (2021). A simplified synthetic community rescues astragalus mongholicus from root rot disease by activating plant-induced systemic resistance. *Microbiome*, *9*(1), 217. https://doi.org/10.1186/s40168-021-01169-9

Libkind, D., Gadanho, M., Van Broock, M., & Sampaio, J. P. (2009). Cystofilobasidium lacus-mascardii sp. nov., a basidiomycetous yeast species isolated from aquatic environments of the patagonian andes, and cystofilobasidium macerans sp. nov., the sexual stage of cryptococcus macerans. *INTERNATIONAL JOURNAL OF SYSTEMATIC AND EVOLUTIONARY MICROBIOLOGY*, *59*(3), 622–630. https://doi.org/10.1099/ijs.0.004390-0

Lilly, D. M., & Stillwell, R. H. (1965). Probiotics: Growth-promoting factors produced by microorganisms. *Science*, *147*(3659), 747–748. https://doi.org/10.1126/science.147.3659.747

Lindow, S. E., & Brandl, M. T. (2003). Microbiology of the phyllosphere. *Applied and Environmental Microbiology*, *69*(4), 1875–1883. https://doi.org/10.1128/AEM.69.4.1875-1883.2003

Links, M. G., Demeke, T., Gräfenhan, T., Hill, J. E., Hemmingsen, S. M., & Dumonceaux, T. J. (2014). Simultaneous profiling of seed-associated bacteria and fungi reveals antagonistic interactions between microorganisms within a shared epiphytic microbiome on *¡span style="font-variant:small-caps;"¿T¡/span¿ riticum* and *¡span style="font-variant:small-caps;"¿B¡/span¿ rassica* seeds. *New Phytologist*, *202*(2), 542–553. https://doi.org/10.1111/nph.12693

Liu, X.-Z., Wang, Q.-M., Göker, M., Groenewald, M., Kachalkin, A., Lumbsch, H., Millanes, A., Wedin, M., Yurkov, A., Boekhout, T., & Bai, F.-Y. (2015). Towards an integrated phylogenetic classification of the *Tremellomycetes*. *Studies in Mycology*, *81*(1), 85–147. https://doi.org/10.1016/j.simyco.2015.12.001

Liu, Y., Chen, L., Wu, G., Feng, H., Zhang, G., Shen, Q., & Zhang, R. (2017). Identification of root-secreted compounds involved in the communication between cucumber, the beneficial *Bacillus amyloliquefaciens* , and the soil-borne pathogen *Fusarium oxysporum*. *Molecular Plant-Microbe Interactions®*, *30*(1), 53–62. https://doi.org/10.1094/MPMI-07-16-0131-R

Liu, Y., Xu, Z., Chen, L., Xun, W., Shu, X., Chen, Y., Sun, X., Wang, Z., Ren, Y., Shen, Q., & Zhang, R. (2024). Root colonization by beneficial rhizobacteria. *FEMS Microbiology Reviews*, *48*(1), fuad066. https://doi.org/10.1093/femsre/fuad066

Loftus, B. J., Fung, E., Roncaglia, P., Rowley, D., Amedeo, P., Bruno, D., Vamathevan, J., Miranda, M., Anderson, I. J., Fraser, J. A., Allen, J. E., Bosdet, I. E., Brent, M. R., Chiu, R., Doering, T. L., Donlin, M. J., D'Souza, C. A., Fox, D. S., Grinberg, V., … Hyman, R. W. (2005). The genome of the basidiomycetous yeast and human pathogen *Cryptococcus neoformans*. *Science*, *307*(5713), 1321–1324. https://doi.org/10.1126/science.1103773

Long, J., Luo, W., Xie, J., Yuan, Y., Wang, J., Kang, L., Li, Y., Zhang, Z., & Hong, M. (2021). Environmental factors influencing phyllosphere bacterial communities in giant pandas' staple food bamboos. *Frontiers in Microbiology*, *12*, 748141. https://doi.org/10.3389/fmicb.2021.748141

Lundberg, D. S., De Pedro Jové, R., Pramoj Na Ayutthaya, P., Karasov, T. L., Shalev, O., Poersch, K., Ding, W., Bollmann-Giolai, A., Bezrukov, I., & Weigel, D. (2022). Contrasting patterns of microbial dominance in the *Arabidopsis thaliana* phyllosphere. *Proceedings of the National Academy of Sciences*, *119*(52), e2211881119. https://doi.org/10.1073/pnas.2211881119

Mahmoudi, M., Almario, J., Hu, Y., Tenzer, L.-M., Nieselt, K., & Kemen, E. (2024, October 26). Biotic interactions shape infection outcomes in *Arabidopsis*. https://doi.org/10.1101/2024.10.25.620230

Maida, I., Chiellini, C., Mengoni, A., Bosi, E., Firenzuoli, F., Fondi, M., & Fani, R. (2016). Antagonistic interactions between endophytic cultivable bacterial communities isolated from the medicinal plant ¡span style="font-variant:small-caps;"¿ *E* ¡/span¿ *chinacea purpurea*. *Environmental Microbiology*, *18*(8), 2357–2365. https://doi.org/10.1111/1462-2920.12911

Makarevitch, I., Waters, A. J., West, P. T., Stitzer, M., Hirsch, C. N., Ross-Ibarra, J., & Springer, N. M. (2015). Transposable elements contribute to activation of maize genes in response to abiotic stress (M. Freeling, Ed.). *PLoS Genetics*, *11*(1), e1004915. https://doi.org/10.1371/journal.pgen.1004915

Marra, D., Karapantsios, T., Caserta, S., Secchi, E., Holynska, M., Labarthe, S., Polizzi, B., Ortega, S., Kostoglou, M., Lasseur, C., Karapanagiotis, I., Lecuyer, S., Bridier, A., Noirot-Gros, M.-F., & Briandet, R. (2023). Migration of surface-associated microbial communities in spaceflight habitats. *Biofilm*, *5*, 100109. https://doi.org/10.1016/j.bioflm.2023.100109

Martins, S. J., Pasche, J., Silva, H. A. O., Selten, G., Savastano, N., Abreu, L. M., Bais, H. P., Garrett, K. A., Kraisitudomsook, N., Pieterse, C. M. J., & Cernava, T. (2023). The use of synthetic microbial communities to improve plant health. *Phytopathology®*, *113*(8), 1369–1379. https://doi.org/10.1094/PHYTO-01-23-0016-IA

Mas, A., Jamshidi, S., Lagadeuc, Y., Eveillard, D., & Vandenkoornhuyse, P. (2016). Beyond the black queen hypothesis. *The ISME Journal*, *10*(9), 2085–2091. https://doi.org/10.1038/ismej.2016.22

Mayo, B., Rodríguez, J., Vázquez, L., & Flórez, A. B. (2021). Microbial interactions within the cheese ecosystem and their application to improve quality and safety. *Foods*, *10*(3), 602. https://doi.org/10.3390/foods10030602

McGowan, J., Byrne, K. P., & Fitzpatrick, D. A. (2019). Comparative analysis of oomycete genome evolution using the oomycete gene order browser (OGOB) (S. Baldauf, Ed.). *Genome Biology and Evolution*, *11*(1), 189–206. https://doi.org/10.1093/gbe/evy267

McLaughlin, D. J., McLaughlin, E. G., & Lemke, P. A. (Eds.). (2001). *Systematics and evolution*. Springer Berlin Heidelberg. https://doi.org/10.1007/978-3-662-10189-6

McMullan, M., Gardiner, A., Bailey, K., Kemen, E., Ward, B. J., Cevik, V., Robert-Seilaniantz, A., Schultz-Larsen, T., Balmuth, A., Holub, E., Van Oosterhout, C., & Jones, J. D. (2015). Evidence for suppression of immunity as a driver for genomic introgressions and host range expansion in races of albugo candida, a generalist parasite. *eLife*, *4*, e04550. https://doi.org/10.7554/eLife.04550

Mercado-Blanco, J., & Bakker, P. A. H. M. (2007). Interactions between plants and beneficial pseudomonas spp.: Exploiting bacterial traits for crop protection. *Antonie van Leeuwenhoek*, *92*(4), 367–389. https://doi.org/10.1007/s10482-007-9167-1

Mercier, J., & Lindow, S. E. (2000). Role of leaf surface sugars in colonization of plants by bacterial epiphytes. *Applied and Environmental Microbiology*, *66*(1), 369–374. https://doi.org/10.1128/AEM.66.1.369-374.2000

Meziane, H., Van Der Sluis, I., Van Loon, L. C., Höfte, M., & Bakker, P. A. H. M. (2005). Determinants of *Pseudomonas putida* WCS358 involved in inducing systemic resistance in plants. *Molecular Plant Pathology*, *6*(2), 177–185. https://doi.org/10.1111/j.1364-3703.2005.00276.x

Millanes, A. M., Diederich, P., Ekman, S., & Wedin, M. (2011). Phylogeny and character evolution in the jelly fungi (tremellomycetes, basidiomycota, fungi). *Molecular Phylogenetics and Evolution*, *61*(1), 12–28. https://doi.org/10.1016/j.ympev.2011.05.014

Moliné, M., Flores, M. R., Libkind, D., Carmen Diéguez, M. D. C., Farías, M. E., & Van Broock, M. (2010). Photoprotection by carotenoid pigments in the yeast rhodotorula mucilaginosa: The role of torularhodin. *Photochemical & Photobiological Sciences*, *9*(8), 1145–1151. https://doi.org/10.1039/c0pp00009d

Monier, J.-M., & Lindow, S. E. (2004). Frequency, size, and localization of bacterial aggregates on bean leaf surfaces. *Applied and Environmental Microbiology*, *70*(1), 346–355. https://doi.org/10.1128/AEM.70.1.346-355.2004

Moore, R. T., & Rij, N. J. W. K.-v. (1972). Ultrastructure of *Filobasidium* olive. *Canadian Journal of Microbiology*, *18*(12), 1949–1951. https://doi.org/10.1139/m72-301

Morris, B. E., Henneberger, R., Huber, H., & Moissl-Eichinger, C. (2013). Microbial syntrophy: Interaction for the common good. *FEMS Microbiology Reviews*, *37*(3), 384–406. https://doi.org/10.1111/1574-6976.12019

Morris, C. E., Monier, J., & Jacques, M. (1997). Methods for observing microbial biofilms directly on leaf surfaces and recovering them for isolation of culturable microorganisms. *Applied and Environmental Microbiology*, *63*(4), 1570–1576. https://doi.org/10.1128/aem.63.4.1570-1576.1997

Muller, E. E., Faust, K., Widder, S., Herold, M., Martínez Arbas, S., & Wilmes, P. (2018). Using metabolic networks to resolve ecological properties of microbiomes. *Current Opinion in Systems Biology*, *8*, 73–80. https://doi.org/10.1016/j.coisb.2017.12.004

Netzker, T., Fischer, J., Weber, J., Mattern, D. J., König, C. C., Valiante, V., Schroeckh, V., & Brakhage, A. A. (2015). Microbial communication leading to the activation of silent fungal secondary metabolite gene clusters. *Frontiers in Microbiology*, *6*. https://doi.org/10.3389/fmicb.2015.00299

Newton, A. C., Fitt, B. D., Atkins, S. D., Walters, D. R., & Daniell, T. J. (2010). Pathogenesis, parasitism and mutualism in the trophic space of microbe–plant interactions. *Trends in Microbiology*, *18*(8), 365–373. https://doi.org/10.1016/j.tim.2010.06.002

Noel, Z. A., Longley, R., Benucci, G. M. N., Trail, F., Chilvers, M. I., & Bonito, G. (2022). Non-target impacts of fungicide disturbance on phyllosphere yeasts in conventional and no-till management. *ISME Communications*, *2*(1), 19. https://doi.org/10.1038/s43705-022-00103-w

Oberwinkler, F., Bandoni, R., Blanz, P., & Kisimova-Horovitz, L. (1983). Cystofilobasidium: A new genus in the filobasidiaceae. *Systematic and Applied Microbiology*, *4*(1), 114–122. https://doi.org/10.1016/S0723-2020(83)80039-3

Ortiz-Castro, R., Díaz-Pérez, C., Martínez-Trujillo, M., Del Río, R. E., Campos-García, J., & López-Bucio, J. (2011). Transkingdom signaling based on bacterial cyclodipeptides with auxin activity in plants. *Proceedings of the National Academy of Sciences*, *108*(17), 7253–7258. https://doi.org/10.1073/pnas.1006740108

Peiffer, J. A., Spor, A., Koren, O., Jin, Z., Tringe, S. G., Dangl, J. L., Buckler, E. S., & Ley, R. E. (2013). Diversity and heritability of the maize rhizosphere microbiome under field conditions. *Proceedings of the National Academy of Sciences*, *110*(16), 6548–6553. https://doi.org/10.1073/pnas.1302837110

Peng, M., Jiang, Z., Zhou, F., & Wang, Z. (2023). From salty to thriving: Plant growth promoting bacteria as nature's allies in overcoming salinity stress in plants. *Frontiers in Microbiology*, *14*, 1169809. https://doi.org/10.3389/fmicb.2023.1169809

Phuengmaung, P., Mekjaroen, J., Saisorn, W., Chatsuwan, T., Somparn, P., & Leelahavanichkul, A. (2022). Rapid synergistic biofilm production of pseudomonas and candida on the pulmonary cell surface and in mice, a possible cause of chronic mixed organismal lung lesions. *International Journal of Molecular Sciences*, *23*(16), 9202. https://doi.org/10.3390/ijms23169202

Piccardi, P., Vessman, B., & Mitri, S. (2019). Toxicity drives facilitation between 4 bacterial species. *Proceedings of the National Academy of Sciences*, *116*(32), 15979–15984. https://doi.org/10.1073/pnas.1906172116

Pieterse, C. M., Zamioudis, C., Berendsen, R. L., Weller, D. M., Van Wees, S. C., & Bakker, P. A. (2014). Induced systemic resistance by beneficial microbes. *Annual Review of Phytopathology*, *52*(1), 347–375. https://doi.org/10.1146/annurev-phyto-082712-102340

Ploch, S., & Thines, M. (2011). Obligate biotrophic pathogens of the genus albugo are widespread as asymptomatic endophytes in natural populations of brassicaceae: OOMYCETES ARE COMMON ASYMPTOMATIC ENDOPHYTES. *Molecular Ecology*, no–no. https://doi.org/10.1111/j.1365-294X.2011.05188.x

Poole, K., Dean, C., Heinrichs, D., Neshat, S., Krebs, K., Young, L., & Kilburn, L. (1996). Siderophore-mediated iron transport in pseudomonas aeruginosa, 371–383.

Poza-Carrion, C., Suslow, T., & Lindow, S. (2013). Resident bacteria on leaves enhance survival of immigrant cells of *Salmonella enterica*. *Phytopathology®*, *103*(4), 341–351. https://doi.org/10.1094/PHYTO-09-12-0221-FI

Preston, G. M., Bertrand, N., & Rainey, P. B. (2001). Type III secretion in plant growth-promoting *Pseudomonas fluorescens* SBW25. *Molecular Microbiology*, *41*(5), 999–1014. https://doi.org/10.1046/j.1365-2958.2001.02560.x

Pruitt, H. M., Zhu, J. C., Riley, S. P., & Shi, M. (2025). The hidden fortress: A comprehensive review of fungal biofilms with emphasis on cryptococcus neoformans. *Journal of Fungi*, *11*(3), 236. https://doi.org/10.3390/jof11030236

Rafiqi, M., Gan, P. H., Ravensdale, M., Lawrence, G. J., Ellis, J. G., Jones, D. A., Hardham, A. R., & Dodds, P. N. (2010). Internalization of flax rust avirulence proteins into flax and tobacco cells can occur in the absence of the pathogen. *The Plant Cell*, *22*(6), 2017–2032. https://doi.org/10.1105/tpc.109.072983

Rainey, P. B. (1999). Adaptation of *Pseudomonas fluorescens* to the plant rhizosphere. *Environmental Microbiology*, *1*(3), 243–257. https://doi.org/10.1046/j.1462-2920.1999.00040.x

Ramage, G., Saville, S. P., Wickes, B. L., & López-Ribot, J. L. (2002). Inhibition of *Candida albicans* biofilm formation by farnesol, a quorum-sensing molecule. *Applied and Environmental Microbiology*, *68*(11), 5459–5463. https://doi.org/10.1128/AEM.68.11.5459-5463.2002

Recinos, D. A., Sekedat, M. D., Hernandez, A., Cohen, T. S., Sakhtah, H., Prince, A. S., Price-Whelan, A., & Dietrich, L. E. P. (2012). Redundant phenazine operons in *Pseudomonas aeruginosa* exhibit environment-dependent expression and differential roles in pathogenicity. *Proceedings of the National Academy of Sciences*, *109*(47), 19420–19425. https://doi.org/10.1073/pnas.1213901109

Records, A. R. (2011). The type VI secretion system: A multipurpose delivery system with a phage-like machinery. *Molecular Plant-Microbe Interactions®*, *24*(7), 751–757. https://doi.org/10.1094/MPMI-11-10-0262

Redford, A. J., Bowers, R. M., Knight, R., Linhart, Y., & Fierer, N. (2010). The ecology of the phyllosphere: Geographic and phylogenetic variability in the distribution of bacteria on tree leaves. *Environmental Microbiology*, *12*(11), 2885–2893. https://doi.org/10.1111/j.1462-2920.2010.02258.x

Reinhold-Hurek, B., Bünger, W., Burbano, C. S., Sabale, M., & Hurek, T. (2015). Roots shaping their microbiome: Global hotspots for microbial activity. *Annual Review of Phytopathology*, *53*(1), 403–424. https://doi.org/10.1146/annurev-phyto-082712-102342

Remus-Emsermann, M. N. P., Tecon, R., Kowalchuk, G. A., & Leveau, J. H. J. (2012). Variation in local carrying capacity and the individual fate of bacterial colonizers in the phyllosphere. *The ISME Journal*, *6*(4), 756–765. https://doi.org/10.1038/ismej.2011.209

Richardson, A. E., & Simpson, R. J. (2011). Soil microorganisms mediating phosphorus availability update on microbial phosphorus. *Plant Physiology*, *156*(3), 989–996. https://doi.org/10.1104/pp.111.175448

Roberts, E., & Lindow, S. (2014). Loline alkaloid production by fungal endophytes of *Fescue* species select for particular epiphytic bacterial microflora. *The ISME Journal*, *8*(2), 359–368. https://doi.org/10.1038/ismej.2013.170

Rueda-Mejia, M. P., Nägeli, L., Lutz, S., Hayes, R. D., Varadarajan, A. R., Grigoriev, I. V., Ahrens, C. H., & Freimoser, F. M. (2021). Genome, transcriptome and secretome analyses of the antagonistic, yeast-like fungus aureobasidium pullulans to identify potential biocontrol genes. *Microbial Cell*, *8*(8), 184–202. https://doi.org/10.15698/mic2021.08.757

Sampaio, J. P., Gadanho, M., & Bauer, R. (2001). Taxonomic studies on the genus cystofilobasidium: Description of cystofilobasidium ferigula sp. nov. and clarification of the status of cystofilobasidium larimarini. *International Journal of Systematic and Evolutionary Microbiology*, *51*(1), 221–229. https://doi.org/10.1099/00207713-51-1-221

Santos Kron, A., Zengerer, V., Bieri, M., Dreyfuss, V., Sostizzo, T., Schmid, M., Lutz, M., Remus-Emsermann, M. N. P., & Pelludat, C. (2020). Pseudomonas orientalis f9 pyoverdine, safracin, and phenazine mutants remain effective antagonists against erwinia amylovora in apple flowers (I. S. Druzhinina, Ed.). *Applied and Environmental Microbiology*, *86*(8), e02620–19. https://doi.org/10.1128/AEM.02620-19

Scher, K., Romling, U., & Yaron, S. (2005). Effect of heat, acidification, and chlorination on *Salmonella enterica* serovar typhimurium cells in a biofilm formed at the air-liquid interface. *Applied and Environmental Microbiology*, *71*(3), 1163–1168. https://doi.org/10.1128/AEM.71.3.1163-1168.2005

Schink, B. (2002). [no title found]. *Antonie van Leeuwenhoek*, *81*(1), 257–261. https://doi.org/10.1023/A:1020579004534

Schlaeppi, K., Dombrowski, N., Oter, R. G., Ver Loren Van Themaat, E., & Schulze-Lefert, P. (2014). Quantitative divergence of the bacterial root microbiota in *Arabidopsis thaliana* relatives. *Proceedings of the National Academy of Sciences*, *111*(2), 585–592. https://doi.org/10.1073/pnas.1321597111

Schoonbeek, H.-j., Raaijmakers, J. M., & De Waard, M. A. (2002). Fungal ABC transporters and microbial interactions in natural environments. *Molecular Plant-Microbe Interactions®*, *15*(11), 1165–1172. https://doi.org/10.1094/MPMI.2002.15.11.1165

Schroeckh, V., Scherlach, K., Nützmann, H.-W., Shelest, E., Schmidt-Heck, W., Schuemann, J., Martin, K., Hertweck, C., & Brakhage, A. A. (2009). Intimate bacterial–fungal interaction triggers biosynthesis of archetypal polyketides in *Aspergillus nidulans*. *Proceedings of the National Academy of Sciences*, *106*(34), 14558–14563. https://doi.org/10.1073/pnas.0901870106

Shalev, O., Karasov, T. L., Lundberg, D. S., Ashkenazy, H., Pramoj Na Ayutthaya, P., & Weigel, D. (2022). Commensal pseudomonas strains facilitate protective response against pathogens in the host plant. *Nature Ecology & Evolution*, *6*(4), 383–396. https://doi.org/10.1038/s41559-022-01673-7

Sharma, M., & Prasad, R. (2011). The quorum-sensing molecule farnesol is a modulator of drug efflux mediated by ABC multidrug transporters and synergizes with drugs in candida albicans. *Antimicrobial Agents and Chemotherapy*, *55*(10), 4834–4843. https://doi.org/10.1128/AAC.00344-11

Shaul, O. (2017). How introns enhance gene expression. *The International Journal of Biochemistry & Cell Biology*, *91*, 145–155. https://doi.org/10.1016/j.biocel.2017.06.016

Shearer, C. A. (1995). Fungal competition. *Canadian Journal of Botany*, *73*, 1259–1264. https://doi.org/10.1139/b95-386

Shiferaw, B., Smale, M., Braun, H.-J., Duveiller, E., Reynolds, M., & Muricho, G. (2013). Crops that feed the world 10. past successes and future challenges to the role played by wheat in global food security. *Food Security*, *5*(3), 291–317. https://doi.org/10.1007/s12571-013-0263-y

Shiraishi, K., Oku, M., Uchida, D., Yurimoto, H., & Sakai, Y. (2015). Regulation of nitrate and methylamine metabolism by multiple nitrogen sources in the methylotrophic yeast *Candida boidinii*. *FEMS Yeast Research*, fov084. https://doi.org/10.1093/femsyr/fov084

Simon, J.-C., Marchesi, J. R., Mougel, C., & Selosse, M.-A. (2019). Host-microbiota interactions: From holobiont theory to analysis. *Microbiome*, *7*(1), 5. https://doi.org/10.1186/s40168-019-0619-4

Sitaraman, R. (2015). Pseudomonas spp. as models for plant-microbe interactions. *Frontiers in Plant Science*, *6*. https://doi.org/10.3389/fpls.2015.00787

Slot, J. C., & Rokas, A. (2011). Horizontal transfer of a large and highly toxic secondary metabolic gene cluster between fungi. *Current Biology*, *21*(2), 134–139. https://doi.org/10.1016/j.cub.2010.12.020

Sorger, Z., Sengupta, P., Beier-Heuchert, K., Bautor, J., Parker, J. E., Kemen, E., & Doehlemann, G. (2025, April 4). GH25 lysozyme mediates tripartite interkingdom interactions and microbial competition on the plant leaf surface. https://doi.org/10.1101/2025.04.04.647216

Spanu, P., & Kämper, J. (2010). Genomics of biotrophy in fungi and oomycetes—emerging patterns. *Current Opinion in Plant Biology*, *13*(4), 409–414. https://doi.org/10.1016/j.pbi.2010.03.004

Sun, P.-F., Fang, W.-T., Shin, L.-Y., Wei, J.-Y., Fu, S.-F., & Chou, J.-Y. (2014). Indole-3-acetic acid-producing yeasts in the phyllosphere of the carnivorous plant drosera indica l (G. Berg, Ed.). *PLoS ONE*, *9*(12), e114196. https://doi.org/10.1371/journal.pone.0114196

Sun, S., Yadav, V., Billmyre, R. B., Cuomo, C. A., Nowrousian, M., Wang, L., Souciet, J.-L., Boekhout, T., Porcel, B., Wincker, P., Granek, J. A., Sanyal, K., & Heitman, J. (2017). Fungal genome and mating system transitions facilitated by chromosomal translocations involving intercentromeric recombination (K. Wolfe, Ed.). *PLOS Biology*, *15*(8), e2002527. https://doi.org/10.1371/journal.pbio.2002527

Sundin, G. W., Kidambi, S. P., Ullrich, M., & Bender, C. L. (1996). Resistance to ultraviolet light in pseudomonas syringae: Sequence and functional analysis of the plasmid-encoded rulAB genes. *Gene*, *177*(1), 77–81. https://doi.org/10.1016/0378-1119(96)00273-9

Svensson, B. (1994). Protein engineering in the ?-amylase family: Catalytic mechanism, substrate specificity, and stability. *Plant Molecular Biology*, *25*(2), 141–157. https://doi.org/10.1007/BF00023233

Swift, C. L., Louie, K. B., Bowen, B. P., Hooker, C. A., Solomon, K. V., Singan, V., Daum, C., Pennacchio, C. P., Barry, K., Shutthanandan, V., Evans, J. E., Grigoriev, I. V., Northen, T. R., & O'Malley, M. A. (2021). Cocultivation of anaerobic fungi with rumen bacteria establishes an antagonistic relationship (J. W. Taylor, Ed.). *mBio*, *12*(4), e01442–21. https://doi.org/10.1128/mBio.01442-21

Thomas, J., Linton, S., Corum, L., Slone, W., Okel, T., & Percival, S. L. (2012). The affect of pH and bacterial phenotypic state on antibiotic efficacy. *International Wound Journal*, *9*(4), 428–435. https://doi.org/10.1111/j.1742-481X.2011.00902.x

Trivedi, P., Leach, J. E., Tringe, S. G., Sa, T., & Singh, B. K. (2020). Plant–microbiome interactions: From community assembly to plant health. *Nature Reviews Microbiology*, *18*(11), 607–621. https://doi.org/10.1038/s41579-020-0412-1

Truyens, S., Weyens, N., Cuypers, A., & Vangronsveld, J. (2015). Bacterial seed endophytes: Genera, vertical transmission and interaction with plants. *Environmental Microbiology Reports*, *7*(1), 40–50. https://doi.org/10.1111/1758-2229.12181

Tsuge, T., Harimoto, Y., Akimitsu, K., Ohtani, K., Kodama, M., Akagi, Y., Egusa, M., Yamamoto, M., & Otani, H. (2013). Host-selective toxins produced by the plant pathogenic fungus *Alternaria alternata*. *FEMS Microbiology Reviews*, *37*(1), 44–66. https://doi.org/10.1111/j.1574-6976.2012.00350.x

Tyc, O., Van Den Berg, M., Gerards, S., Van Veen, J. A., Raaijmakers, J. M., De Boer, W., & Garbeva, P. (2014). Impact of interspecific interactions on antimicrobial activity among soil bacteria. *Frontiers in Microbiology*, *5*. https://doi.org/10.3389/fmicb.2014.00567

Velez, P., Espinosa-Asuar, L., Figueroa, M., Gasca-Pineda, J., Aguirre-von-Wobeser, E., Eguiarte, L. E., Hernandez-Monroy, A., & Souza, V. (2018). Nutrient dependent cross-kingdom interactions: Fungi and bacteria from an oligotrophic desert oasis. *Frontiers in Microbiology*, *9*, 1755. https://doi.org/10.3389/fmicb.2018.01755

Vergin, F. (1954). Anti- und probiotika. (4), 16–119.

Villa, F., Cappitelli, F., Cortesi, P., & Kunova, A. (2017). Fungal biofilms: Targets for the development of novel strategies in plant disease management. *Frontiers in Microbiology*, *8*. https://doi.org/10.3389/fmicb.2017.00654

Vorholt, J. A. (2012). Microbial life in the phyllosphere [Medium: application/pdf,33 p. accepted version Publisher: ETH Zurich]. https://doi.org/10.3929/ETHZ-B-000059727

Vylkova, S. (2017). Environmental pH modulation by pathogenic fungi as a strategy to conquer the host (D. A. Hogan, Ed.). *PLOS Pathogens*, *13*(2), e1006149. https://doi.org/10.1371/journal.ppat.1006149

Wandersman, C., & Delepelaire, P. (2004). Bacterial iron sources: From siderophores to hemophores. *Annual Review of Microbiology*, *58*(1), 611–647. https://doi.org/10.1146/annurev.micro.58.030603.123811

Wang, K., Sipilä, T. P., & Overmyer, K. (2016). The isolation and characterization of resident yeasts from the phylloplane of arabidopsis thaliana. *Scientific Reports*, *6*(1), 39403. https://doi.org/10.1038/srep39403

Whipps, J., Hand, P., Pink, D., & Bending, G. (2008). Phyllosphere microbiology with special reference to diversity and plant genotype. *Journal of Applied Microbiology*, *105*(6), 1744–1755. https://doi.org/10.1111/j.1365-2672.2008.03906.x

Whooley, M. A., & McLoughlin, A. J. (1982). The regulation of pyocyanin production in pseudomonas aeruginosa. *European Journal of Applied Microbiology and Biotechnology*, *15*(3), 161–166. https://doi.org/10.1007/BF00511241

Winski, C. J., Qian, Y., Mobashery, S., & Santiago-Tirado, F. H. (2022). An atypical ABC transporter is involved in antifungal resistance and host interactions in the pathogenic fungus cryptococcus neoformans (J. Andrew Alspaugh, Ed.). *mBio*, *13*(4), e01539–22. https://doi.org/10.1128/mbio.01539-22

Wintermute, E. H., & Silver, P. A. (2010). Emergent cooperation in microbial metabolism. *Molecular Systems Biology*, *6*(1), 407. https://doi.org/10.1038/msb.2010.66

Woodward, F. I., & Lomas, M. R. (2004). Vegetation dynamics – simulating responses to climatic change. *Biological Reviews*, *79*(3), 643–670. https://doi.org/10.1017/S1464793103006419

World Health Organization. (1990). *Public health impact of pesticides used in agriculture*.

Wright, R., Douglas, B., Royal Botanic Gardens Kew Genome Acquisition Lab, Darwin Tree of Life Barcoding collective, Wellcome Sanger Institute Tree of Life Management, Samples and Laboratory team, Wellcome Sanger Institute Scientific Operations: Sequencing Operations, Wellcome Sanger Institute Tree of Life Core Informatics team, Tree of Life Core Informatics collective, & Darwin Tree of Life Consortium. (2024). The genome sequence of a basidiomycete yeast, tausonia pullulans (lindner) x.z. liu, f.y. bai, m. groenew. & boekhout, 2016 (mrakiaceae). *Wellcome Open Research*, *9*, 685. https://doi.org/10.12688/wellcomeopenres.23350.1

Xin, X.-F., Nomura, K., Aung, K., Velásquez, A. C., Yao, J., Boutrot, F., Chang, J. H., Zipfel, C., & He, S. Y. (2016). Bacteria establish an aqueous living space in plants crucial for virulence. *Nature*, *539*(7630), 524–529. https://doi.org/10.1038/nature20166

Xu, Y., & Zhong, J.-J. (2011). Significance of oxygen supply in production of a novel antibiotic by pseudomonas sp. SJT25. *Bioresource Technology*, *102*(19), 9167–9174. https://doi.org/10.1016/j.biortech.2011.07.011

Yan, L., Boyd, K. G., Adams, D. R., & Burgess, J. G. (2003). Biofilm-specific cross-species induction of antimicrobial compounds in bacilli. *Applied and Environmental Microbiology*, *69*(7), 3719–3727. https://doi.org/10.1128/AEM.69.7.3719-3727.2003

Yasmin, S., Hafeez, F. Y., Mirza, M. S., Rasul, M., Arshad, H. M. I., Zubair, M., & Iqbal, M. (2017). Biocontrol of bacterial leaf blight of rice and profiling of secondary metabolites produced by rhizospheric pseudomonas aeruginosa BRp3. *Frontiers in Microbiology*, *8*, 1895. https://doi.org/10.3389/fmicb.2017.01895

Yokoi, S., Quintero, F. J., Cubero, B., Ruiz, M. T., Bressan, R. A., Hasegawa, P. M., & Pardo, J. M. (2002). Differential expression and function of *Arabidopsis thaliana* NHX na^+ /h^+ antiporters in the salt stress response. *The Plant Journal*, *30*(5), 529–539. https://doi.org/10.1046/j.1365-313X.2002.01309.x

Zamioudis, C., & Pieterse, C. M. J. (2012). Modulation of host immunity by beneficial microbes. *Molecular Plant-Microbe Interactions®*, *25*(2), 139–150. https://doi.org/10.1094/MPMI-06-11-0179

Zelezniak, A., Andrejev, S., Ponomarova, O., Mende, D. R., Bork, P., & Patil, K. R. (2015). Metabolic dependencies drive species co-occurrence in diverse microbial communities. *Proceedings of the National Academy of Sciences*, *112*(20), 6449–6454. https://doi.org/10.1073/pnas.1421834112

Zgadzaj, R., Garrido-Oter, R., Jensen, D. B., Koprivova, A., Schulze-Lefert, P., & Radutoiu, S. (2016). Root nodule symbiosis in *Lotus japonicus* drives the establishment of distinctive rhizosphere, root, and nodule bacterial communities. *Proceedings of the National Academy of Sciences*, *113*(49). https://doi.org/10.1073/pnas.1616564113

Zhalnina, K., Louie, K. B., Hao, Z., Mansoori, N., Da Rocha, U. N., Shi, S., Cho, H., Karaoz, U., Loqué, D., Bowen, B. P., Firestone, M. K., Northen, T. R., & Brodie, E. L. (2018). Dynamic root exudate chemistry and microbial substrate preferences drive patterns in rhizosphere microbial community assembly. *Nature Microbiology*, *3*(4), 470–480. https://doi.org/10.1038/s41564-018-0129-3

Zhou, N., Swamy, K. B. S., Leu, J.-Y., McDonald, M. J., Galafassi, S., Compagno, C., & Piškur, J. (2017). Coevolution with bacteria drives the evolution of aerobic fermentation in lachancea kluyveri (J. Schacherer, Ed.). *PLOS ONE*, *12*(3), e0173318. https://doi.org/10.1371/journal.pone.0173318

Zhou, X., Wang, J., Liu, F., Liang, J., Zhao, P., Tsui, C. K. M., & Cai, L. (2022). Cross-kingdom synthetic microbiota supports tomato suppression of fusarium wilt disease. *Nature Communications*, *13*(1), 7890. https://doi.org/10.1038/s41467-022-35452-6

Zhu, H.-Y., Wei, X.-Y., Liu, X.-Z., & Bai, F.-Y. (2023). Cystofilobasidium josepaulonis sp. nov., a novel basidiomycetous yeast species. *International Journal of Systematic and Evolutionary Microbiology*, *73*(5). https://doi.org/10.1099/ijsem.0.005865

Zhu, S., Vivanco, J. M., & Manter, D. K. (2016). Nitrogen fertilizer rate affects root exudation, the rhizosphere microbiome and nitrogen-use-efficiency of maize. *Applied Soil Ecology*, *107*, 324–333. https://doi.org/10.1016/j.apsoil.2016.07.009

Żymańczyk-Duda, E., Brzezińska-Rodak, M., Klimek-Ochab, M., Duda, M., & Zerka, A. (2017, November 8). Yeast as a versatile tool in biotechnology. In A. Morata & I. Loira (Eds.), *Yeast - industrial applications*. InTech. https://doi.org/10.5772/intechopen.70130

12 Acknowledgment

First, I would like to thank Eric for giving me the opportunity to perform my PhD in his lab, for his supervision and confidence in me. It was not an easy journey, but one I hope we both grew and learned from. Additionally, I thank my other TAC-members Hannes Link and Farid El Kasmi for giving invaluable insights and suggestions. Without the three of you I wouldn't be where I am today.

Of course, I want to thank the whole Kemen lab and ZMBP 4th floor for an open and inviting environment and all the input, as well as support over the years. Every presentation, every progress report, you guys brought me a step closer to the finish line. On that note, special thanks to Monja and Lukas for reading and correcting my thesis. Wishing you all the best in your future endeavors — I'm looking forward to sharing many more coffees together!

Angi, mein Stups. Danke auch für deine Unterstützung über die letzten 4 Jahre! Ich bin froh dich in meinem Leben zu haben und *freue* mich schon auf viele weitere Wochenendstalldienste vor Sonnenaufgang bei Wind und Wetter mit dir!
Vielen Dank an meine Eltern, Tanja und Andreas, die mich, vor allem während meines Studiums, immer voll und ganz unterstützt haben. Sowas ist nicht selbstverständlich, und darum danke ich euch von ganzem Herzen! Ich *verspreche* euch natürlich, nie wieder euren Kühlschrank zu plündern oder Wäsche mitzubringen, wenn ich zu Besuch komme. Wirklich. Ganz bestimmt. Vielleicht.

13 Affidavit / Eidesstaatliche Erklärung

Ich versichere, dass ich die von mir vorgelegte Dissertation selbständig angefertigt, die benutzten Quellen und Hilfsmittel vollständig angegeben und die Stellen der Arbeit, die - einschließlich Tabellen, Karten und Abbildungen - anderen Werken im Wortlaut oder dem Sinn nach entnommen sind, in jedem Einzelfall als Entlehnung kenntlich gemacht habe; dass diese Dissertation noch keiner anderen Fakultät oder Universität zur Prüfung vorgelegen hat; dass sie noch nicht veröffentlicht worden ist, sowie, dass ich eine solche Veröffentlichung vor Abschluss des Promotionsverfahrens nicht vornehmen werde.

Die Bestimmungen der Promotionsordnung sind mir bekannt. Die von mir vorgelegte Dissertation ist von Prof. Dr. Eric Kemen betreut worden.

Ich versichere, dass ich alle Angaben wahrheitsgemäß nach bestem Wissen und Gewissen gemacht habe und verpflichte mich, jedmögliche, die obigen Angaben betreffenden Veränderungen, dem Dekanat unverzüglich mitzuteilen.

Tübingen, den

Samuel Quinzer